Istituto Nazionale di Fisica Nucleare
SEZIONE DI ROMA TOR VERGATA

国家自然科学基金委员会
National Natural Science Foundation of China

Granted by a NSFC Project: U1931201

Ground-based gamma-ray astronomy with LHAASO

G. Di Sciascio
INFN - Roma Tor Vergata, Italy
IHEP - Chinese Academy of Sciences, Beijing, China (PIFI program)
disciascio@roma2.infn.it

SEXTEN CENTER FOR ASTROPHYSICS

Summer School on Gamma-Ray Astrophysics
Sesto - Sexten (Italy) July 18 - 22, 2022

All-particle Energy Spectrum

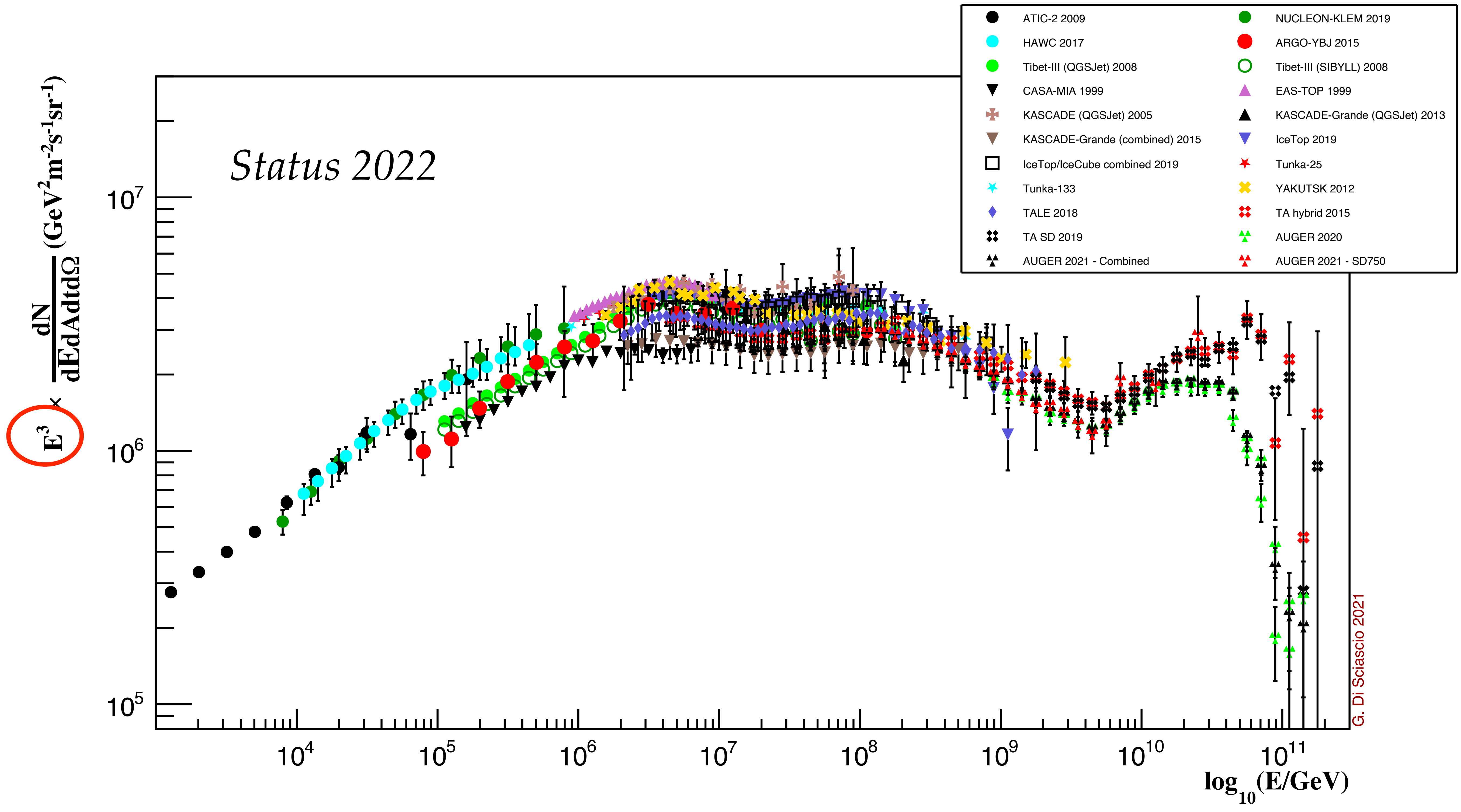

All-particle Energy Spectrum

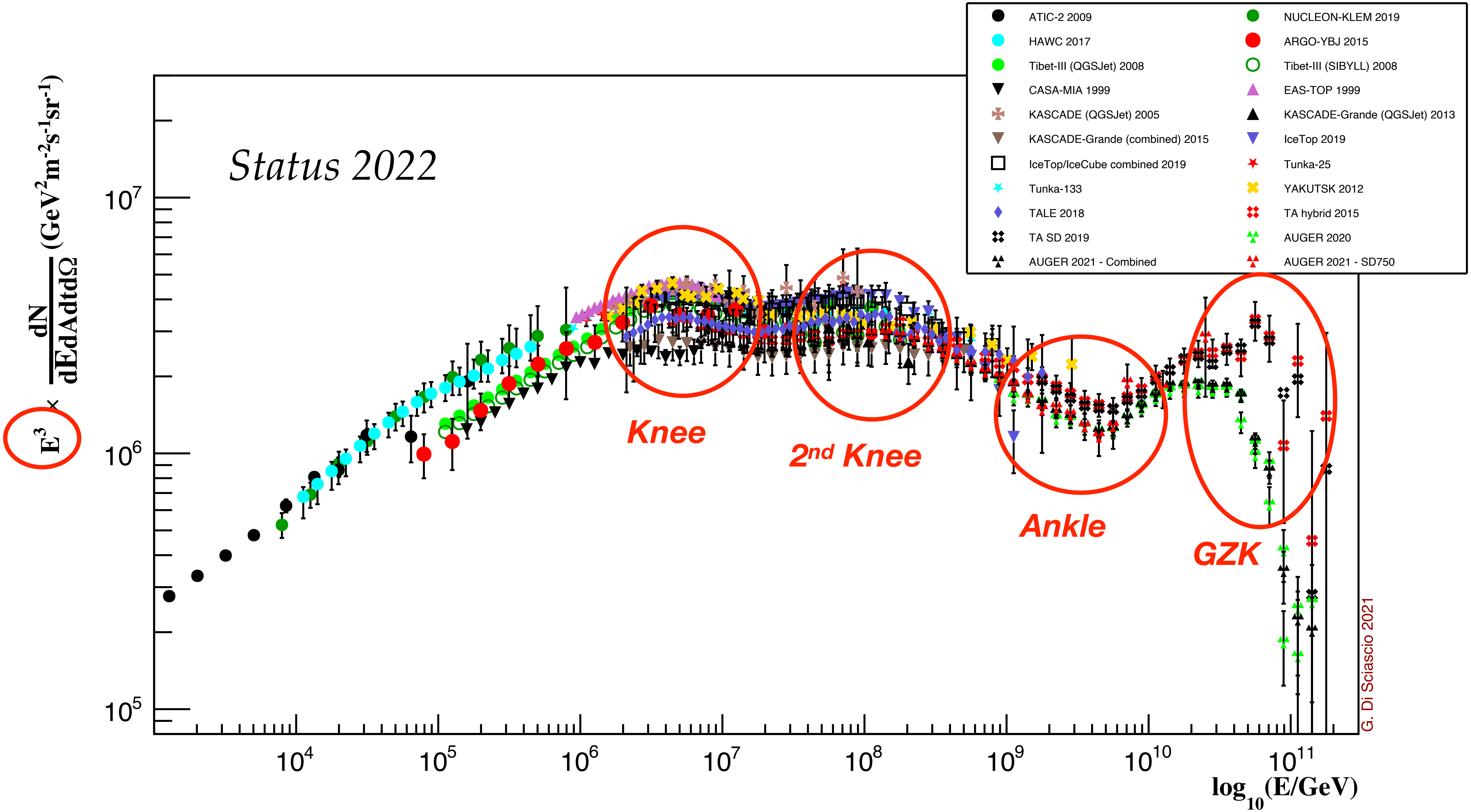

A closer look to the knee region

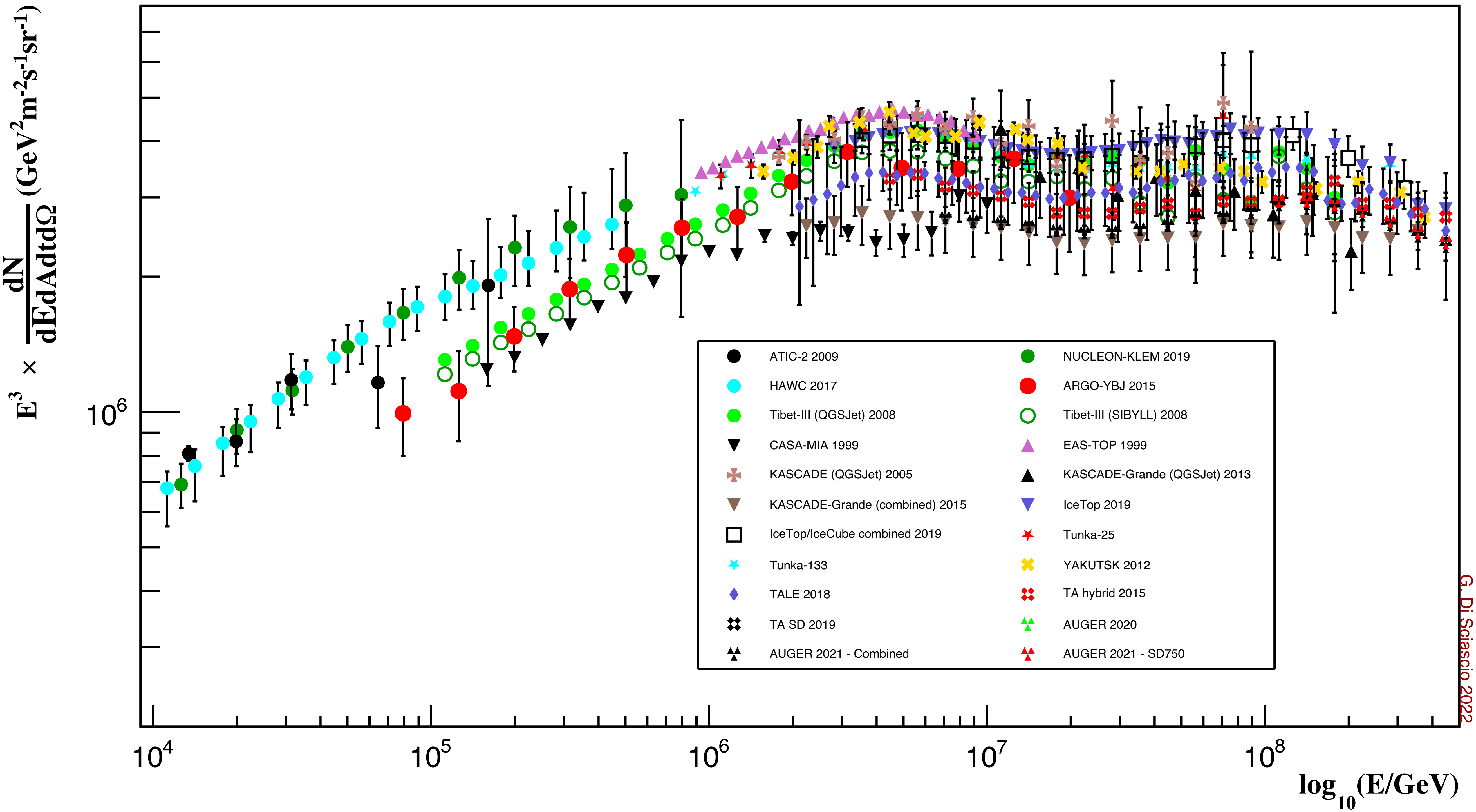

A closer look to the knee region

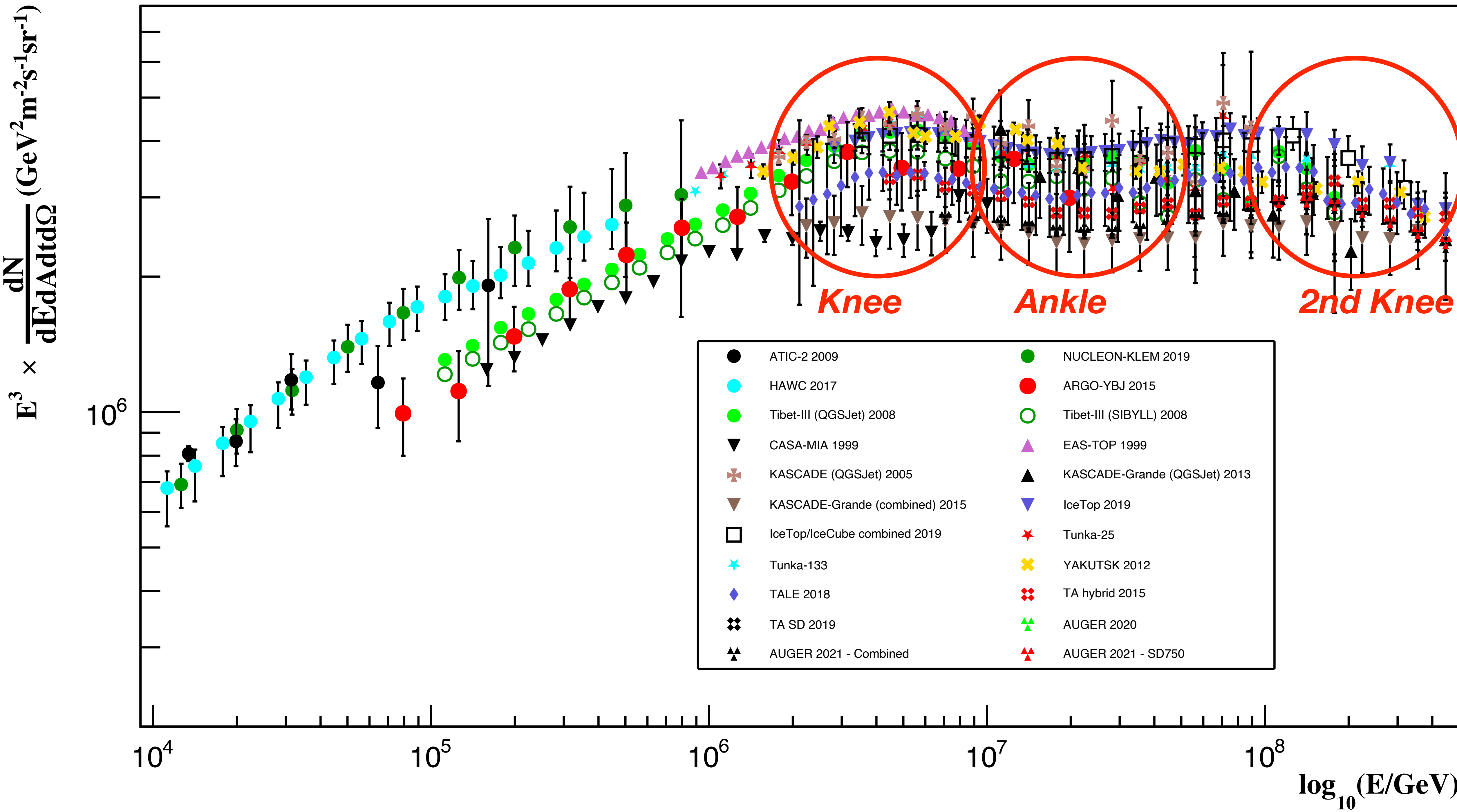

Open questions in Cosmic Ray Physics

Much of CR research in the past century has been devoted to answering a set of classical questions:

(1) Which ***classes of sources*** contribute to the CR flux in different energy ranges? How many types of sources provide a significant contribution to the overall CR flux?

(2) Which sources are capable of reaching the ***highest particle energies and how***?

(3) Which are the relevant processes responsible for CR ***confinement*** in the Galaxy?

(4) Where is the ***transition between Galactic and EG-CRs*** and how can we explain the well-known features such as knee, second knee, ankle?

(5) What is the origin of the difference between the ***chemical composition*** of CRs and the solar one?

A description

The CR spectrum can be described as an ensemble of adjacent energy intervals, where the energy distribution is a simple power law, separated by *"spectral features"*, that is narrow regions where the slope (or spectral index) of the flux undergoes a rapid change.

The features can be softenings or hardenings of the spectrum, and appear as "knee–like" or "ankle–like" in the usual log–log graphic representation of the spectrum.

$$\phi(E) = K_0 \left(\frac{E}{E_0}\right)^{-\alpha_1} \left[1 + \left(\frac{E}{E_b}\right)^{\frac{1}{w}}\right]^{-(\alpha_2-\alpha_1)\,w}$$

The absolute flux K_0 and the spectral index α_1 quantify the power law. The flux above the cut-off energy E_b is modeled by a second and steeper power law. The parameters α_2, the slope beyond the knee, and $w > 0$, the smoothness of the transition from the first to the second power law, characterize the change in the spectrum at the cut-off energy. A value $w = 0$ corresponds to a steep transition that soften with increasing values[?].

P. Lipari / Astroparticle Physics 97 (2018) 197–204

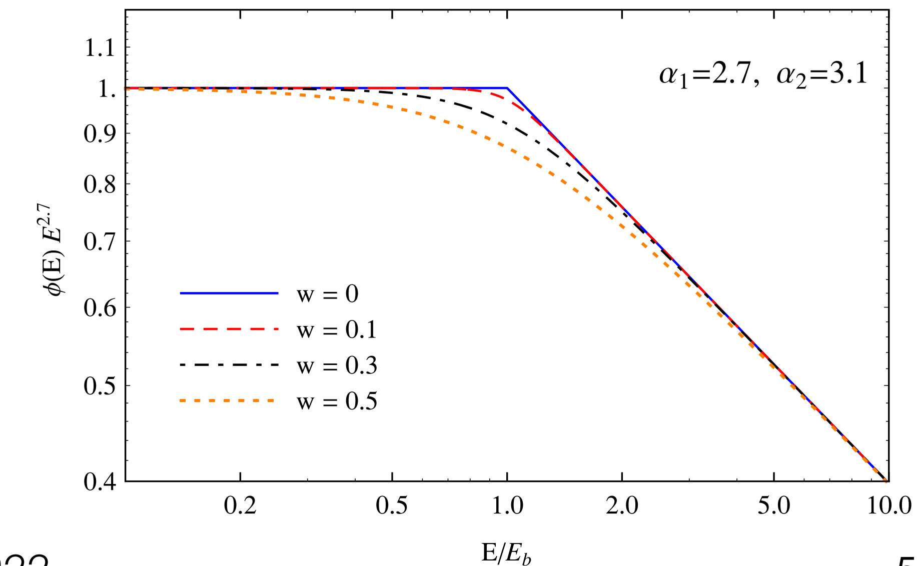

The knee region by selected experiments

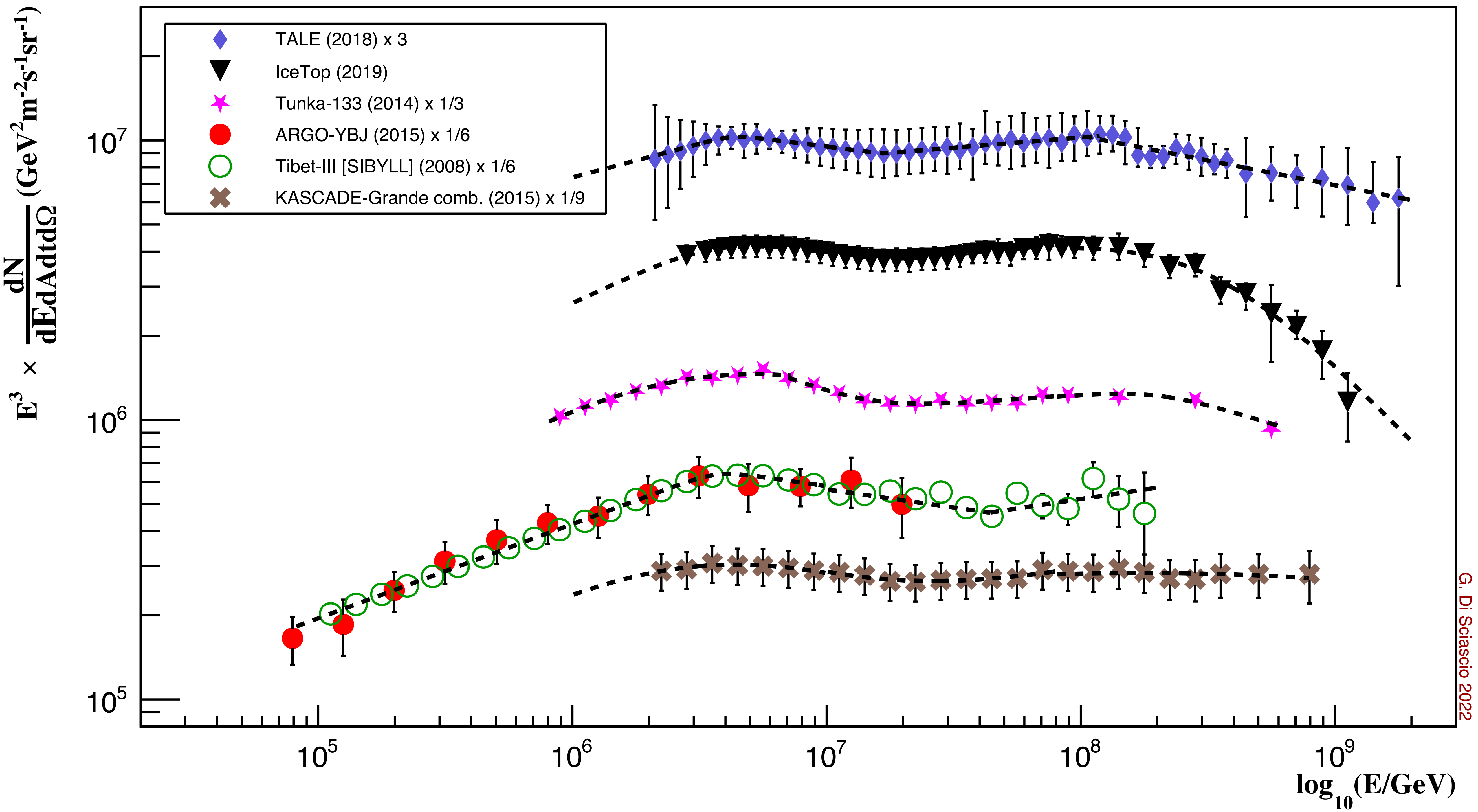

Fits to the all-particle spectra in the knee region

Table 1: Fits to the all–particle CR spectra in the energy range $8 \cdot 10^4$ to $2 \cdot 10^9$ GeV.

(a) Parameters for the first Knee.

Experiment	E_{b1} (PeV)	α_1	α_2	w_1
TALE	4.26 ± 1.65	2.76 ± 0.18	3.11 ± 0.07	0.07 ± 0.18
IceTop	3.30 ± 1.23	2.48 ± 0.08	3.12 ± 0.12	0.30 ± 0.46
Tunka–133	4.18 ± 0.83	2.76 ± 0.09	3.20 ± 0.04	0.15 ± 0.16
ARGO–YBJ/Tibet ASγ	3.72 ± 0.03	2.66 ± 0.01	3.13 ± 0.01	0.11 ± 0.01
Kascade–Grande	2.10 ± 0.87	2.47 ± 0.04	3.16 ± 0.14	0.60 ± 0.51

(b) Parameters for the ankle feature.

Experiment	E_{b2} (PeV)	α_2	α_3	w_2
TALE	16.61 ± 8.36	3.11 ± 0.05	2.93 ± 0.05	0.07 ± 0.05
IceTop	18.66 ± 6.65	3.12 ± 0.12	2.92 ± 0.05	0.05 ± 0.05
Tunka–133	18.70 ± 3.88	3.20 ± 0.04	2.96 ± 0.05	0.17 ± 0.45
ARGO–YBJ/Tibet ASγ	43.8 ± 4.81	3.13 ± 0.01	2.86 ± 0.05	0.01 ± 0.01
Kascade–Grande	18.01 ± 17.4	3.16 ± 0.14	2.83 ± 0.45	0.66 ± 1.74

(c) Parameters for the second Knee.

Experiment	E_{b3} (PeV)	α_3	α_4	w_3
TALE	104.5 ± 40.0	2.93 ± 0.05	3.18 ± 0.06	0.02 ± 0.02
IceTop	168.4 ± 17.4	2.92 ± 0.05	3.50 ± 0.40	0.25 ± 0.16
Tunka–133	238.2 ± 56.8	2.96 ± 0.05	3.34 ± 0.19	0.05 ± 0.50
Kascade–Grande	274.5 ± 122	2.83 ± 0.45	3.20 ± 0.13	2.47 ± 0.97

Galactic CRs: mainstream interpretation

- CRs below 10^{17} eV are predominantly Galactic.

- *Standard paradigm*: Galactic CRs accelerated in SN shocks via 1^0 order Fermi mechanism

- Somehow released into the ISM, CRs are *diffusively confined* within a magnetized *Galactic halo*

- CRs reside from some time before escaping the Galaxy

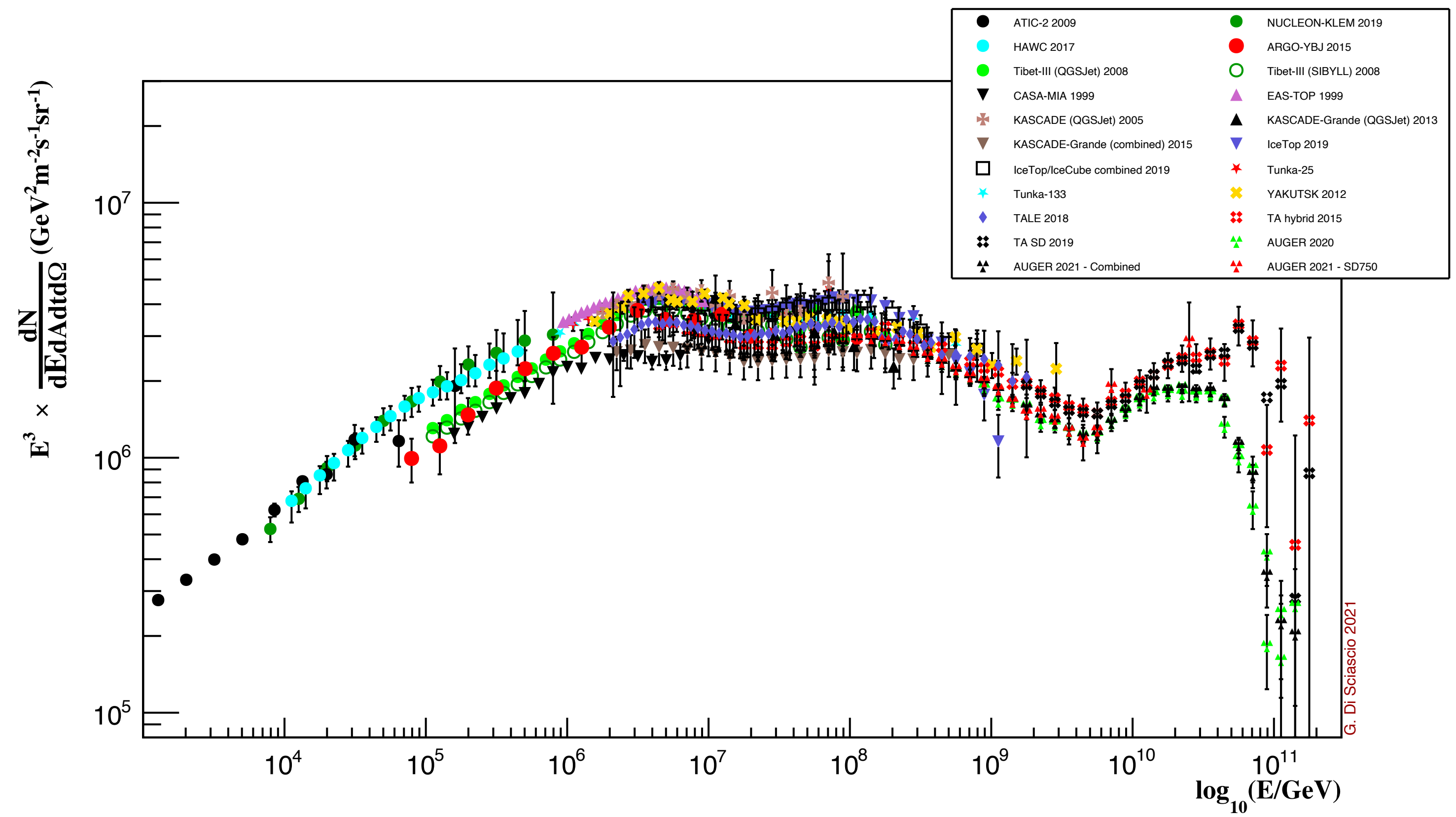

- Galactic CRs are scrambled by galactic magnetic field over very long time ➜ arrival direction *mostly isotropic*

Galactic CRs: mainstream interpretation

- CRs below 10^{17} eV are predominantly Galactic.

- ***Standard paradigm***: Galactic CRs accelerated in SN shocks via 1^0 order Fermi mechanism
- Somehow released into the ISM, CRs are ***diffusively confined*** within a magnetized ***Galactic halo***
- CRs reside from some time before escaping the Galaxy

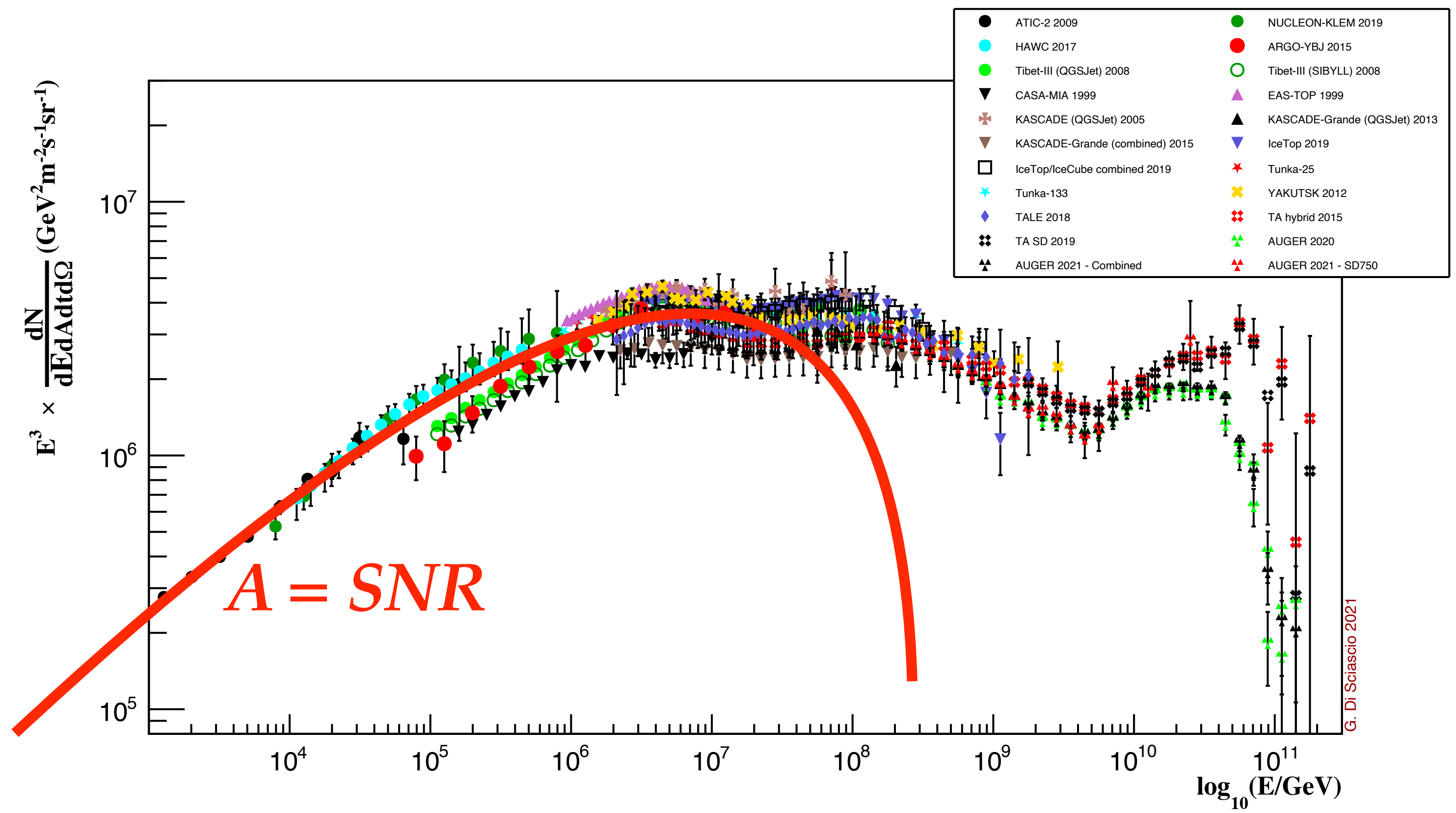

- Galactic CRs are scrambled by galactic magnetic field over very long time ➜ arrival direction ***mostly isotropic***

Galactic CRs: mainstream interpretation

- CRs below 10^{17} eV are predominantly Galactic.

- *Standard paradigm*: Galactic CRs accelerated in SN shocks via 1^0 order Fermi mechanism

- Somehow released into the ISM, CRs are *diffusively confined* within a magnetized *Galactic halo*

- CRs reside from some time before escaping the Galaxy

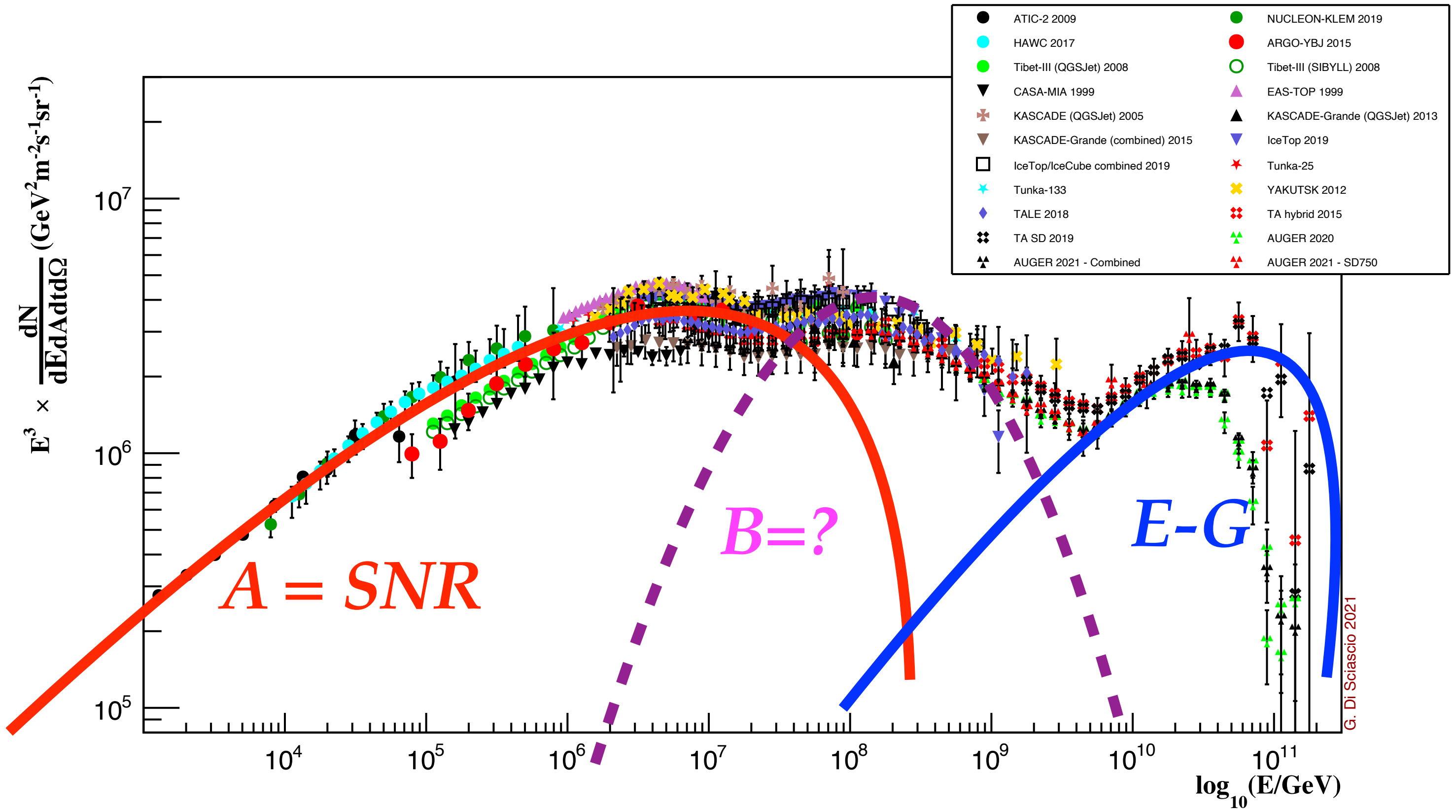

- Galactic CRs are scrambled by galactic magnetic field over very long time ➜ arrival direction *mostly isotropic*

- Transition to *extragalactic* CRs occurs somewhere between 10^{17} and 10^{19} eV

The 'knee' in the CR energy spectrum

- Why should we study CRs at the knee?
  - ★ E_{knee} → *most extreme Galactic accelerators* of CR protons

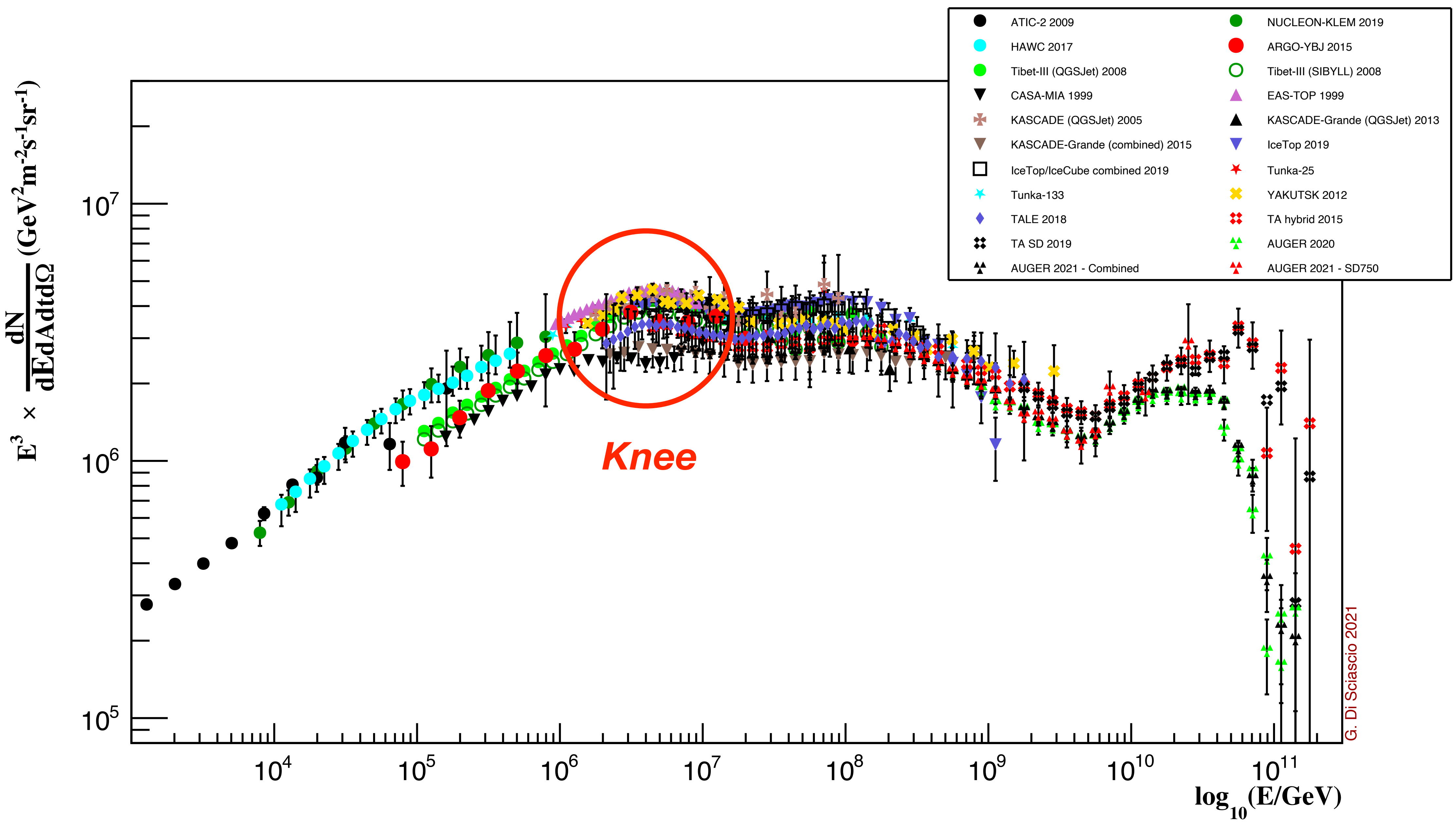

The 'knee' in the CR energy spectrum

- Why should we study CRs at the knee?
  - ★ *E_{knee}* → ***most extreme Galactic accelerators*** of CR protons

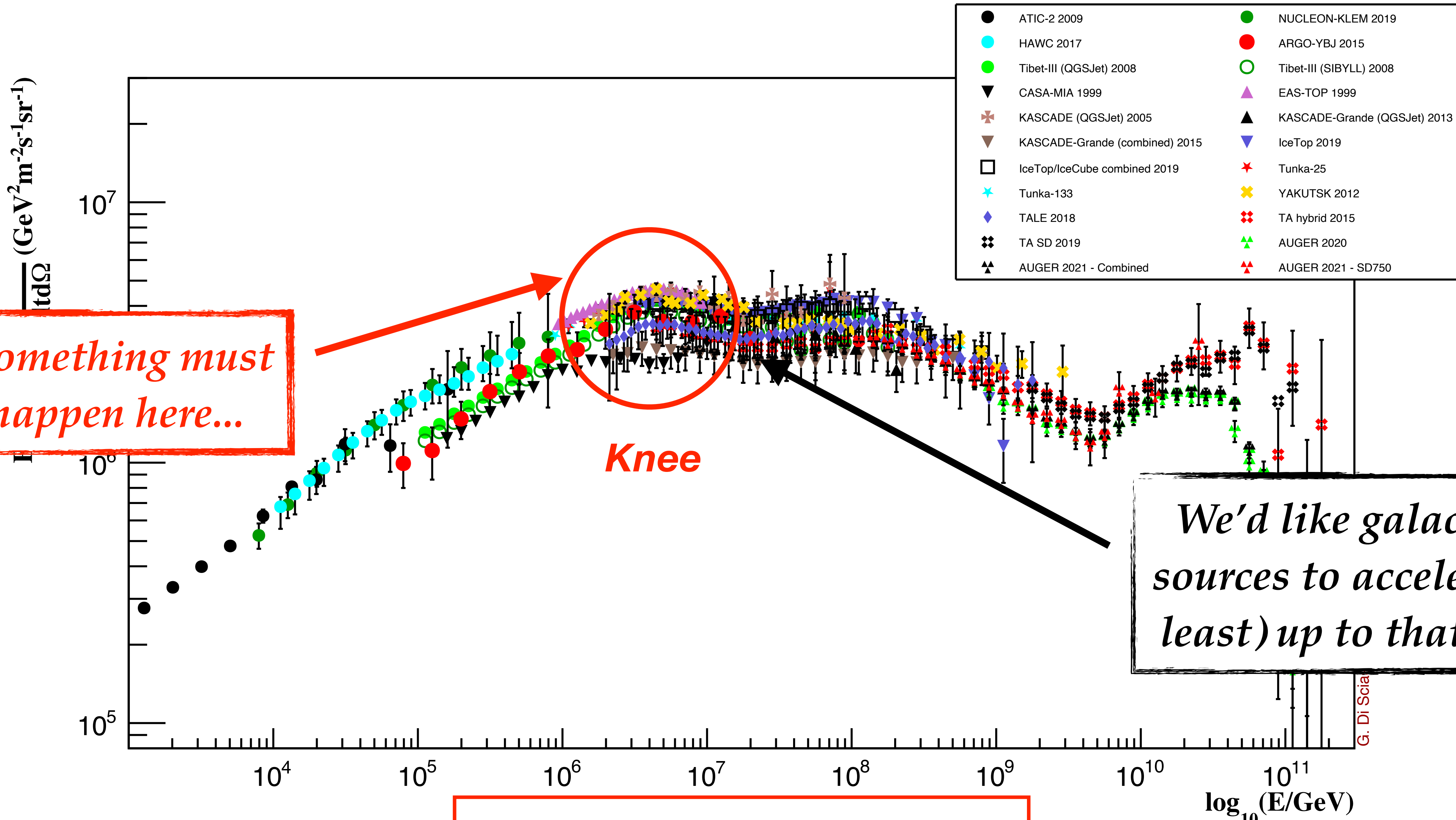

Something must happen here...

We'd like galactic CR sources to accelerate (at least) up to that energy

We would like SNRs to be Galactic PeVatrons…!

LSA energy dependence: IceCube/IceTop

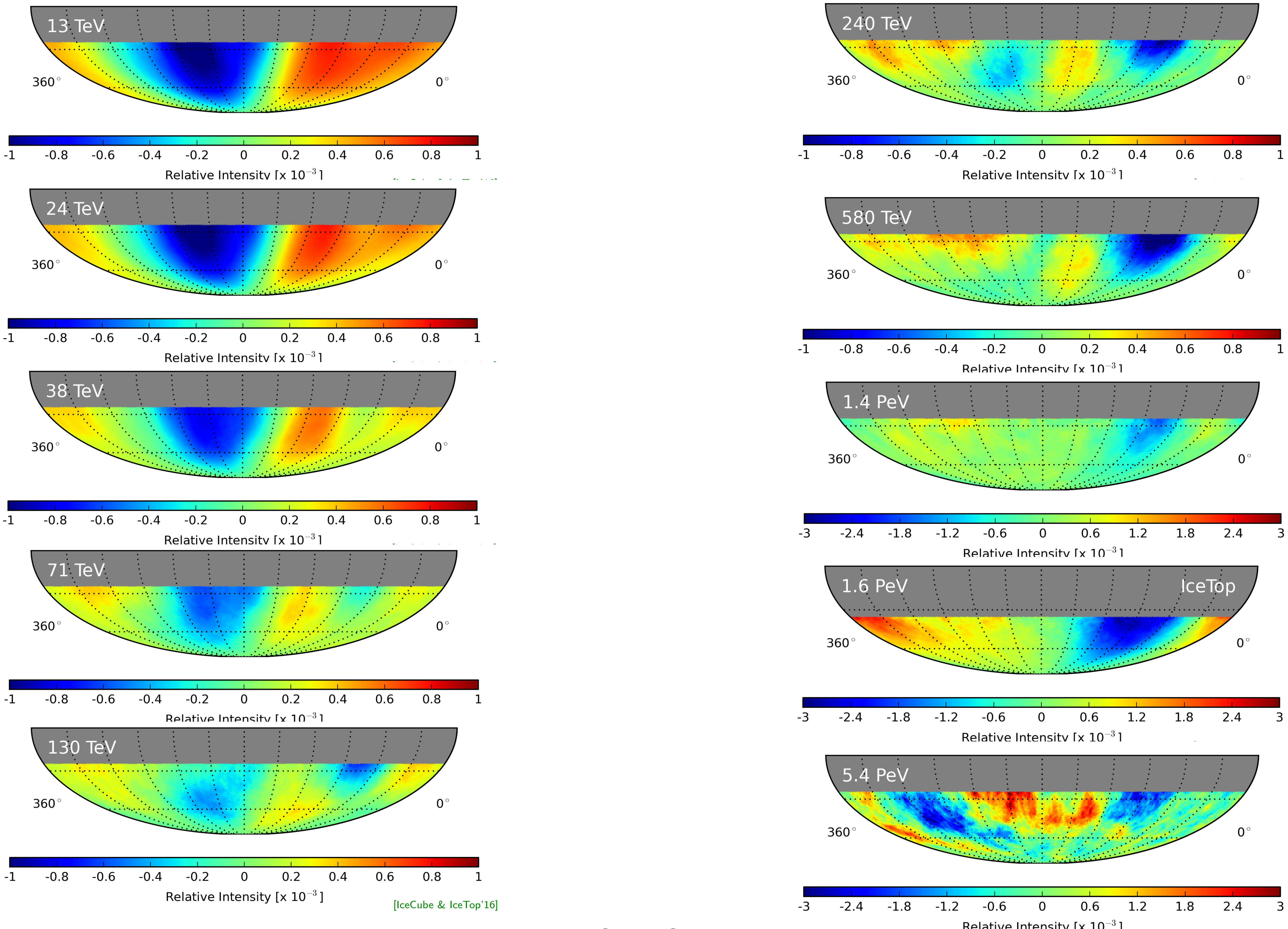

LSA energy dependence: IceCube/IceTop

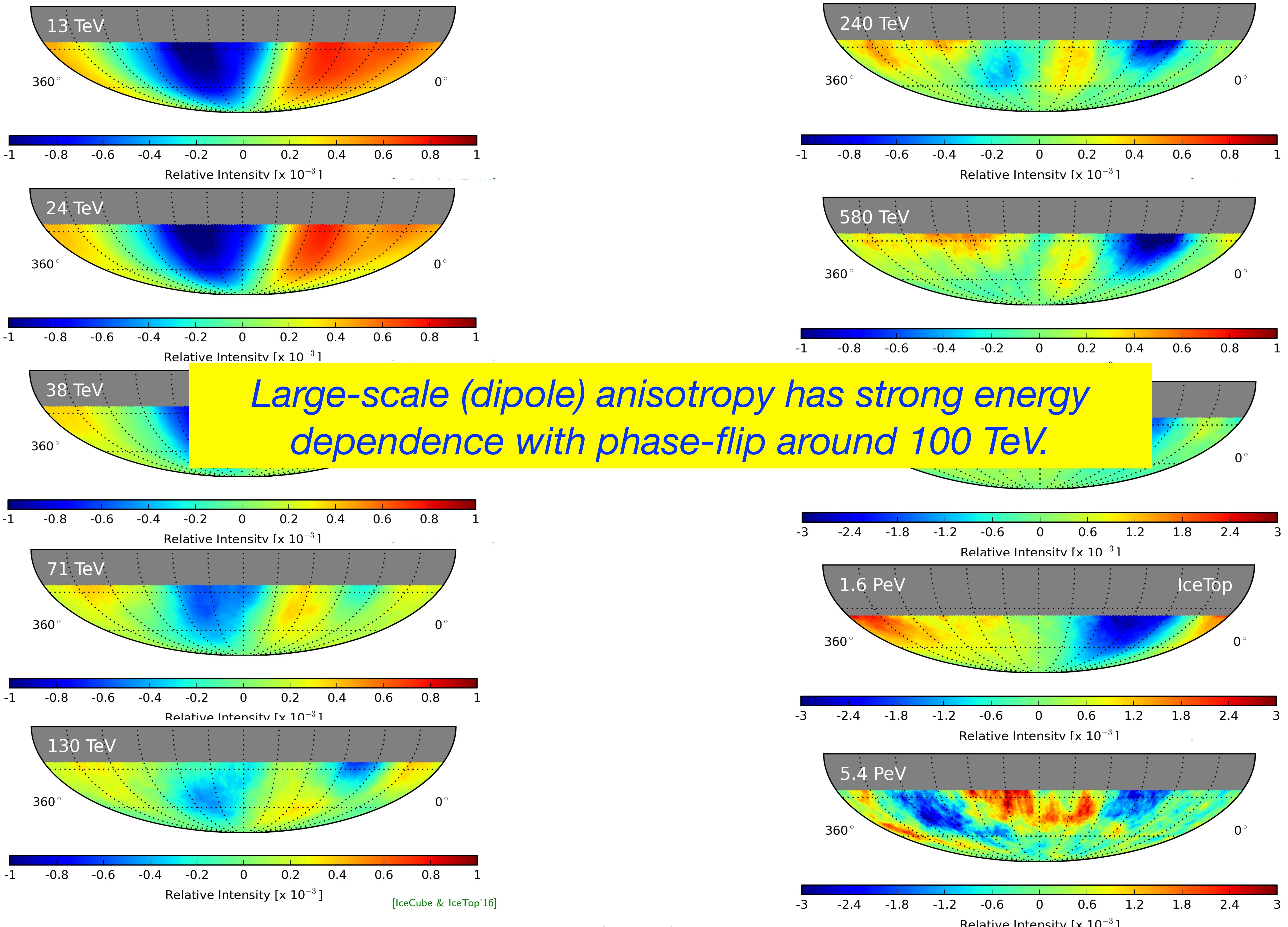

Large-scale (dipole) anisotropy has strong energy dependence with phase-flip around 100 TeV.

The origin of the 'knee'

In ***1961 B. Peters*** postulated a ***rigidity cutoff model.***

B. Peters, Nuovo Cimento 22 (1961) 800

$$E_{max} \approx Ze \cdot L \cdot B$$

$\rightarrow$ E_{total} **(knee) ~ Z × R(knee)**

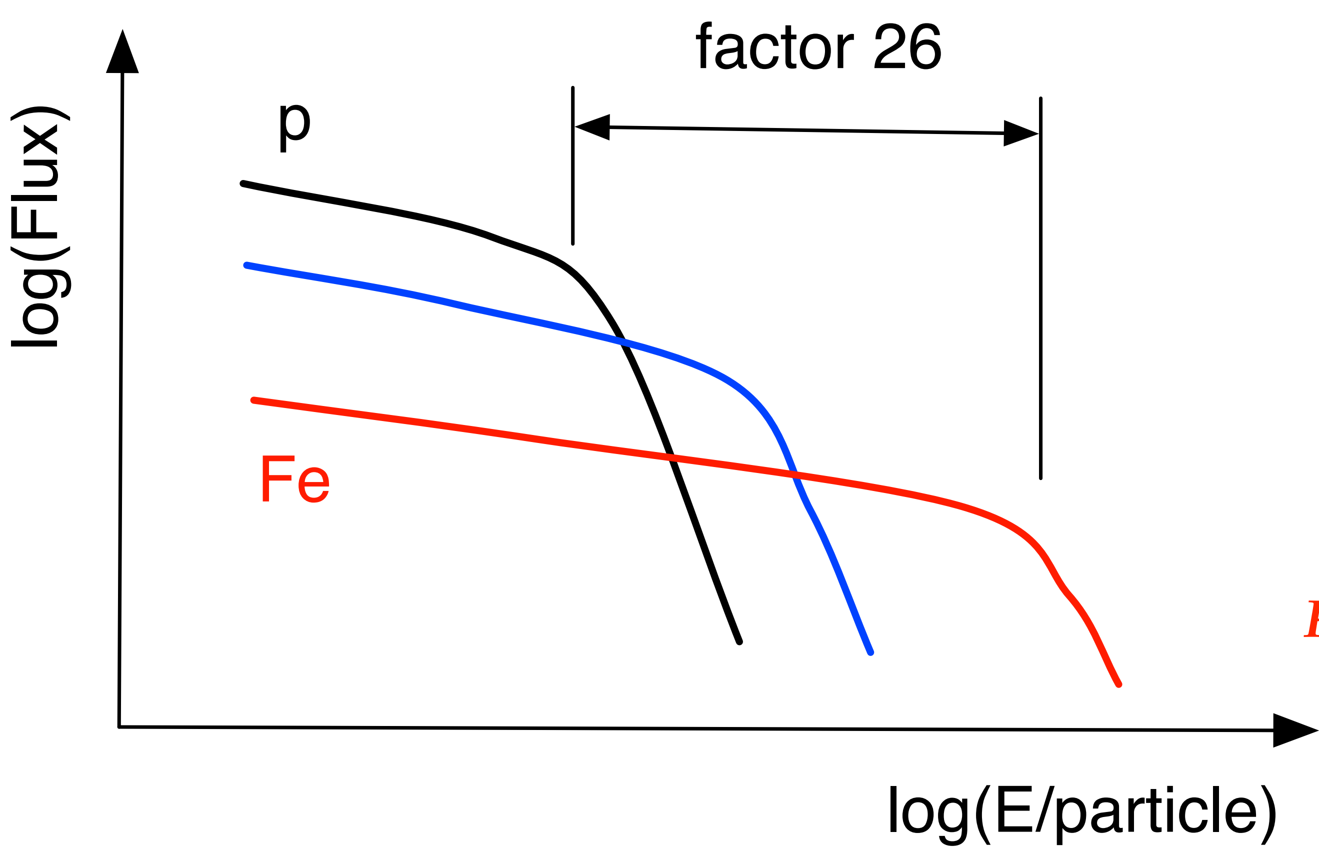

If E_{max} ***depends on B*** then p disappear first, then He, C, O, etc

$$R_L(\text{p}, \mathbf{E}) = R_L(\text{Fe}, \mathbf{26\ E})$$

Fe confined longer ➜ *accelerated to higher energies*

- Not only does the spectrum become steeper due to such a cutoff but also heavier
- <A> should begin to decrease again for E > 30 x E_{knee} ≈ 100 PeV

The standard model

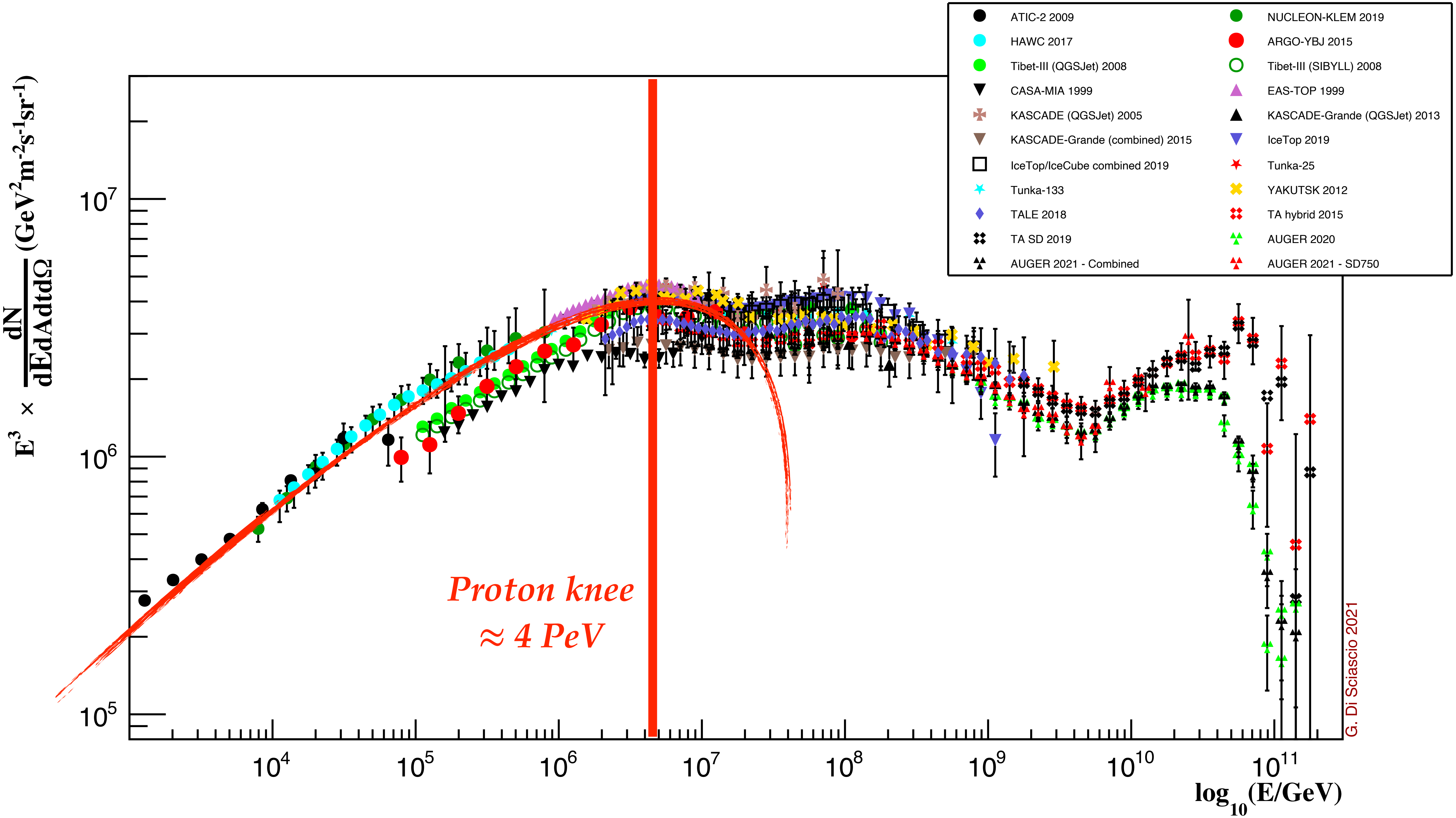

The standard model

Determining elemental composition in the knee energy region is crucial to understand where Galactic CR spectrum ends

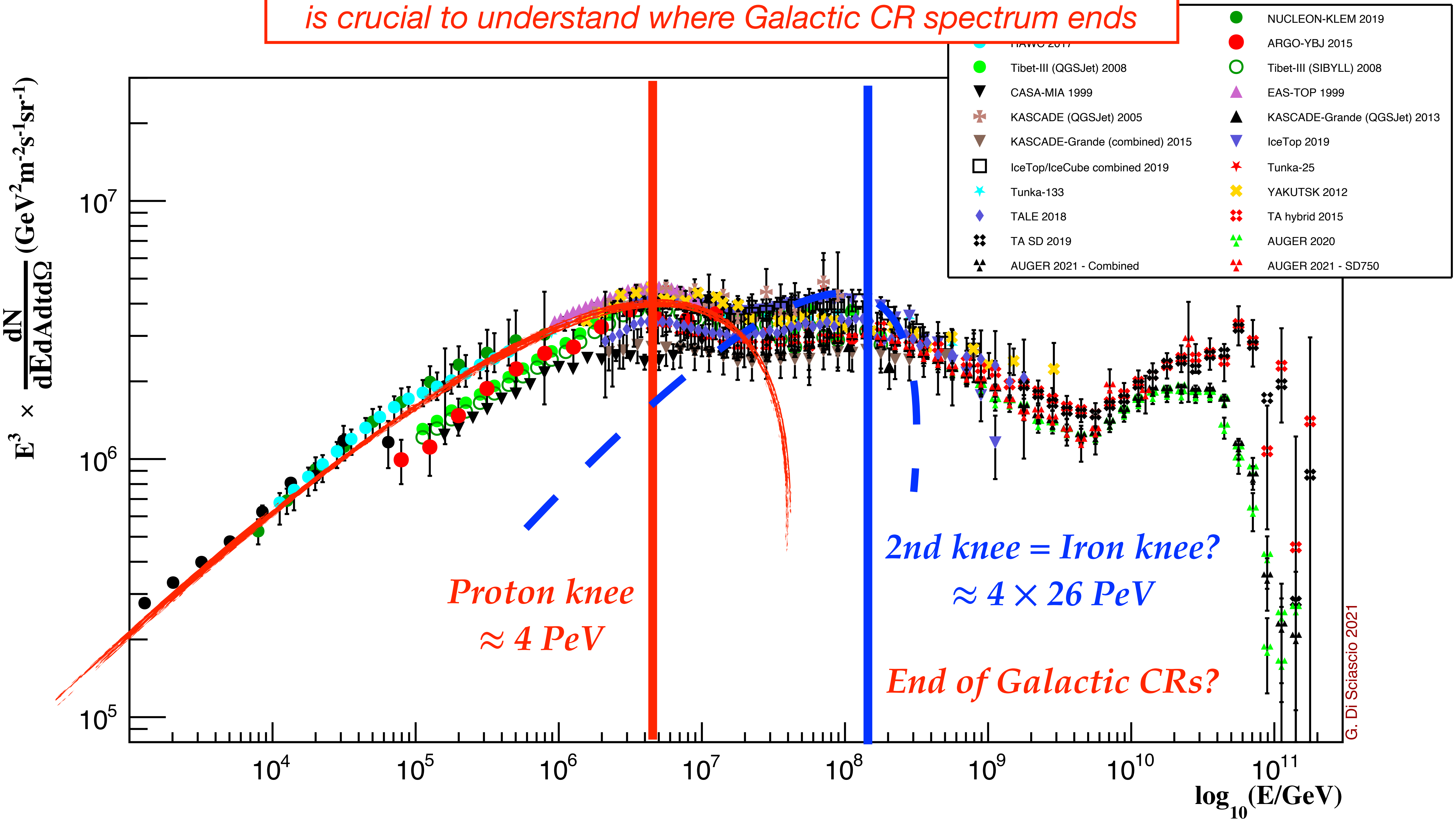

Conflicting results: ARGO-YBJ and Tibet ASγ

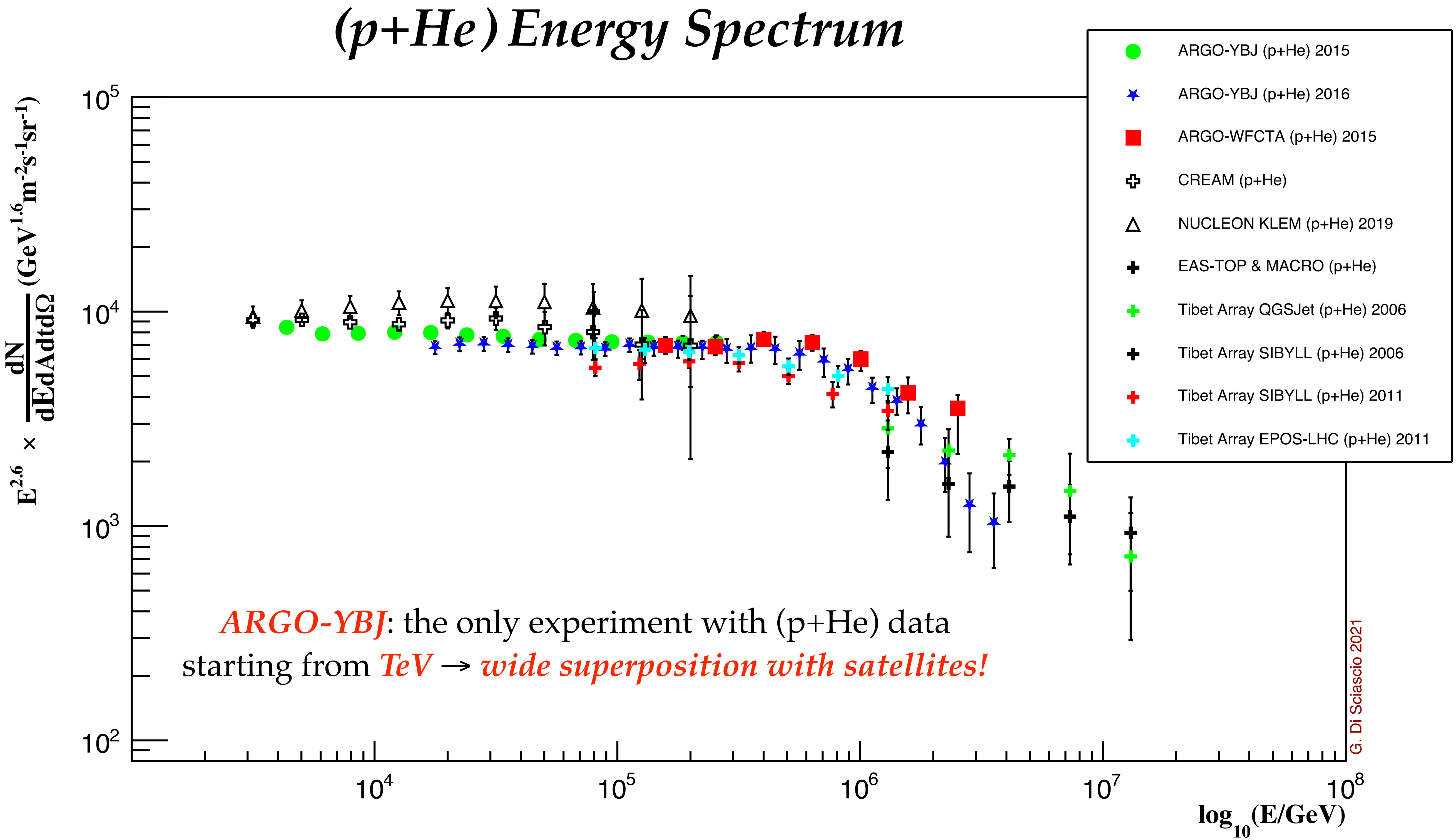

Conflicting results: ARGO-YBJ and Tibet ASγ

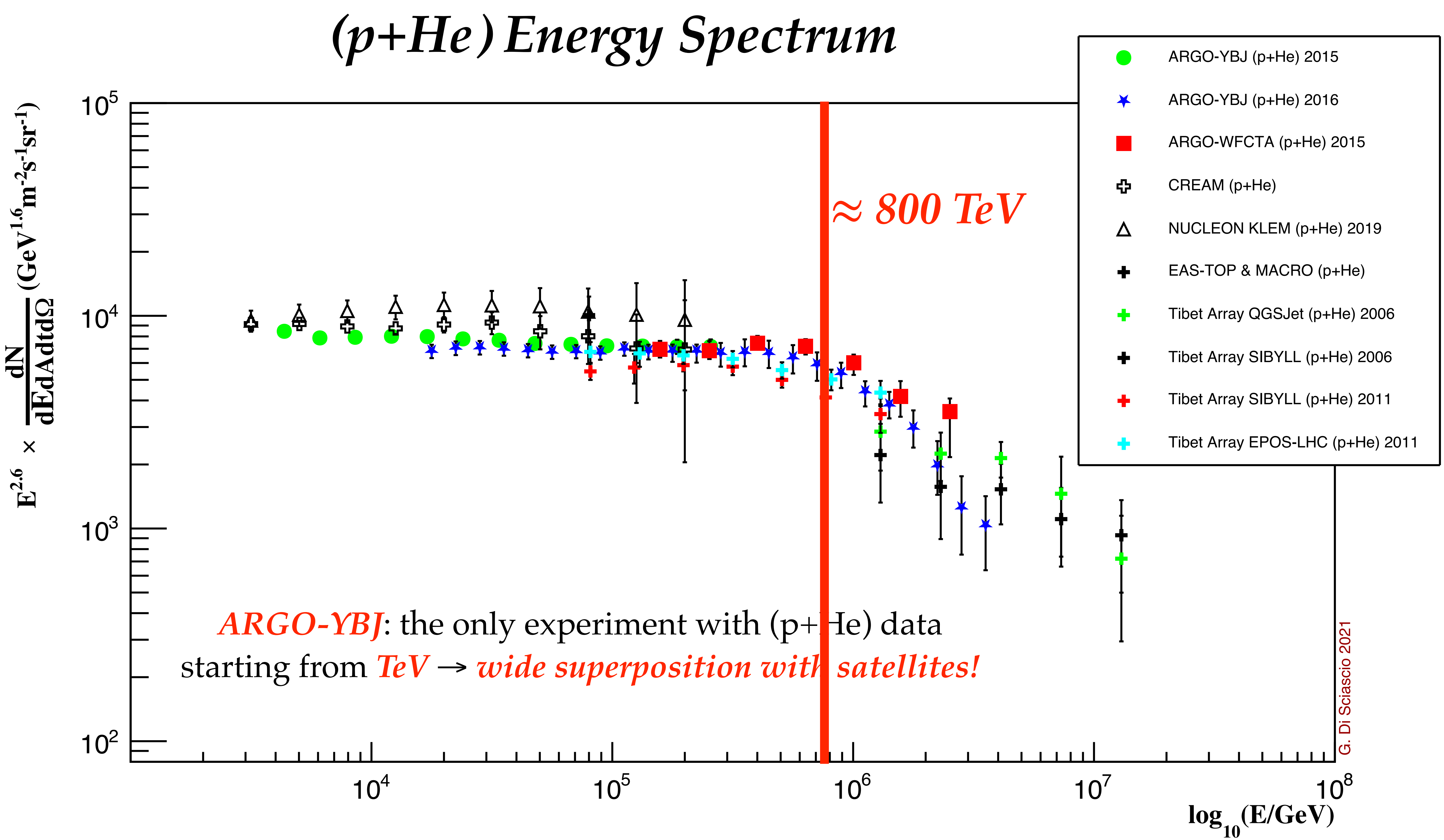

ARGO-YBJ: the only experiment with (p+He) data starting from *TeV* → *wide superposition with satellites!*

The ARGO-YBJ light knee

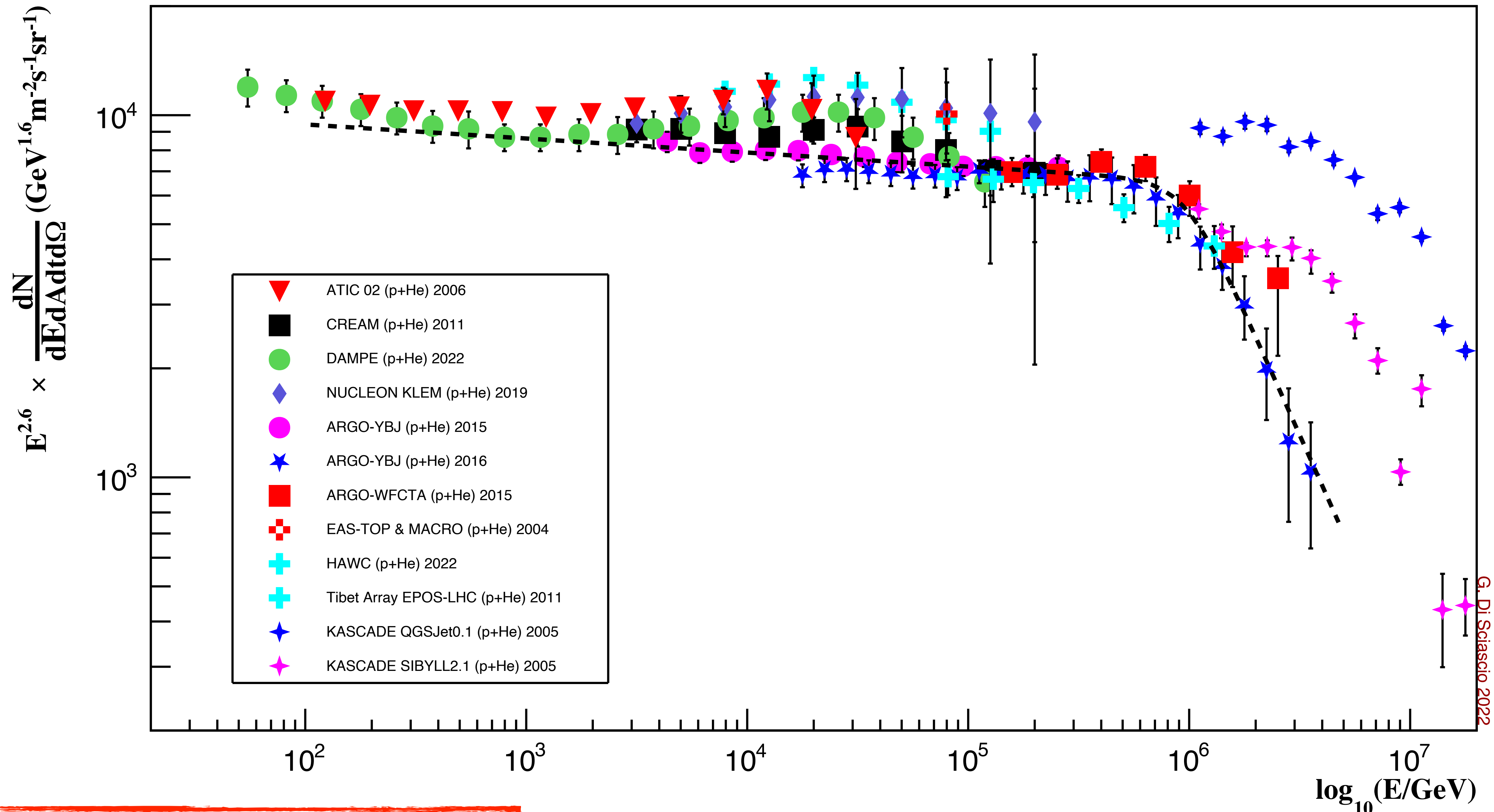

Break energy = 914 ± 260 TeV

$\alpha_1 = 2.64 \pm 0.01$

$\alpha_2 = 3.85 \pm 0.48$

$w = 0.18 \pm 0.14$

Knee region: quite confusing situation

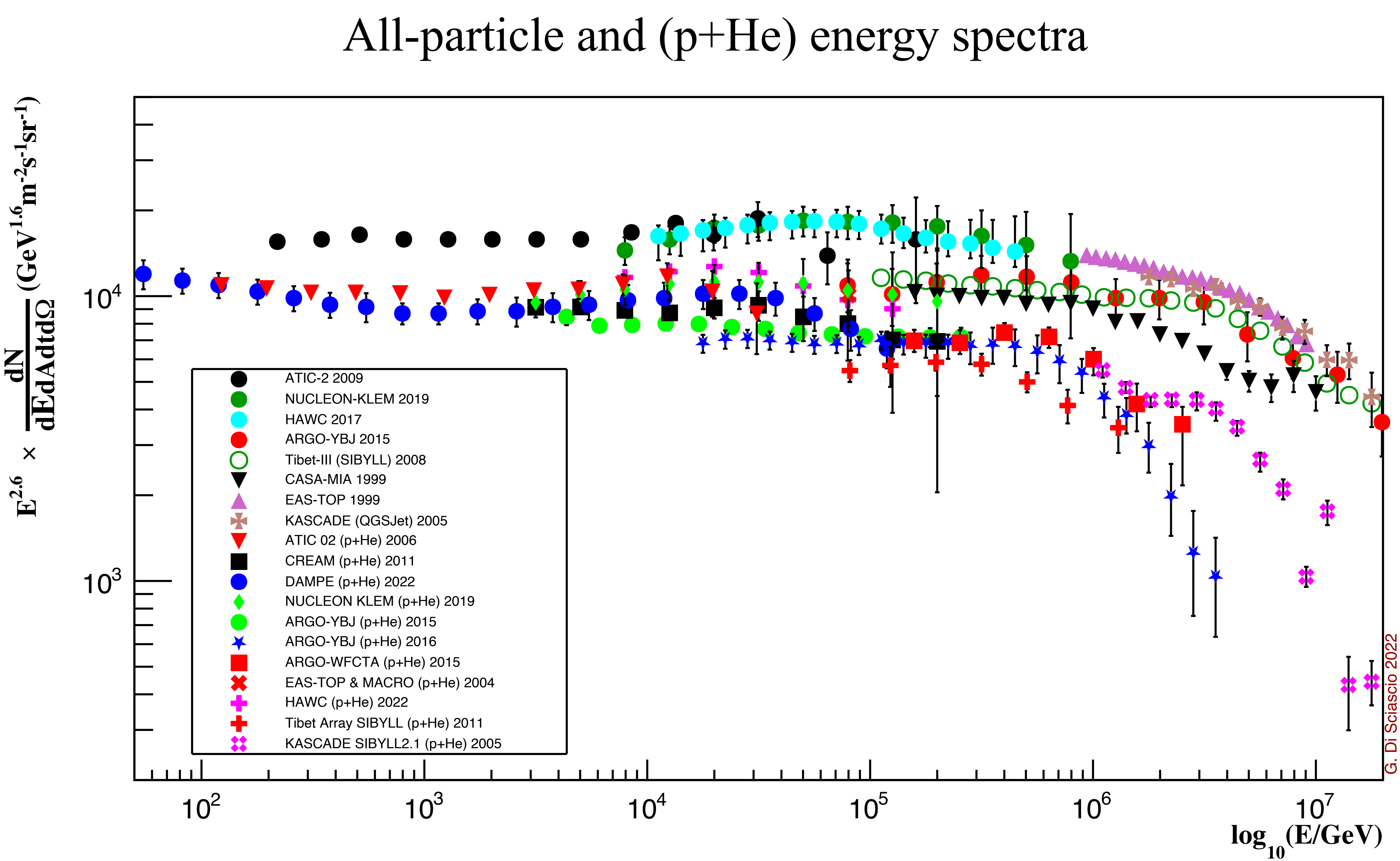

Maximum energy: in numbers…

$$E_{\kappa}^{max} \approx 3 \times 10^{12} Z \left(\frac{B}{\mu\mathrm{G}}\right)\left(\frac{U}{1000\ \mathrm{km/s}}\right)\left(\frac{L}{\mathrm{pc}}\right)\ \mathrm{eV} \quad \approx 100\ \mathrm{TeV}$$

magnetic field: ~ 3 ***velocity: ~ 10*** ***dimension: ~ 3***

well below the knee!!!

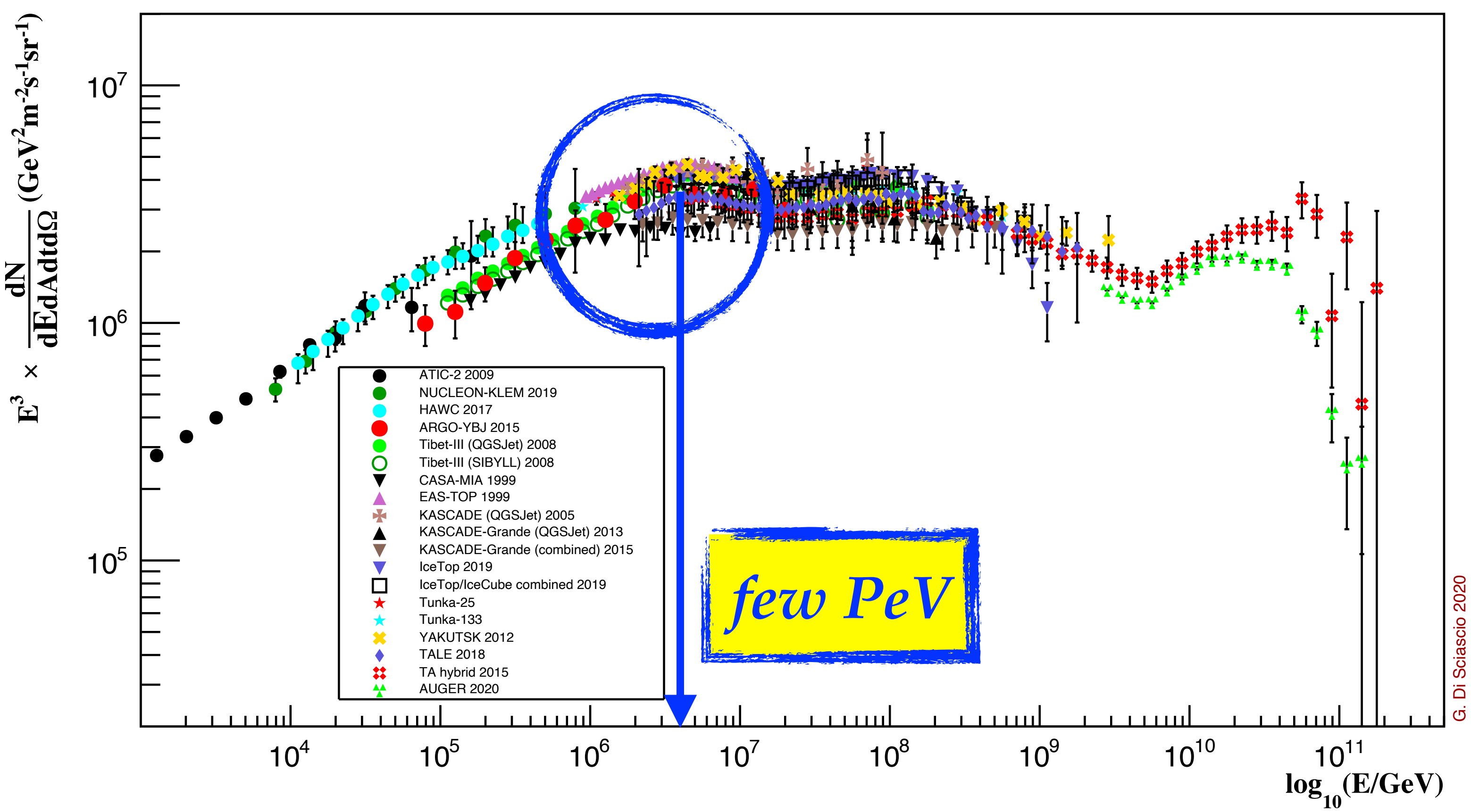

$$E_{max} \approx B\, u\, R$$

The only way is to increase B

→ *magnetic field amplification* at shocks (Bell, 2004)?

But can SNRs accelerate enough protons to the knee?

Gamma – Cosmic Ray connection

$$E_\gamma \approx \frac{E_p}{10}$$

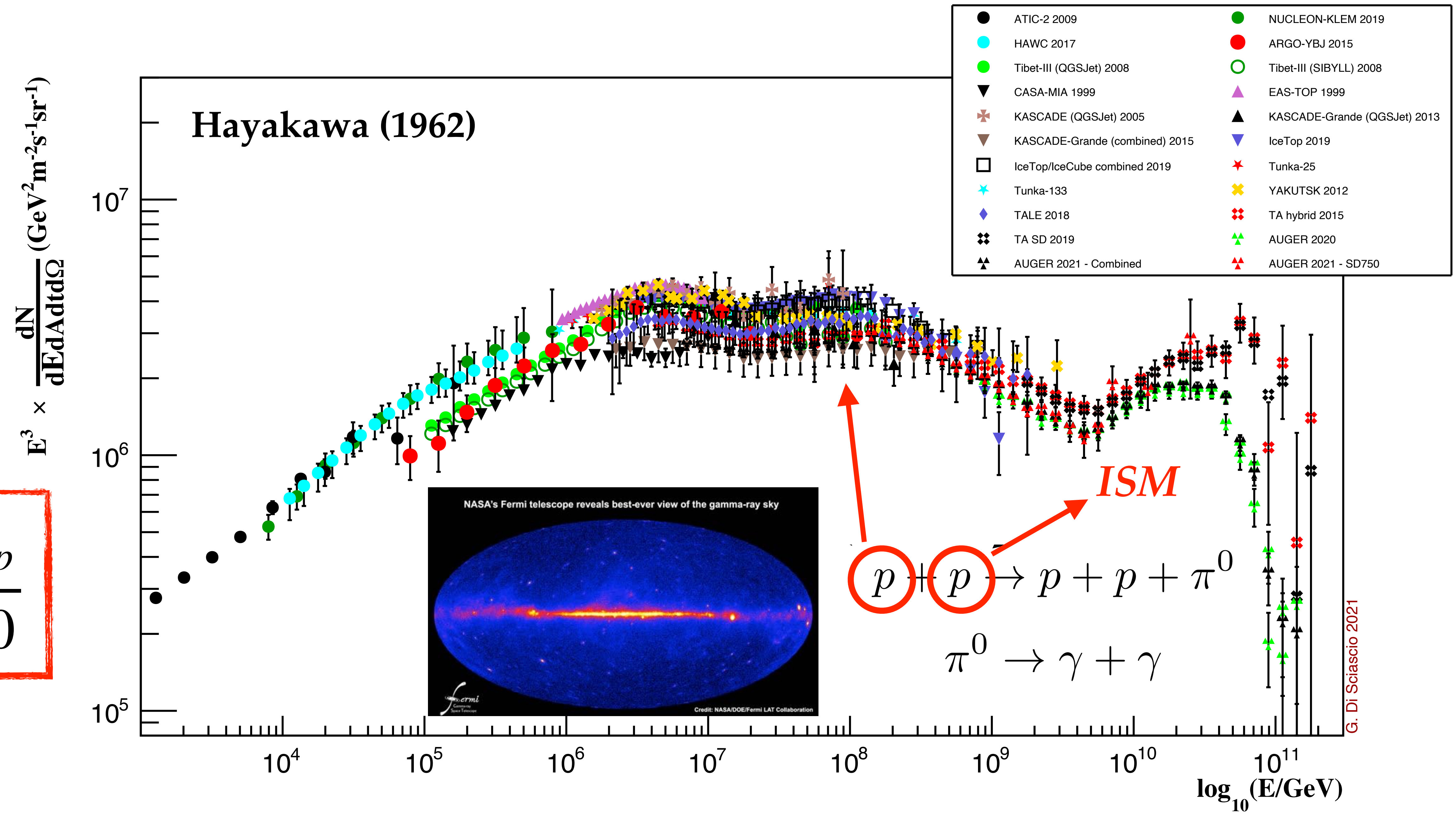

Gamma – Cosmic Ray connection

$$E_\gamma \approx \frac{E_p}{10}$$

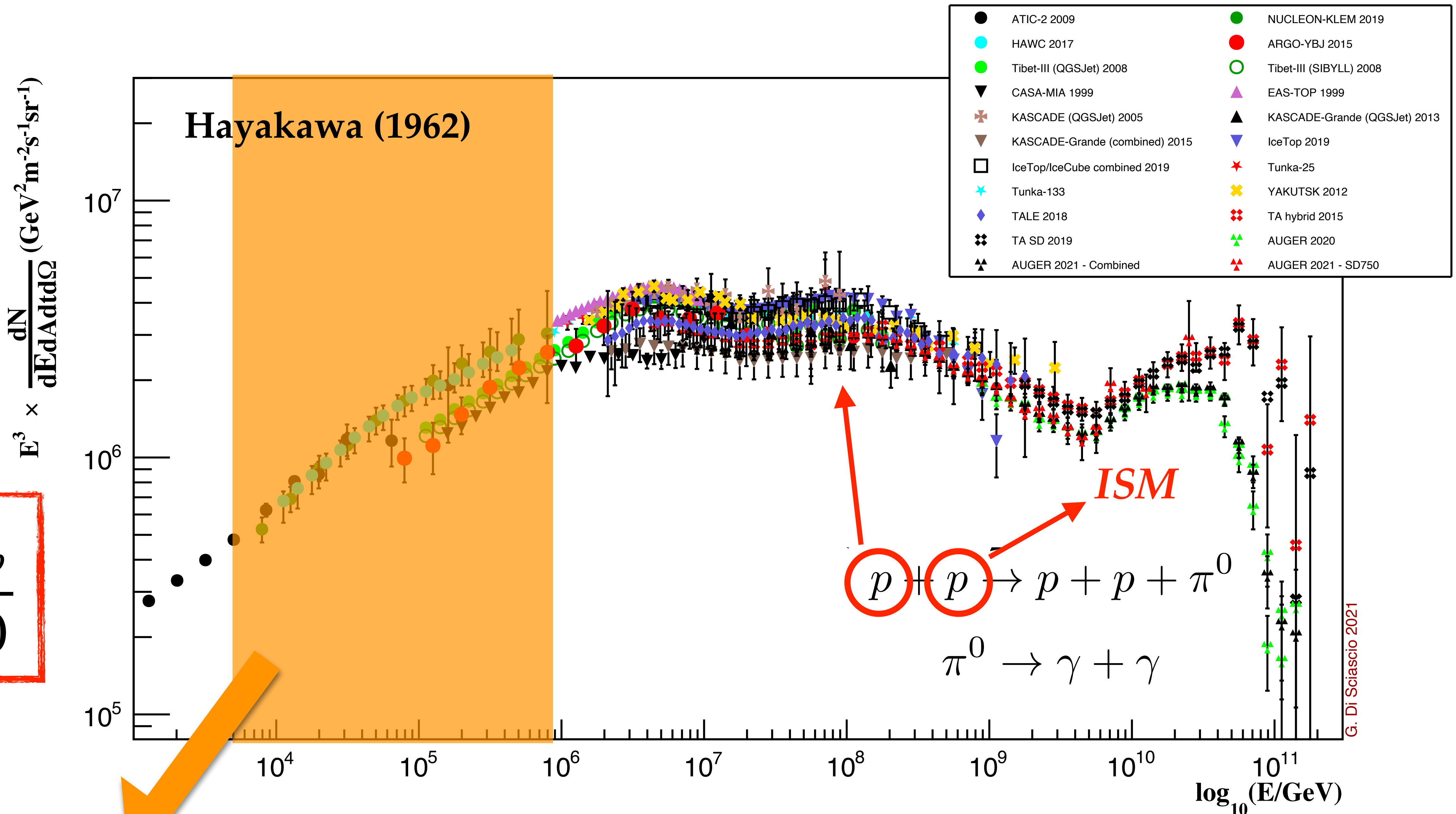

TeV Cosmic Rays?
→ Photons >100 GeV !

Satellites and Cherenkov Telescopes

Gamma – Cosmic Ray connection

$$E_\gamma \approx \frac{E_p}{10}$$

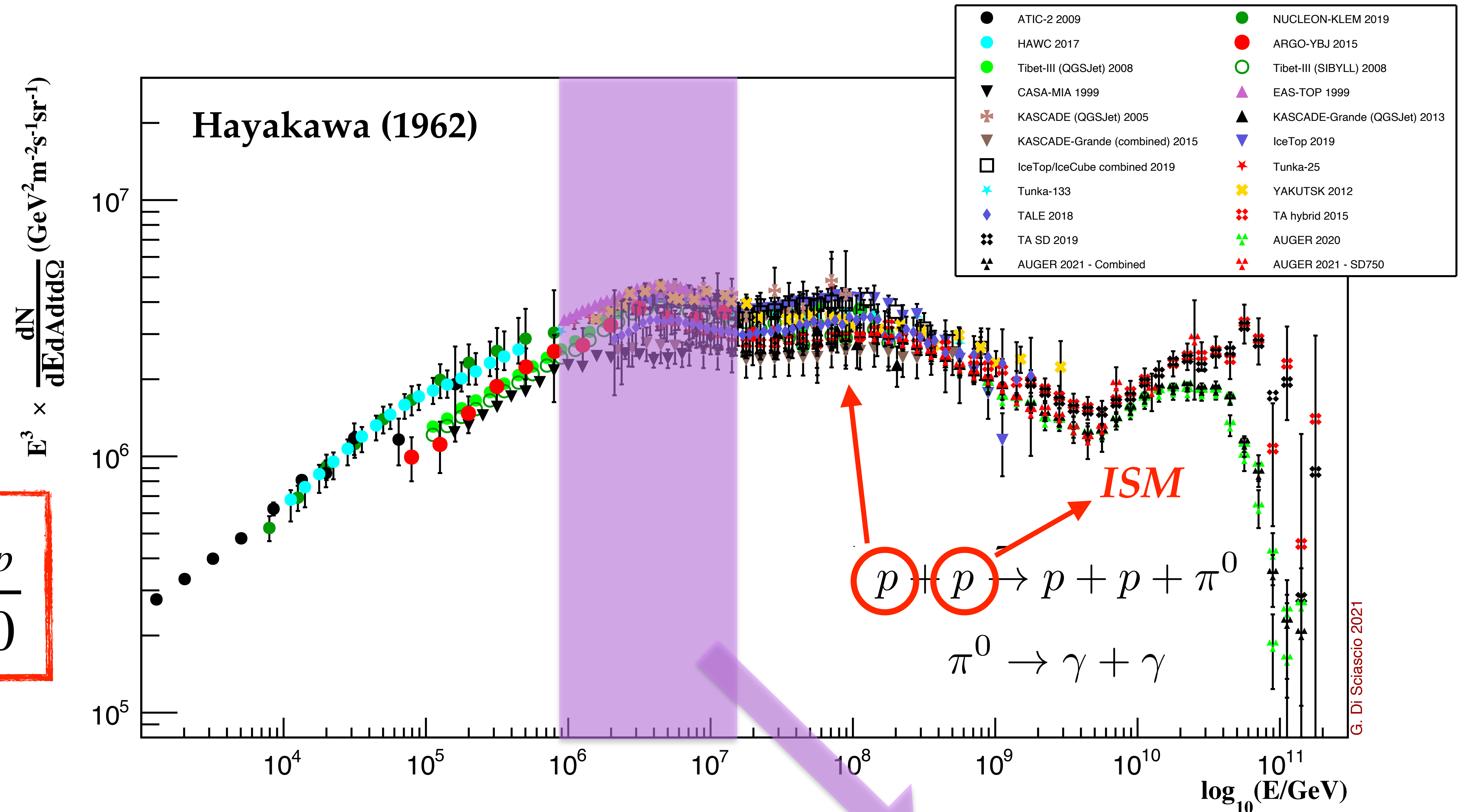

PeV Cosmic Rays?

→ Photons >100 TeV !

Air shower arrays

Production mechanisms for gamma rays

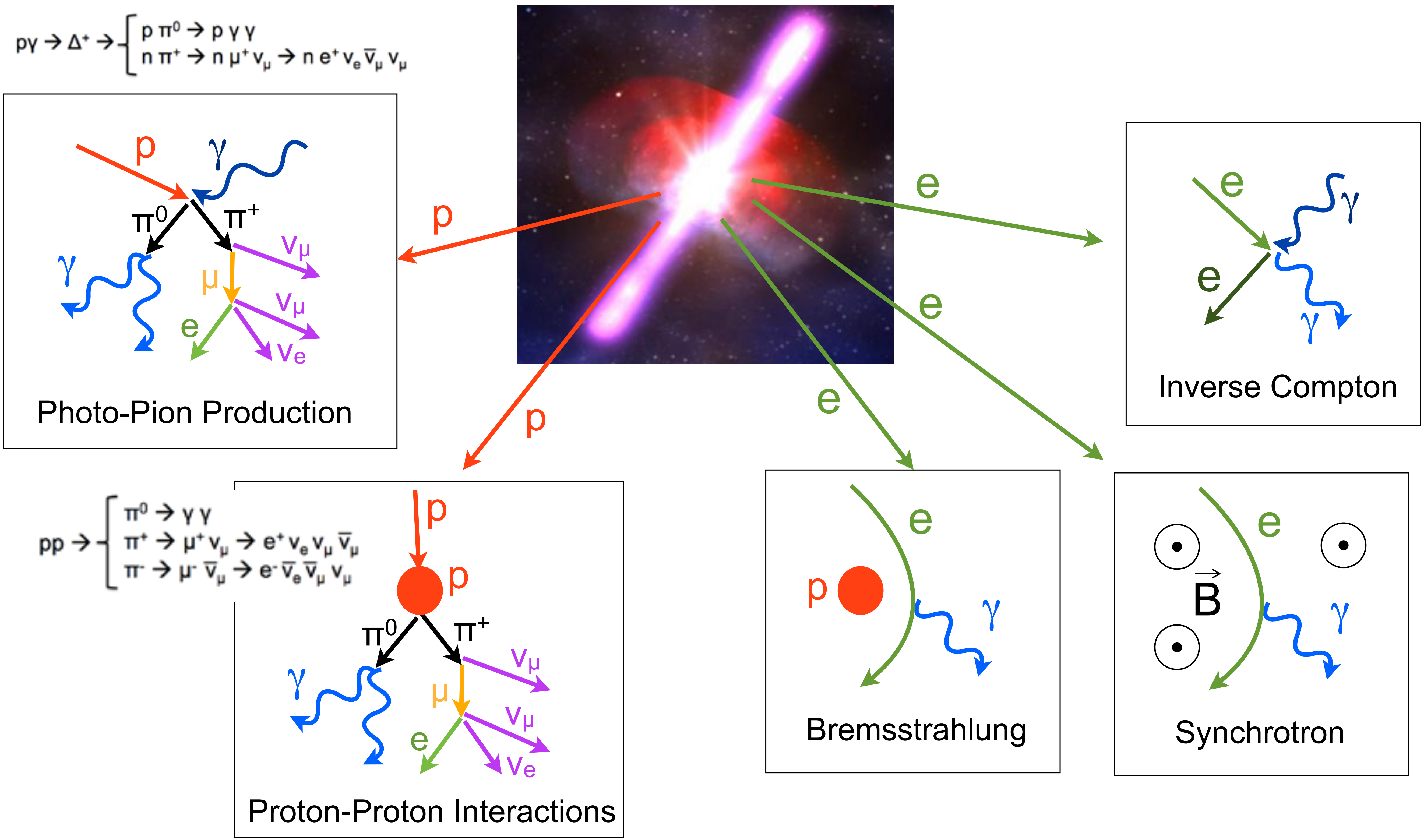

Production mechanisms for gamma rays

$p\gamma \rightarrow \Delta^+ \rightarrow \begin{cases} p\,\pi^0 \rightarrow p\,\gamma\,\gamma \\ n\,\pi^+ \rightarrow n\,\mu^+\nu_\mu \rightarrow n\,e^+\nu_e\bar{\nu}_\mu\,\nu_\mu \end{cases}$

$pp \rightarrow \begin{cases} \pi^0 \rightarrow \gamma\,\gamma \\ \pi^+ \rightarrow \mu^+\nu_\mu \rightarrow e^+\nu_e\,\nu_\mu\,\bar{\nu}_\mu \\ \pi^- \rightarrow \mu^-\bar{\nu}_\mu \rightarrow e^-\bar{\nu}_e\bar{\nu}_\mu\,\nu_\mu \end{cases}$

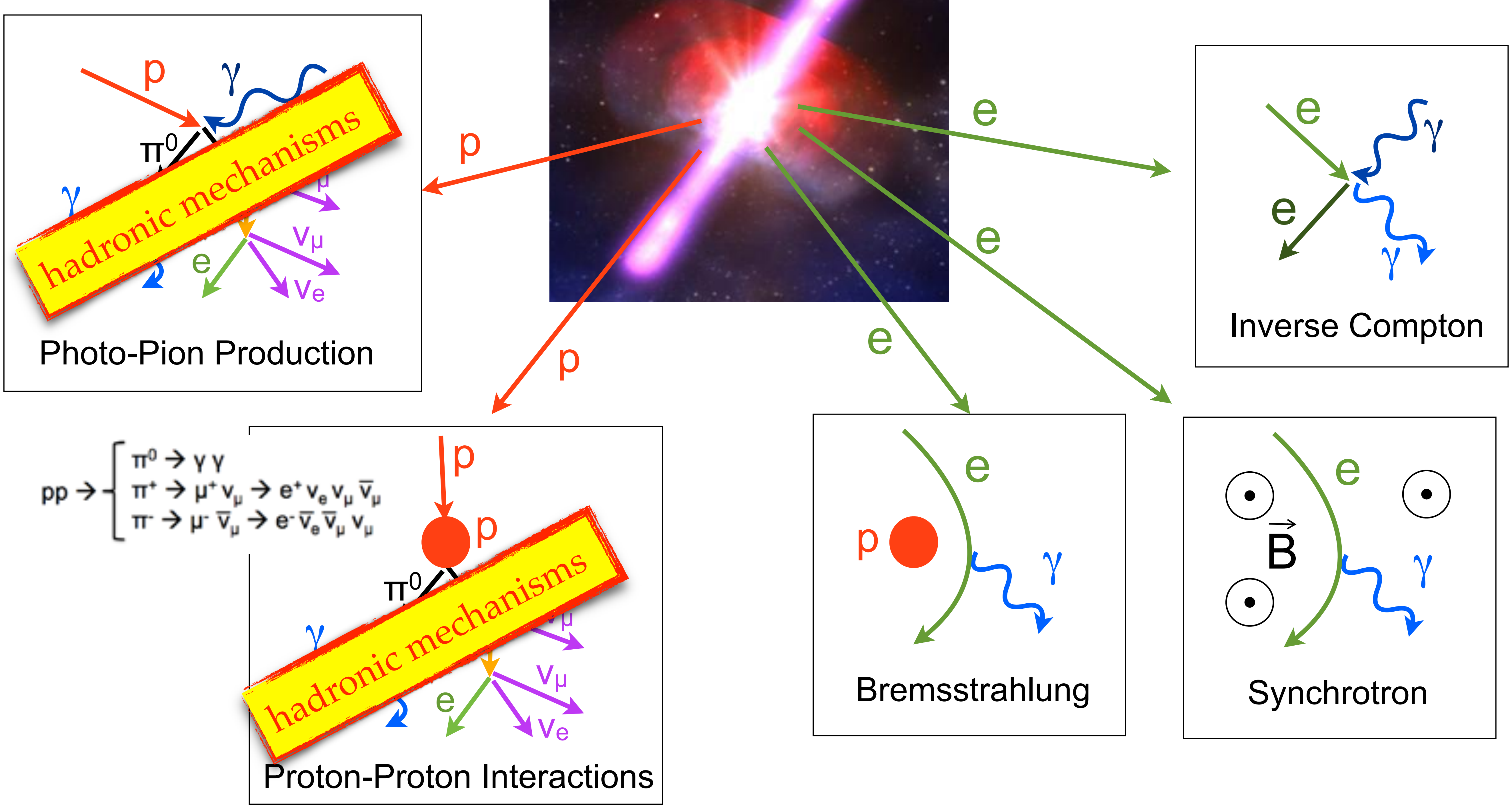

Production mechanisms for gamma rays

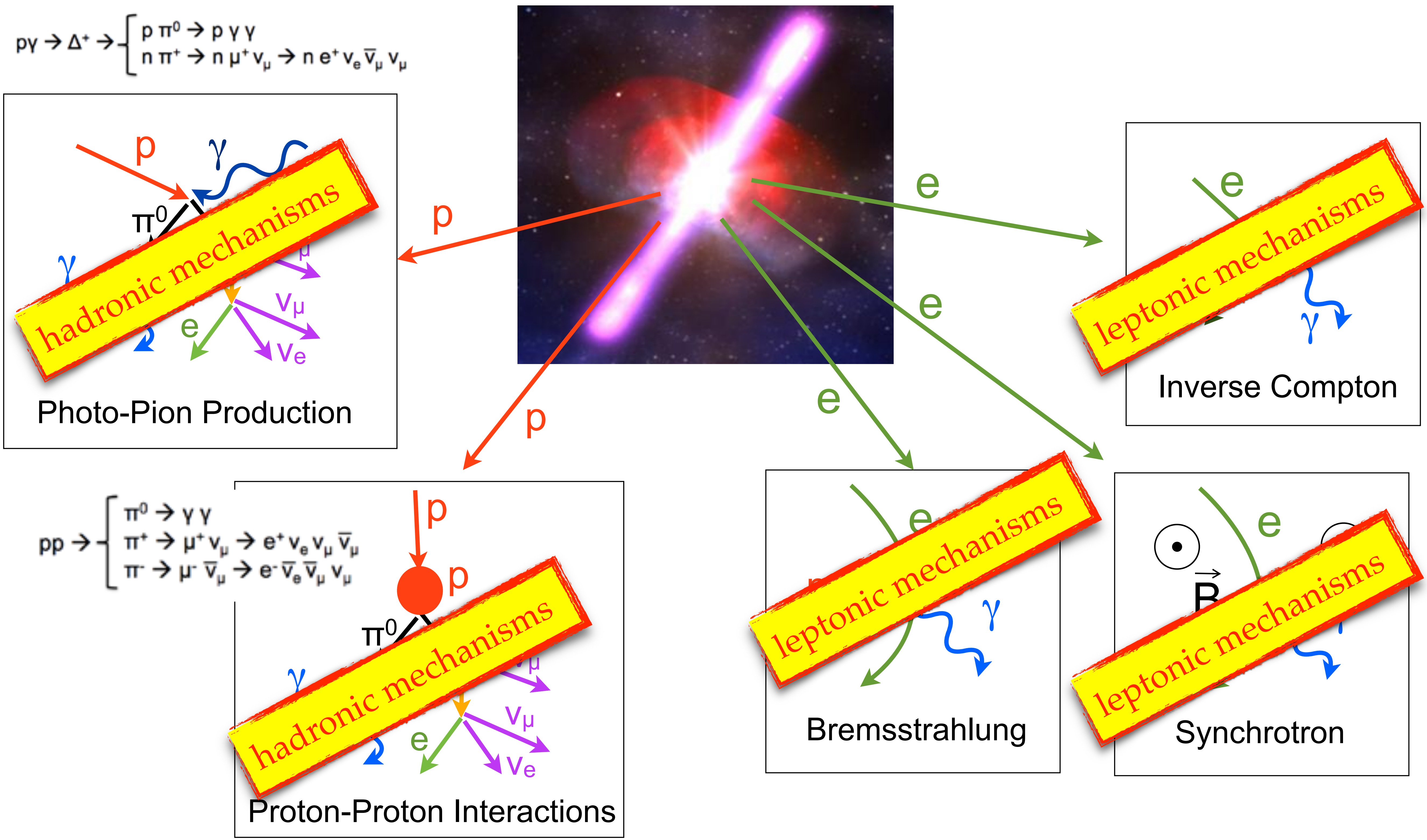

From particle to photon spectra

Hadronic: proton spectrum E^{-2} → p-p interaction → gamma-ray spectrum E^{-2}

Leptonic: electron spectrum E^{-2} → inverse Compton scattering → gamma-ray spectrum $E^{-1.5}$

$$E_{p,e}^{-\delta} \rightarrow E_{\gamma}^{-\alpha}$$

p-p interactions	$\alpha = \delta$	$E_\gamma \approx 0.1 \times E_p$
bremsstrahlung	$\alpha = \delta$	$E_\gamma \approx E_e$
inverse Compton	$\alpha = \dfrac{\delta + 1}{2}$	$E_\gamma \approx 1 \left(\dfrac{E_e}{20\ \mathrm{TeV}} \right)^2\ \mathrm{TeV}$

Complex scenario: each source is individual and has a unique behaviour.
In general one expects a ***combination of leptonic and hadronic emission !***
Multi-wavelength observations crucial but high energy spectra similar.

From particle to photon spectra

Hadronic: proton spectrum E^{-2} → p-p interaction → gamma-ray spectrum E^{-2}

Leptonic: electron spectrum E^{-2} → inverse Compton scattering → gamma-ray spectrum $E^{-1.5}$

$$E_{p,e}^{-\delta} \rightarrow E_{\gamma}^{-\alpha}$$

p-p interactions $\alpha = \delta$ $E_\gamma \approx 0.1 \times E_p$

bremsstrahlung

inverse Compton $\alpha = \frac{[illegible]}{2}$ $E_\gamma \approx 1 \left(\frac{E_e}{20\ \text{TeV}} \right)^2$ TeV

What is accelerated ?
Electrons or Hadrons ?

Complex scenario: each source is individual and has a unique behaviour.
In general one expects a *combination of leptonic and hadronic emission !*
Multi-wavelength observations crucial but high energy spectra similar.

Data above 50 TeV are very important…

…to discriminate between Leptonic/Hadronic emission of photons

✦ *Leptonic emission:*

1) Thomson regime

$E_e \epsilon \ll 4m_e^2$ (ε = seed photon energy)

Constant cross section: Thomson cross section

Electron spectrum $E^{-\delta}$

➜ Gamma ray spectrum $E^{-\alpha}$, $\alpha = \dfrac{\delta + 1}{2}$

2) Klein-Nishina regime

The cross section decreases

Photon index $\alpha = \delta + 1$

In case of CMB seed photons, the KN regime starts below 100 TeV

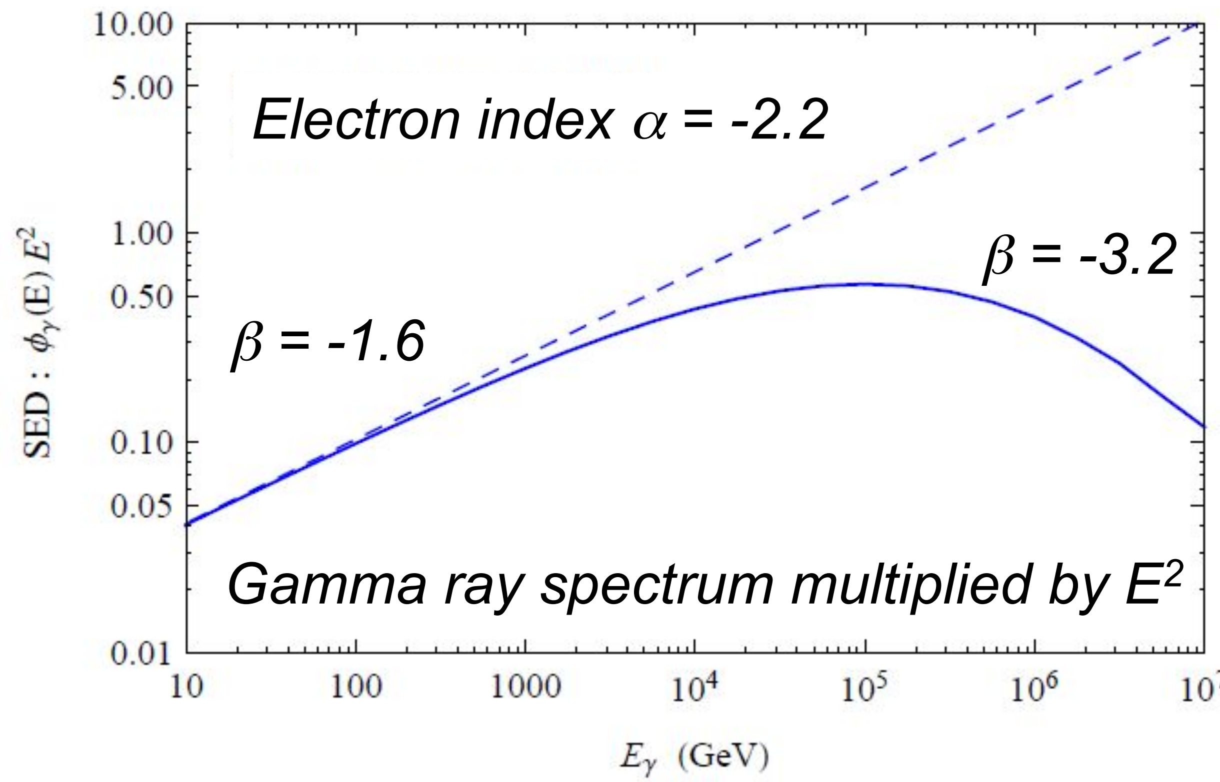

Inverse Compton is suppressed by the Klein-Nishina effect

✦ *Hadronic emission:*

π^0 decay from proton/nuclei interactions with the ambient nuclei

There is *NO suppression at high energy* as IC, unless the parent proton spectrum has a cutoff

Data above 50 TeV are very important…

…to discriminate between Leptonic/Hadronic emission of photons

✦ *Leptonic emission:*

1) Thomson regime

$E_e\epsilon \ll 4m_e^2$ (ε = seed photon energy)

Constant cross section: Thomson cross section

Electron spectrum $E^{-\delta}$

➜ Gamma ray spectrum $E^{-\alpha}$, $\alpha = \dfrac{\delta+1}{2}$

2) Klein-Nishina regime

The cross section decreases

Photon index $\alpha = \delta + 1$

In case of CMB seed photons, the I…

starts below 100 TeV

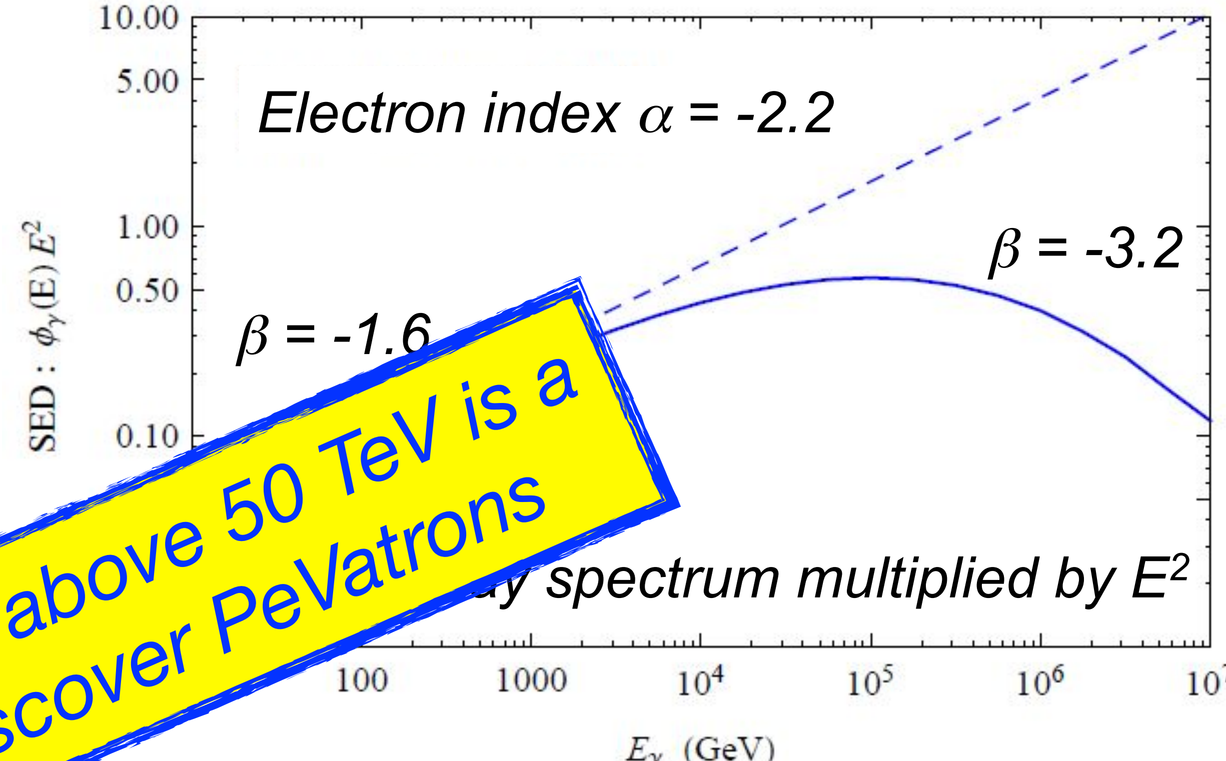

…erse Compton is suppressed by the Klein-Nishina effect

Gamma ray astronomy above 50 TeV is a important tool to discover PeVatrons

✦ *Hadronic e…*

π⁰ decay fr… …uclei interactions with the ambient nuclei

There is *NO suppression at high energy* as IC, unless the parent proton spectrum has a cutoff

★ *A power law spectrum reaching 100 TeV without a cutoff* is a strong indication of the hadronic origin of the emission

Gamma-ray detectors

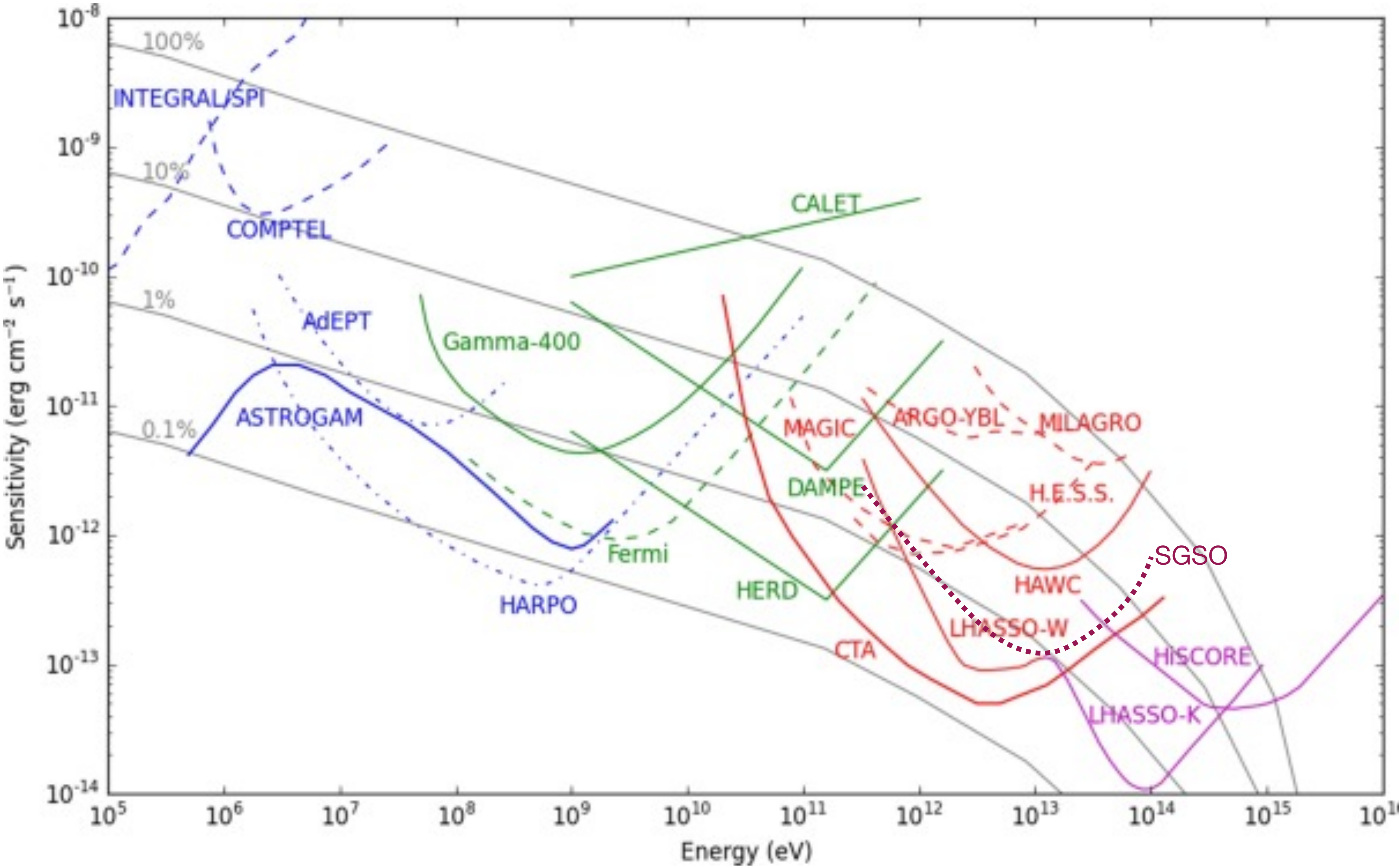

Knoedlseder 2016

Gamma-ray detectors

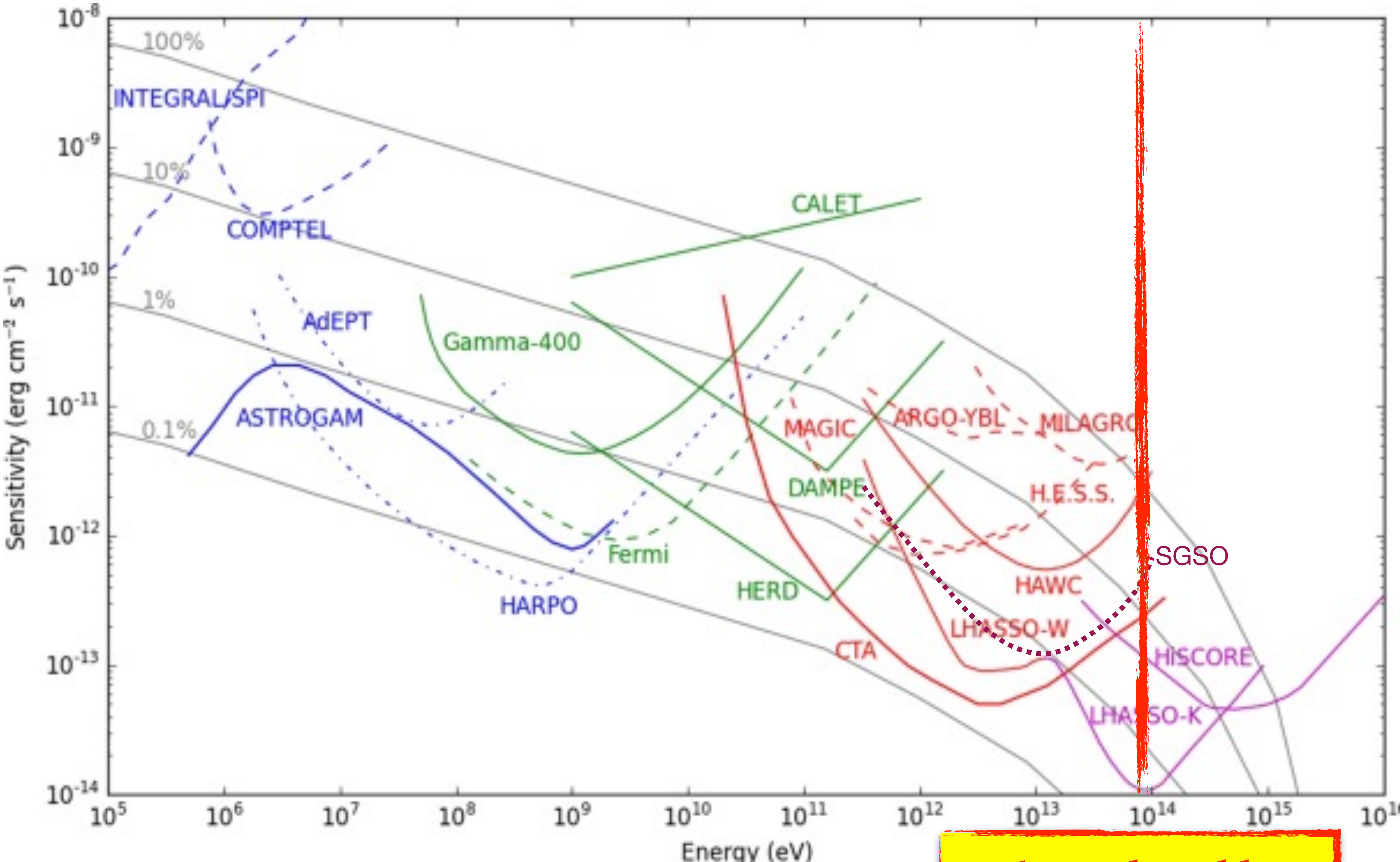

Knoedlseder 2016

γ's produced by PeV protons

Gamma-ray detectors

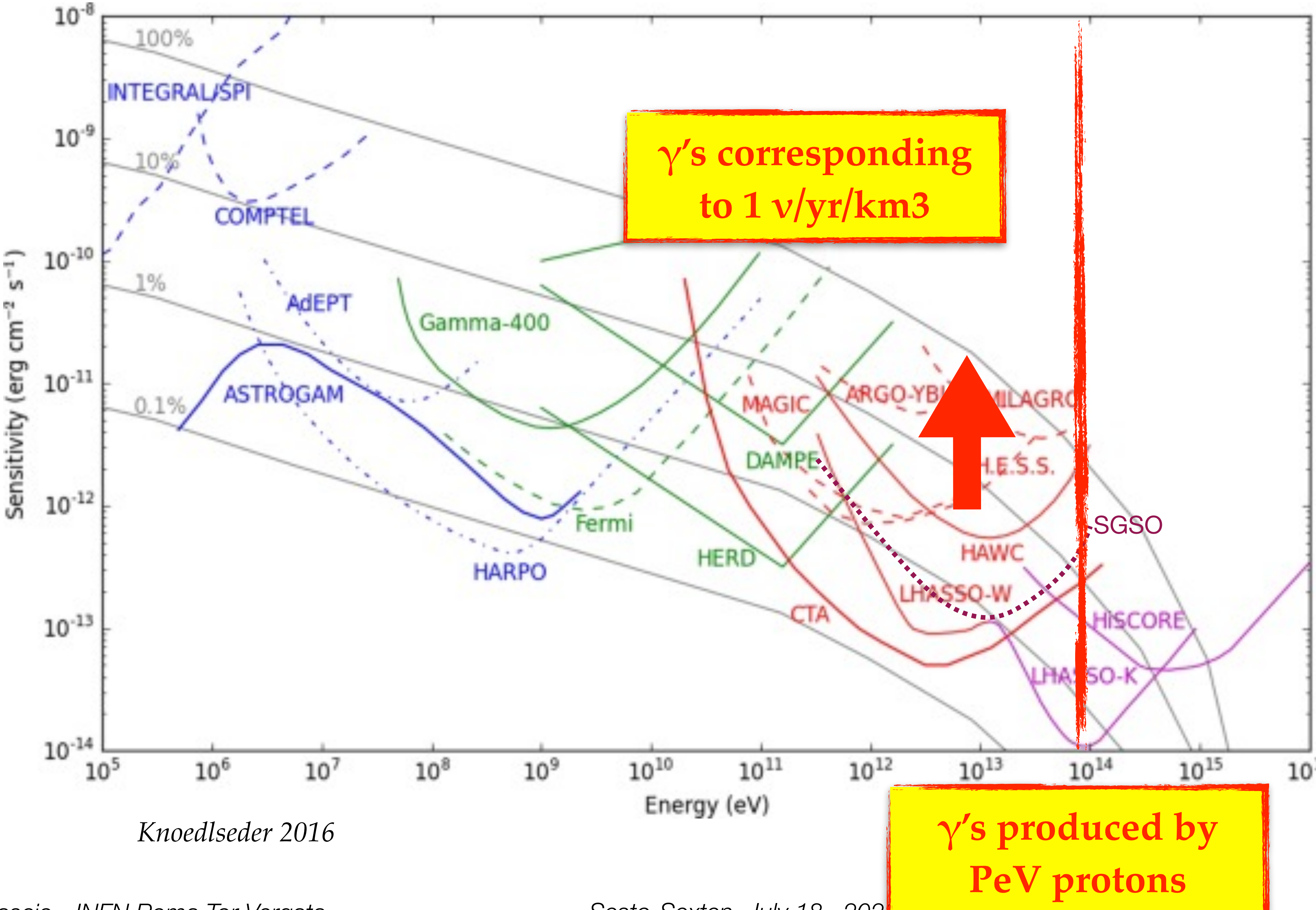

Knoedlseder 2016

LHAASO layout

- 1.3 km^2 array, including 5195 scintillator detectors 1 m^2 each, with 15 m spacing.
- An overlapping 1 km^2 array of 1171, underground water Cherenkov tanks 36 m^2 each, with 30 m spacing, for muon detection (total sensitive area ≈ 42,000 m^2).

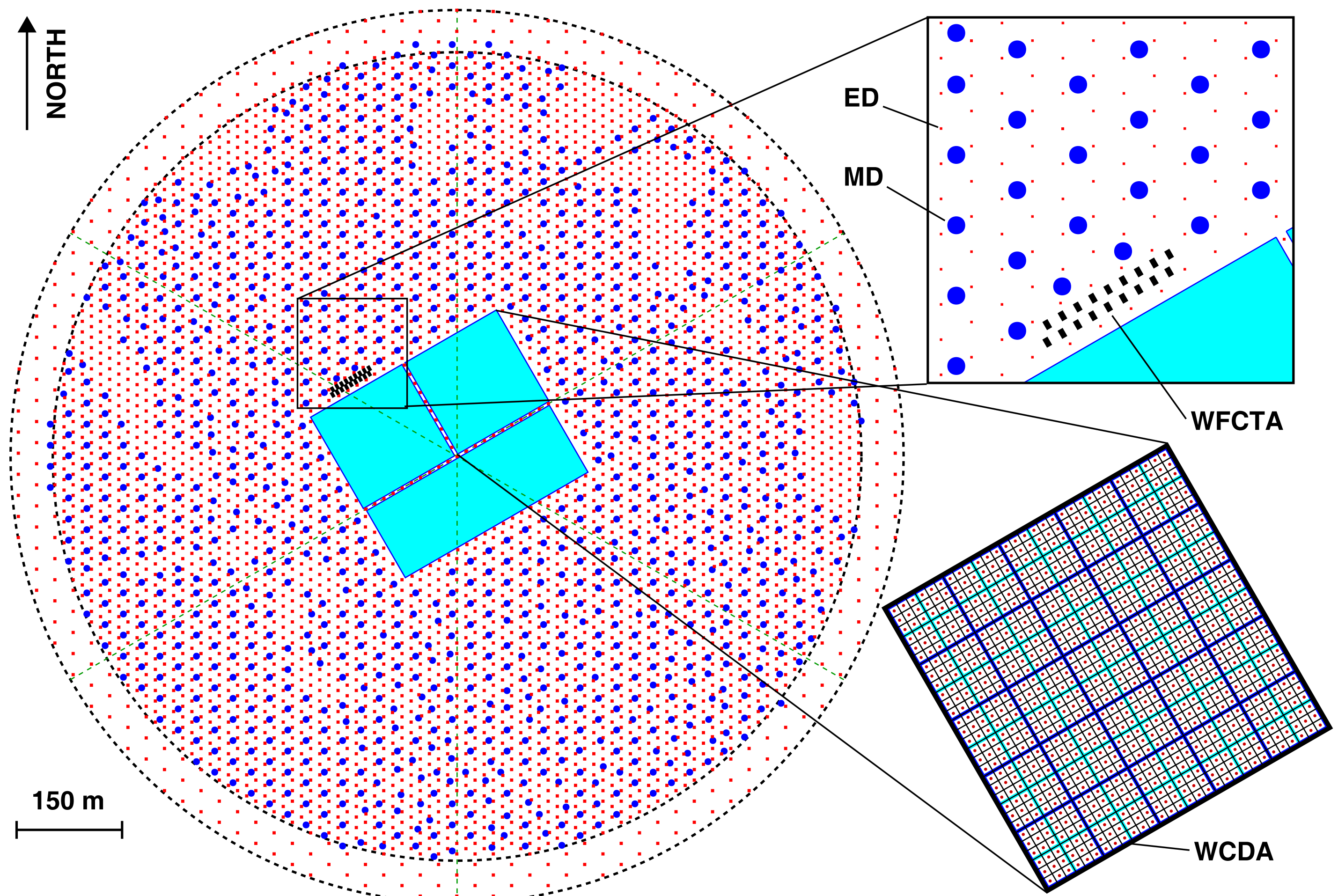

- A close-packed, surface water Cherenkov detector facility with a total area of 80,000 m^2.
- 18 wide field-of-view air Cherenkov (and fluorescence) telescopes.
- Neutron detectors

The LHAASO site

The experiment is located at ***4400 m*** asl (600 g/cm^2) in the Haizishan (Lakes' Mountain) site, Sichuan province

Coordinates: 29º 21' 31'' N, 100º 08' 15'' E

700 km to Chengdu
50 km to Daocheng City (3700 m asl, guest house)
10 km to the highest airport in the world

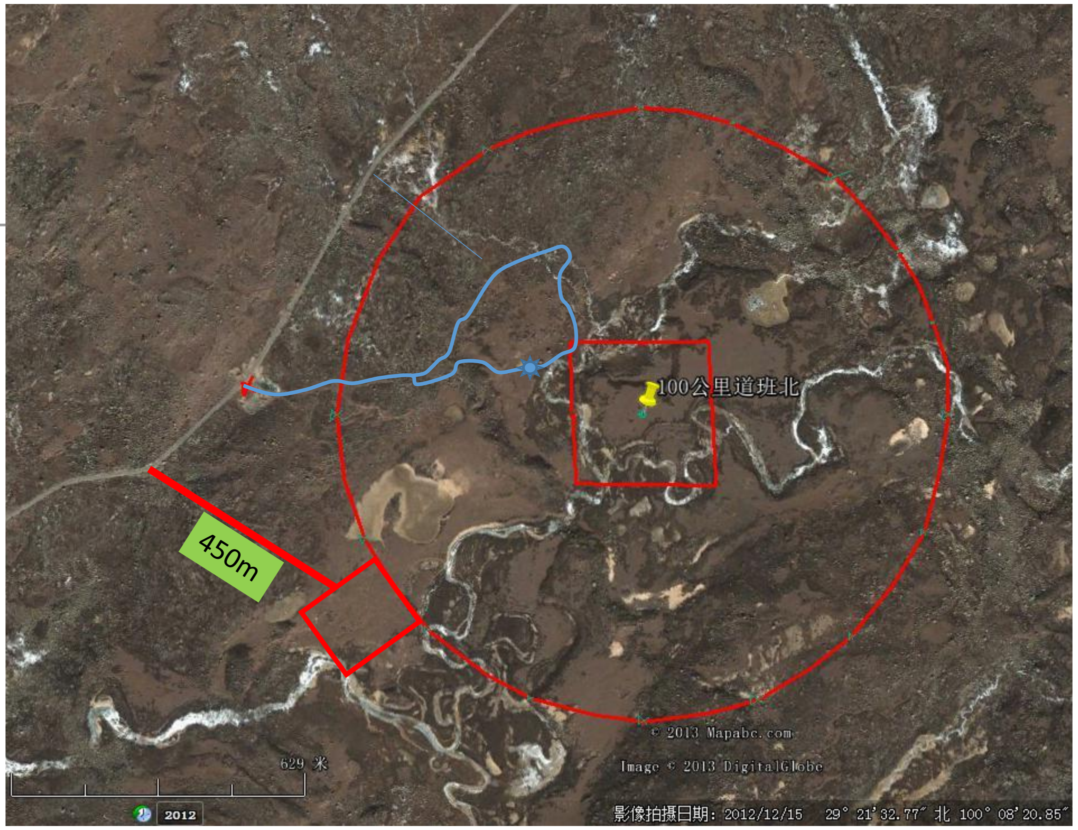

LHAASO Sky >100 TeV with half array

LHAASO Coll., Nature 2021

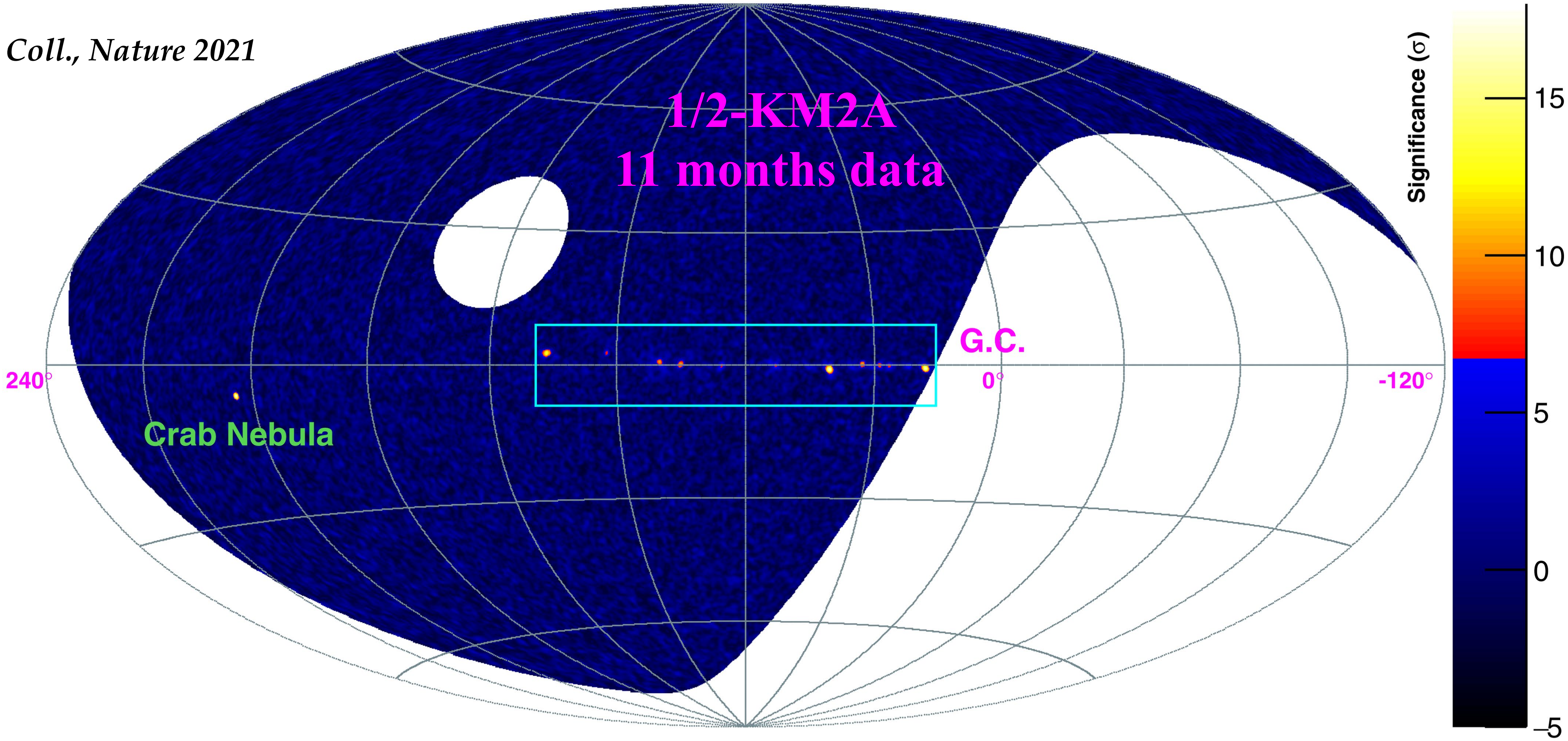

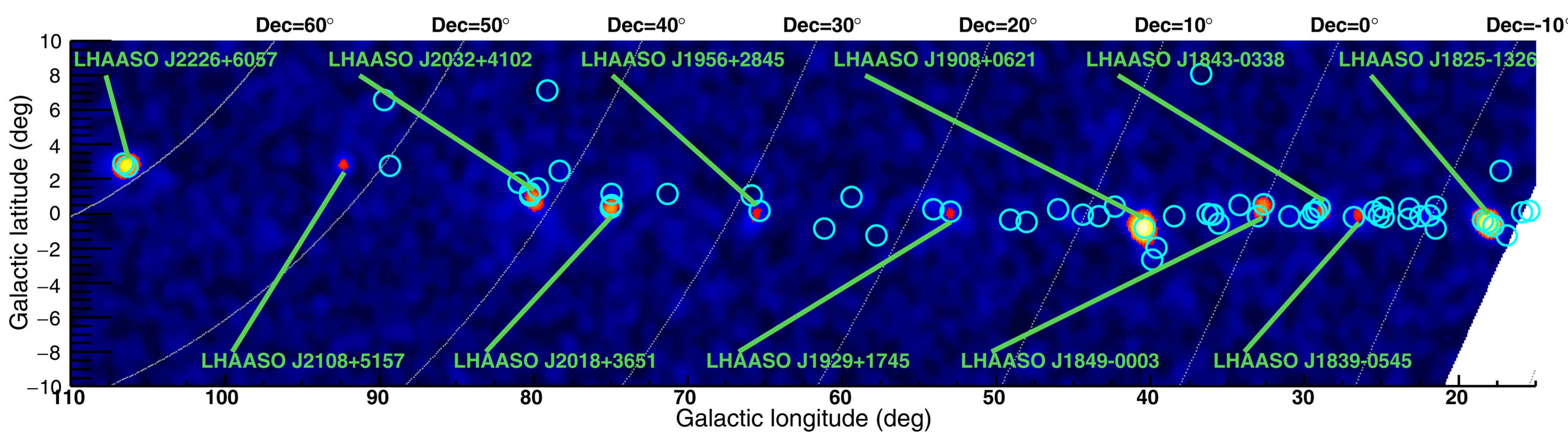

Detection of >1 PeV photons from Crab

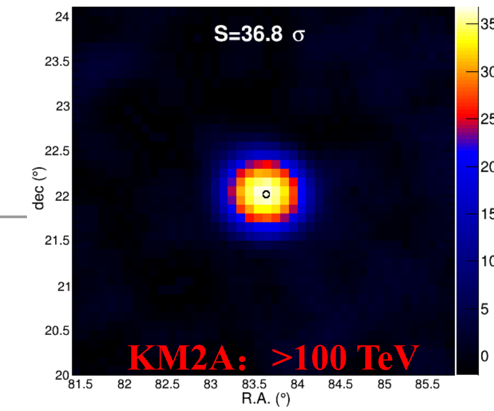

Electron accelerator over 22 energy decades

Mechanism: Inverse Compton on 2.7 K CMBR: direct relation $E_e \sim 2.15\left(\frac{E_\gamma}{1\ PeV}\right)^{0.77}$

$E_\gamma = 1.1$ PeV $\rightarrow E_e \sim 2.5$ PeV

$\log_{10}(E/\mathrm{TeV})$	N_{on}	N_b
2.0-2.2	55	1.413
2.2-2.4	23	0.459
2.4-2.6	6	0.176
2.6-2.8	3	0.045
2.8-3.0	1	0.008
3.0-3.2	1	0.000

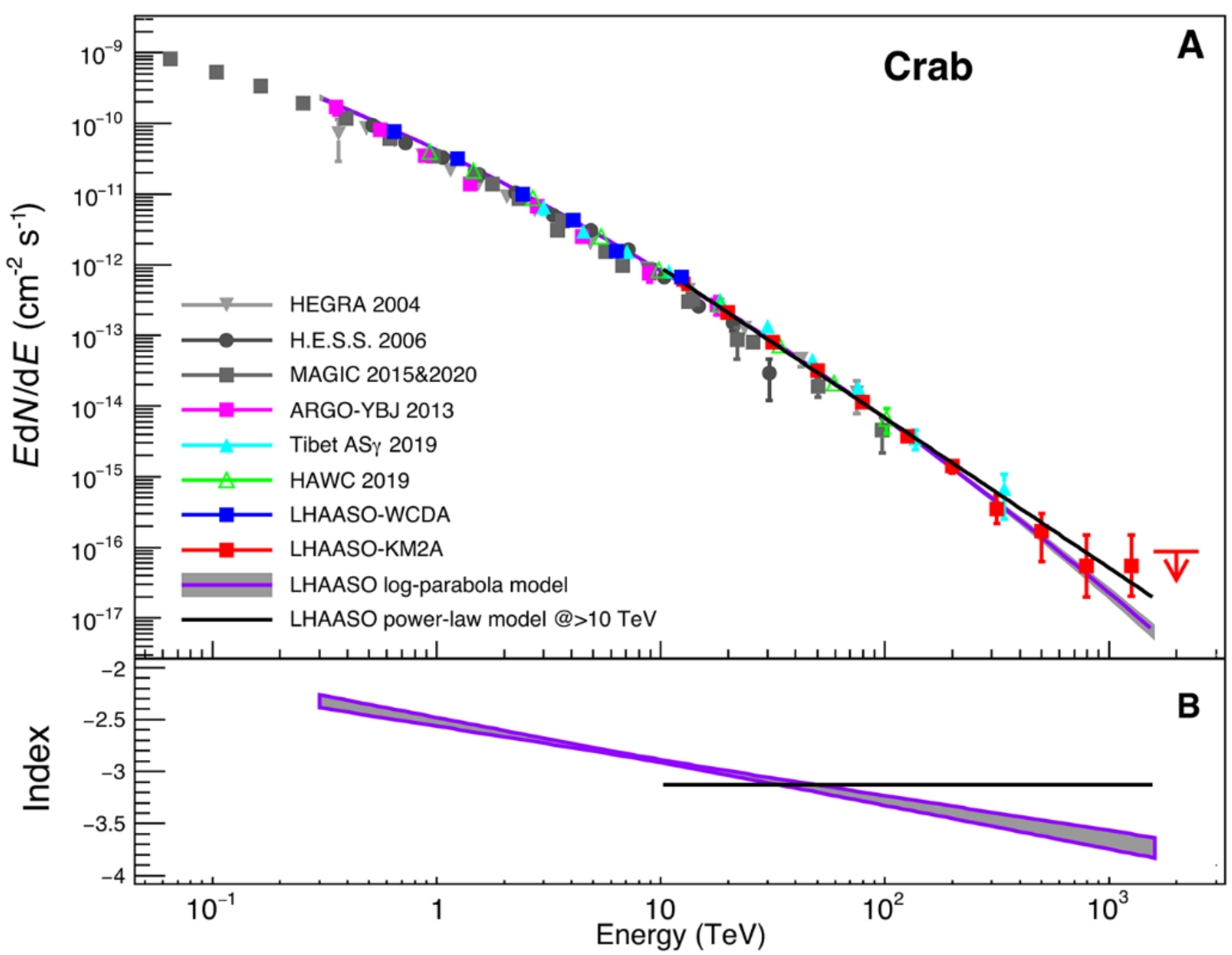

Science, 373 (2021) 425

1~ 2 PeV photon per year

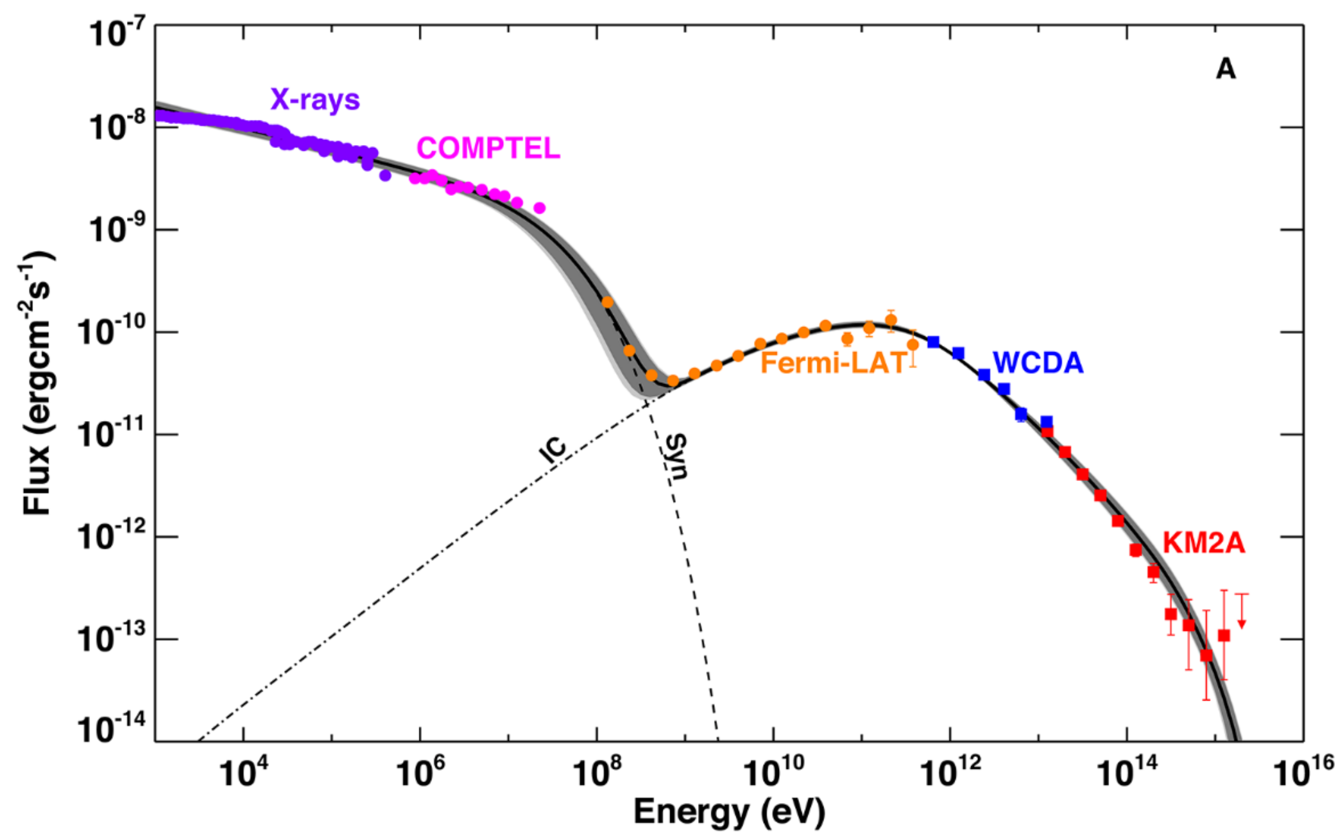

0.9 PeV photon from the Crab

Observed by 3 LHAASO detectors: WCDA, KM2A and WFCTA

Excellent Energy Intercalibration

KM2A 0.88 ± 0.11 PeV
WFCTA $0.92^{+0.28}_{-0.20}$ PeV

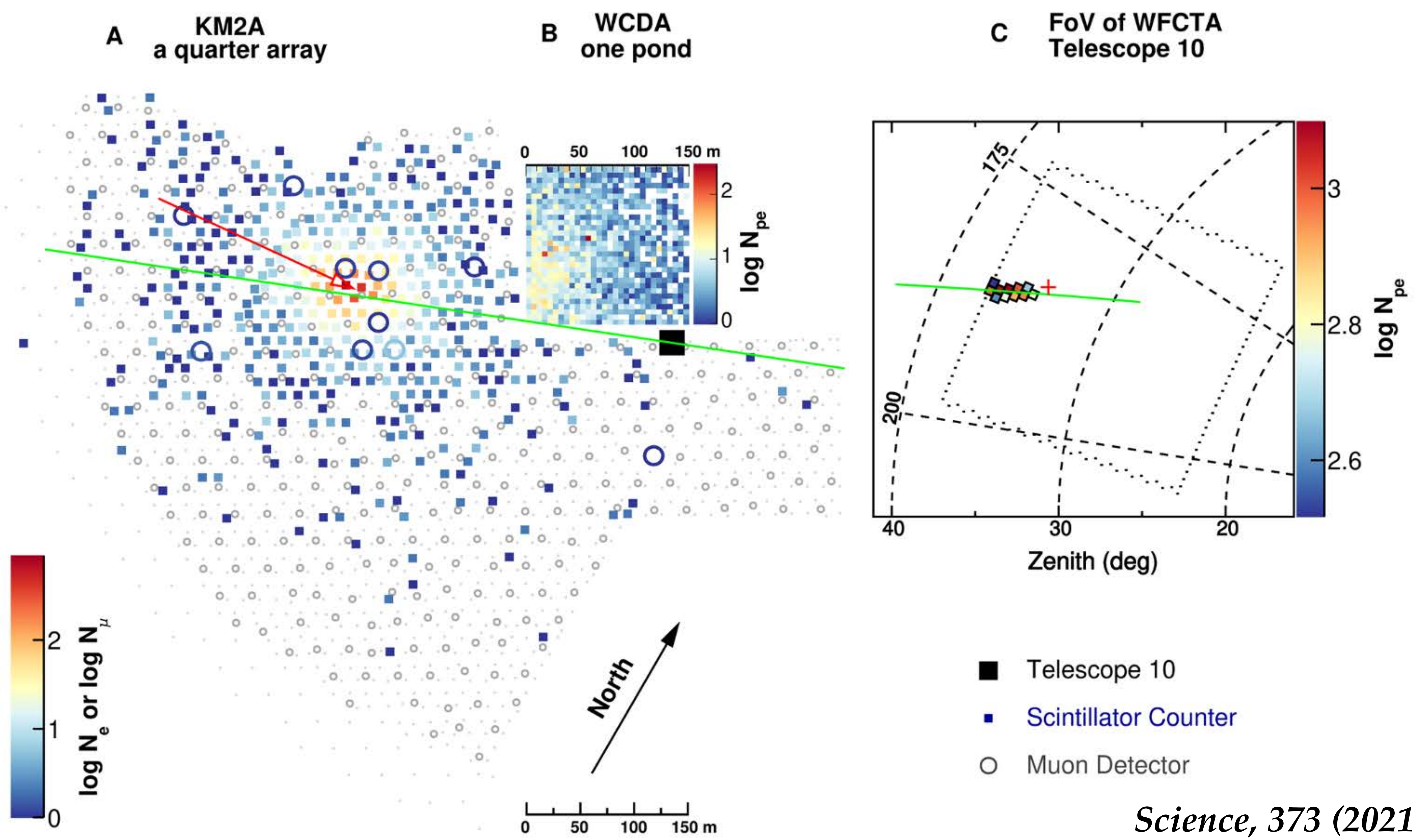

Science, 373 (2021) 425

LHAASO: γ-ray sources above 100 TeV

***Nature* 594: 33-36 (2021)**

- High statistical significance: >7σ
- High statistics: 543 HE photons vs 65 CR bkg
- High flux at 100 TeV
- ***Maximum energy: 1.4 PeV***

Source name	RA (°)	dec. (°)	Significance above 100 TeV (×σ)	E_{max} (PeV)	Flux at 100 TeV (CU)
LHAASO J0534+2202	83.55	22.05	17.8	0.88 ± 0.11	1.00(0.14)
LHAASO J1825-1326	276.45	−13.45	16.4	0.42 ± 0.16	3.57(0.52)
LHAASO J1839-0545	279.95	−5.75	7.7	0.21 ± 0.05	0.70(0.18)
LHAASO J1843-0338	280.75	−3.65	8.5	$0.26\,{}_{-0.10}^{+0.16}$	0.73(0.17)
LHAASO J1849-0003	282.35	−0.05	10.4	0.35 ± 0.07	0.74(0.15)
LHAASO J1908+0621	287.05	6.35	17.2	0.44 ± 0.05	1.36(0.18)
LHAASO J1929+1745	292.25	17.75	7.4	$0.71\,{}_{-0.07}^{+0.16}$	0.38(0.09)
LHAASO J1956+2845	299.05	28.75	7.4	0.42 ± 0.03	0.41(0.09)
LHAASO J2018+3651	304.75	36.85	10.4	0.27 ± 0.02	0.50(0.10)
LHAASO J2032+4102	308.05	41.05	10.5	1.42 ± 0.13	0.54(0.10)
LHAASO J2108+5157	317.15	51.95	8.3	0.43 ± 0.05	0.38(0.09)
LHAASO J2226+6057	336.75	60.95	13.6	0.57 ± 0.19	1.05(0.16)

Celestial coordinates (RA, dec.); statistical significance of detection above 100 TeV (calculated using a point-like template for the Crab Nebula and LHAASO J2108+5157 and 0.3° extension templates for the other sources); the corresponding differential photon fluxes at 100 TeV; and detected highest photon energies. Errors are estimated as the boundary values of the area that contains ±34.14% of events with respect to the most probable value of the event distribution. In most cases, the distribution is a Gaussian and the error is 1σ.

***SNRs are likely not the main sources of PeV CRs in our galaxy*.**

No young SNRs (Cas A, Tycho)

None of these sources can be clearly described with hadronic mechanisms operating in SNR

Residual CR background >100 TeV and exposure

source	Number of on-source events	number of background events	exposure (hr)
LHAASO J0534+2202	67	5.5	2236.4
LHAASO J1825-1326	61	3.2	1149.3
LHAASO J1839-0545	26	4.2	1614.5
LHAASO J1843-0338	30	4.3	1715.4
LHAASO J1849-0003	36	4.8	1865.3
LHAASO J1908+0621	74	5.1	2058.0
LHAASO J1929+1745	29	5.8	2282.6
LHAASO J1956+2845	34	6.1	2461.5
LHAASO J2018+3651	42	6.3	2610.7
LHAASO J2032+4102	45	6.7	2648.2
LHAASO J2108+5157	30	6.4	2525.8
LHAASO J2226+6057	60	6.2	2401.3

Above 400 TeV, KM2A measures γ-rays essentially background-free

CR rejection power 10^{-4} at 100 TeV and 10^{-5} at 1 PeV

Muon-poor technique

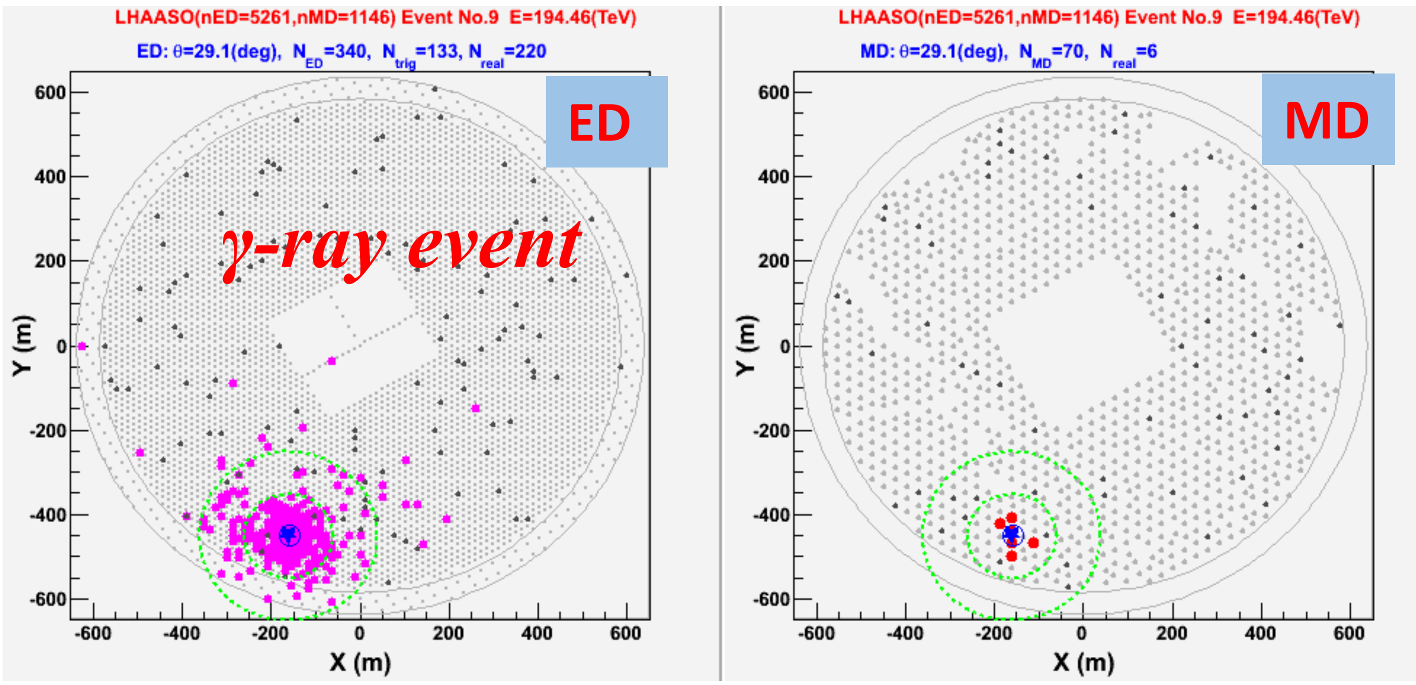

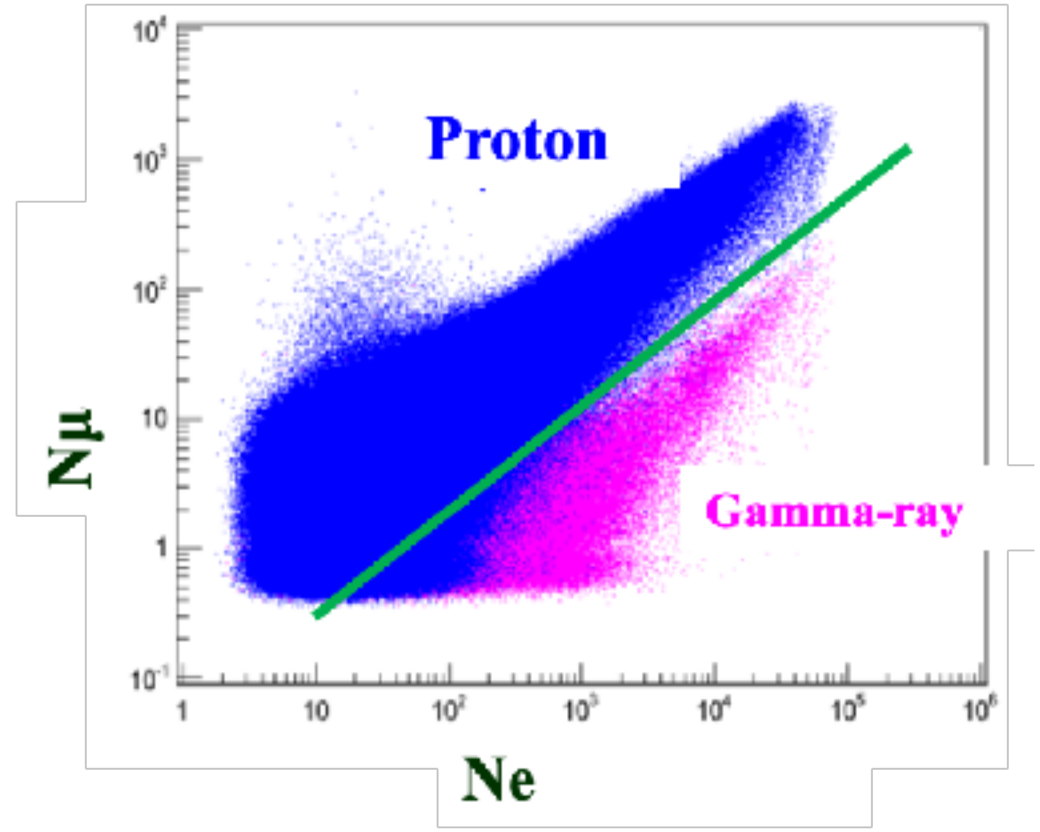

Detection rate of the full KM2A array

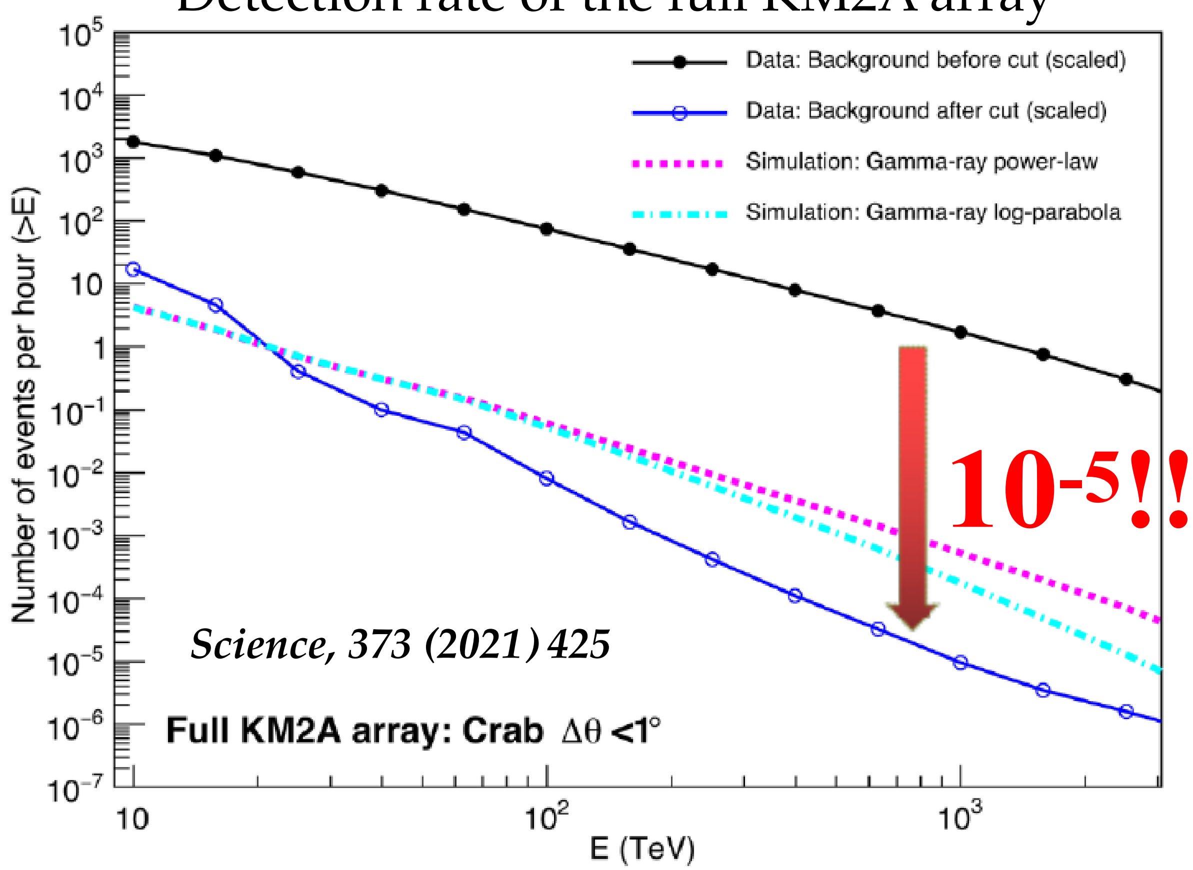

Impressive background rejection capability!

Cosmic ray rate before cut

Gamma-ray rate

Cosmic ray rate after cut

LHAASO-KM2A

	ARGO	AS+MD	HAWC	KM2A	CTA
Area	6,500 m^2	50,000 m^2	22,500 m^2	1 km^2	10 km^2
σ_θ (deg)	0.2-0.5	0.2-0.5	0.1-0.5	0.1-0.5	0.05
BG rejection power		10^4	100	10^4	100
Duty Cycle	>90%	>90%	>90%	>90%	10%
FOV (sr)	2	2	2	2	0.015
Sensitivity (c.u.) @100TeV		0.25		0.01	0.3
Energy resolution	30%	30%	>50%	30%	15%

KM2A Energy and Angular Resolutions

★ **θ<20°: 24% @ 20 TeV, 13% at 100 TeV**

★ **0.25˚ – 0.30˚ at 100 TeV**

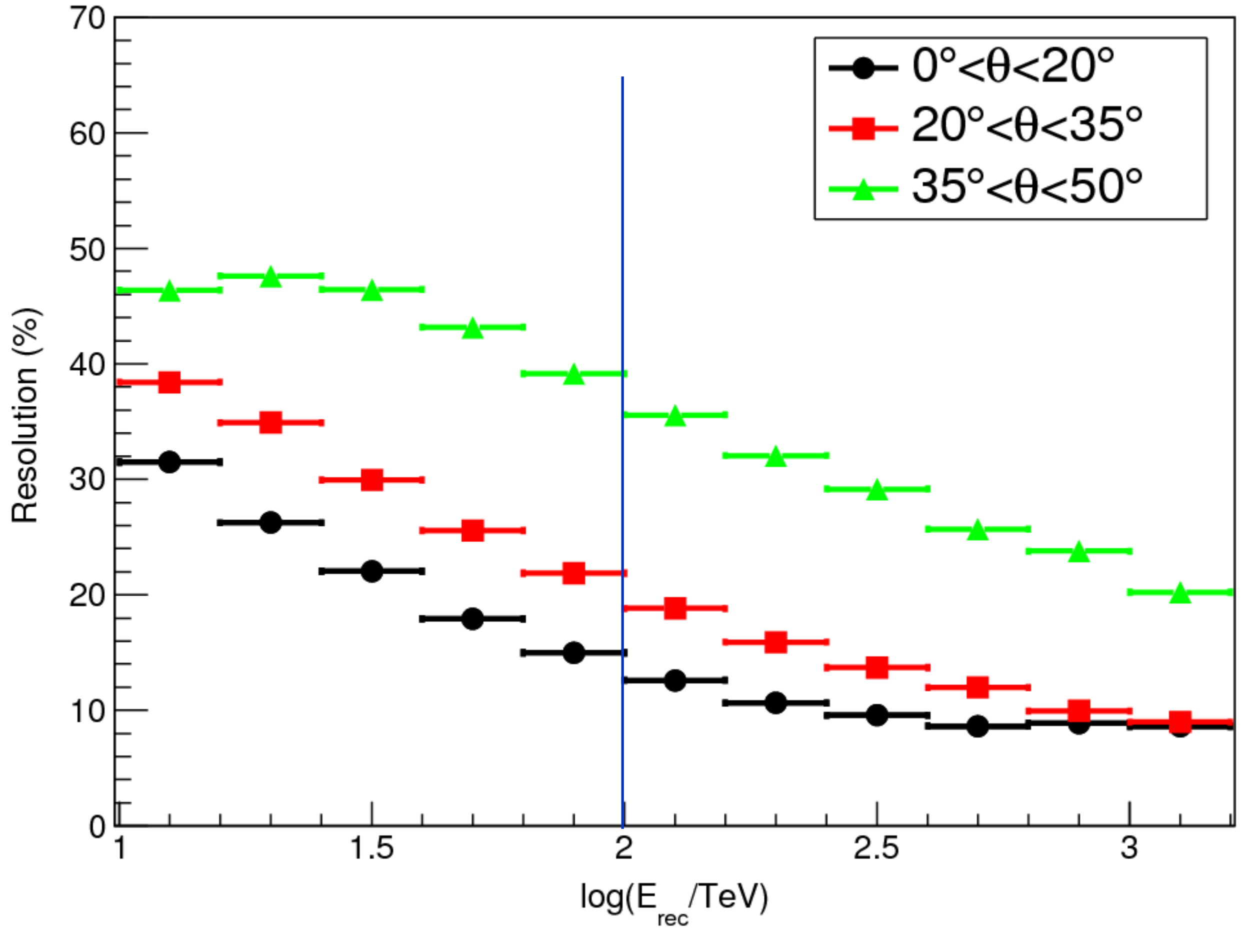

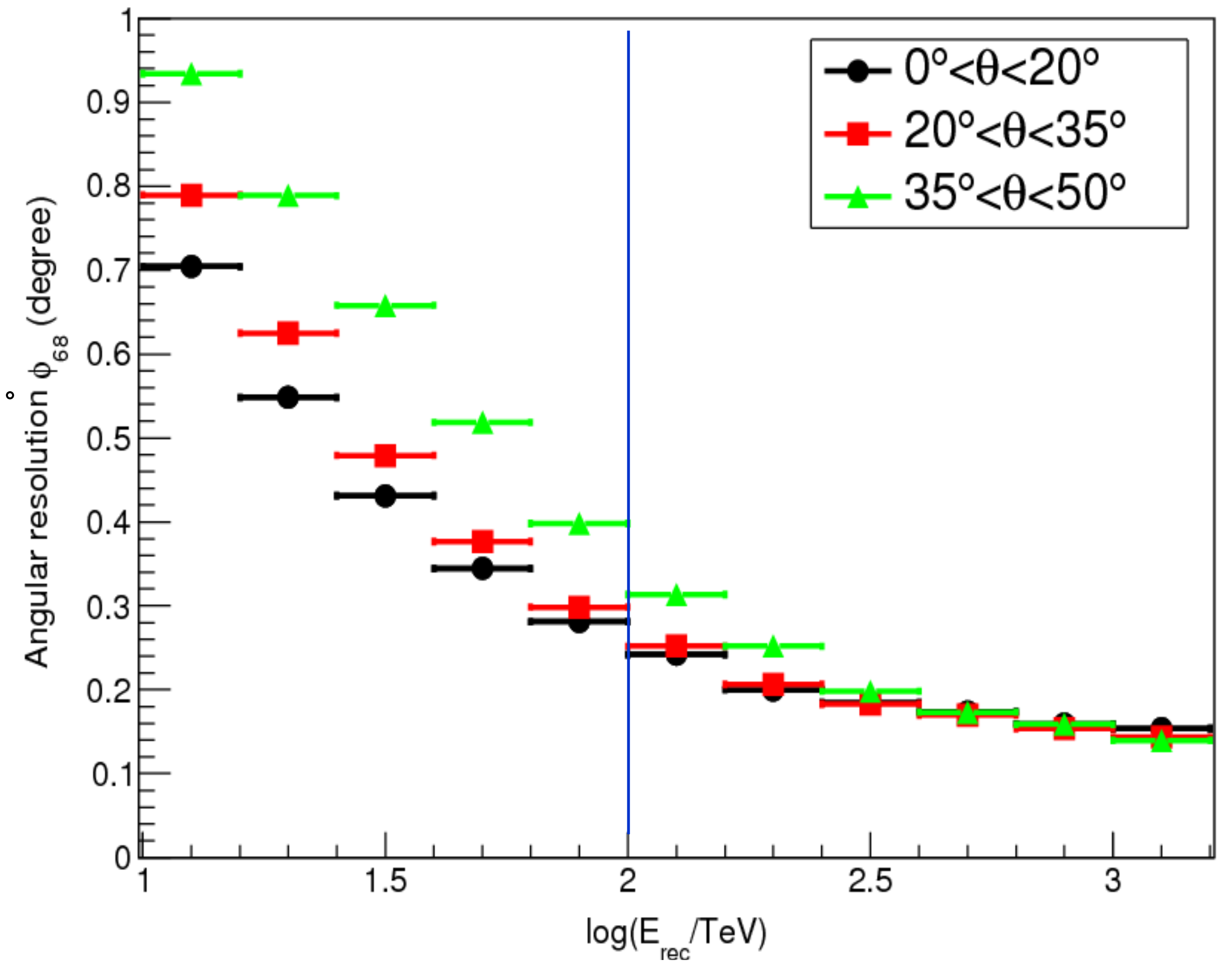

Chinese Physics C 45: 025002 (2021)

Very important to measure cutoffs of PeVatrons!

Opening the PeV γ-ray sky to observations

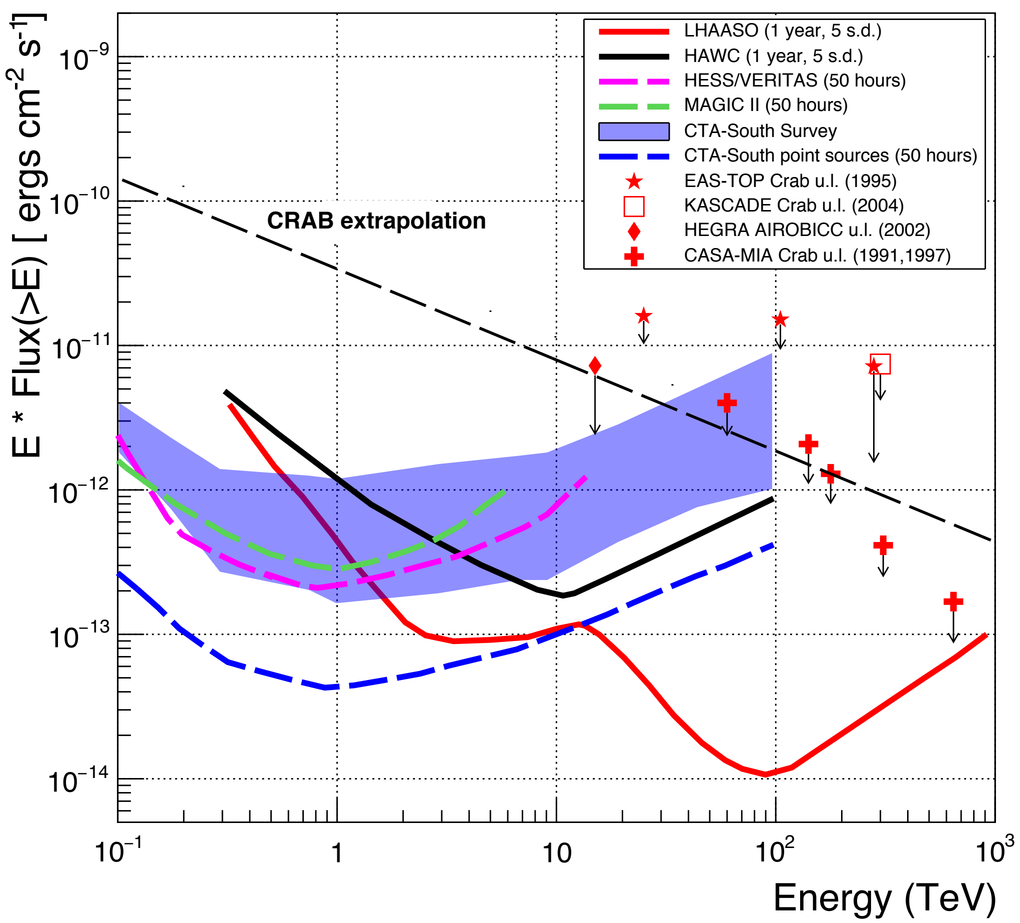

- background-free detection of extended 1 deg sources of >100 TeV
- gamma-rays of strength 0.1 Crab by KM2A with a rate 1 ph/100 h
- Exposure/year: >2000 km² hr (CTA: 100 km²hr)

This achievement is the result of the combination of:

(1) a ***1-km^2 detection area*** providing adequate UHE photon statistics;

(2) suppression of the CR background at the level of ***10^{-5}***, enabling ***background-free*** detection of γ-rays above 100 TeV;

(3) KM2A - PSF: 25′ at 20 TeV 12′ at 100 TeV;

(4) an energy resolution of ***<20%*** constraining the spillover that mainly occurs in the neighbouring energy channels with a width of $\Delta(\log E) = 0.2$.

SEDs of 3 most powerful sources

Very steep spectra $\Gamma \approx 3$

Klein-Nishina regime???

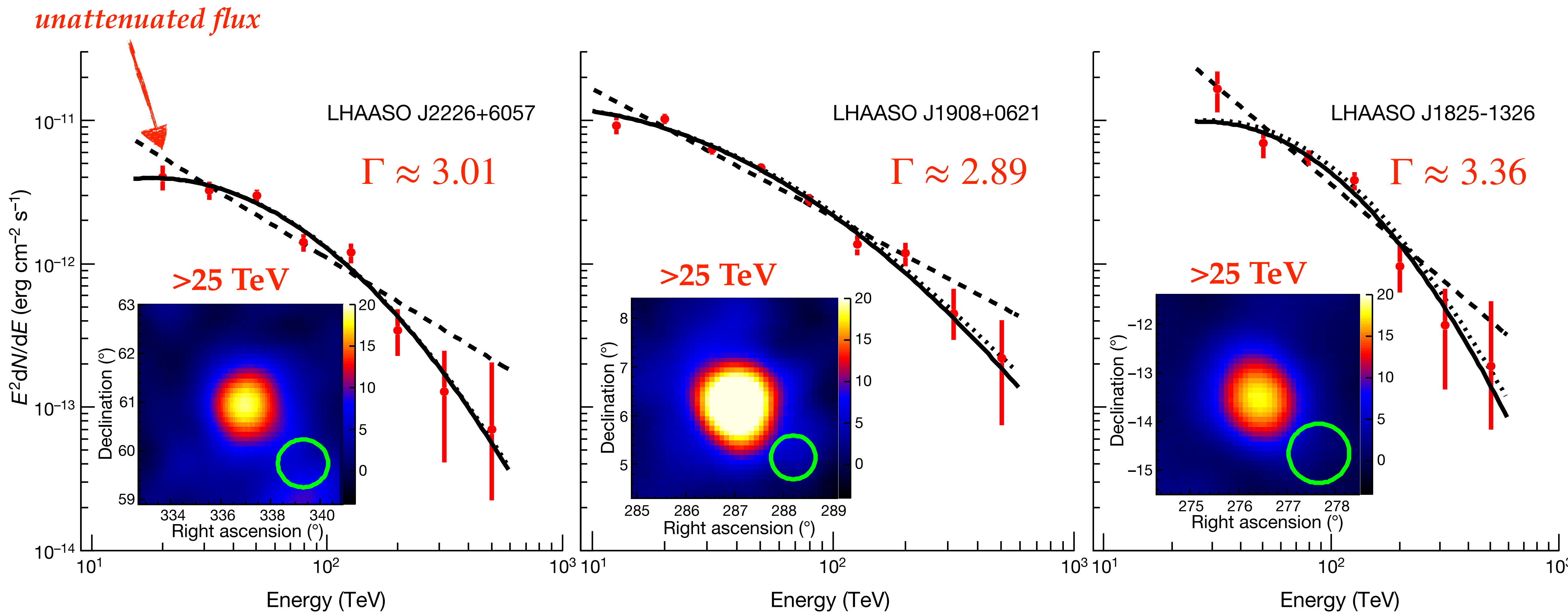

Fit with log-parabola function $\left(\frac{E}{10\ TeV}\right)^{-a-b\cdot log\left(\frac{E}{10\ TeV}\right)}$ with $\Gamma(E) = a + b \cdot log(E)$

The first SNR as PeVatron?

LHAASO J1908+0621 = SNR G40.5-0.5 + GMC ?

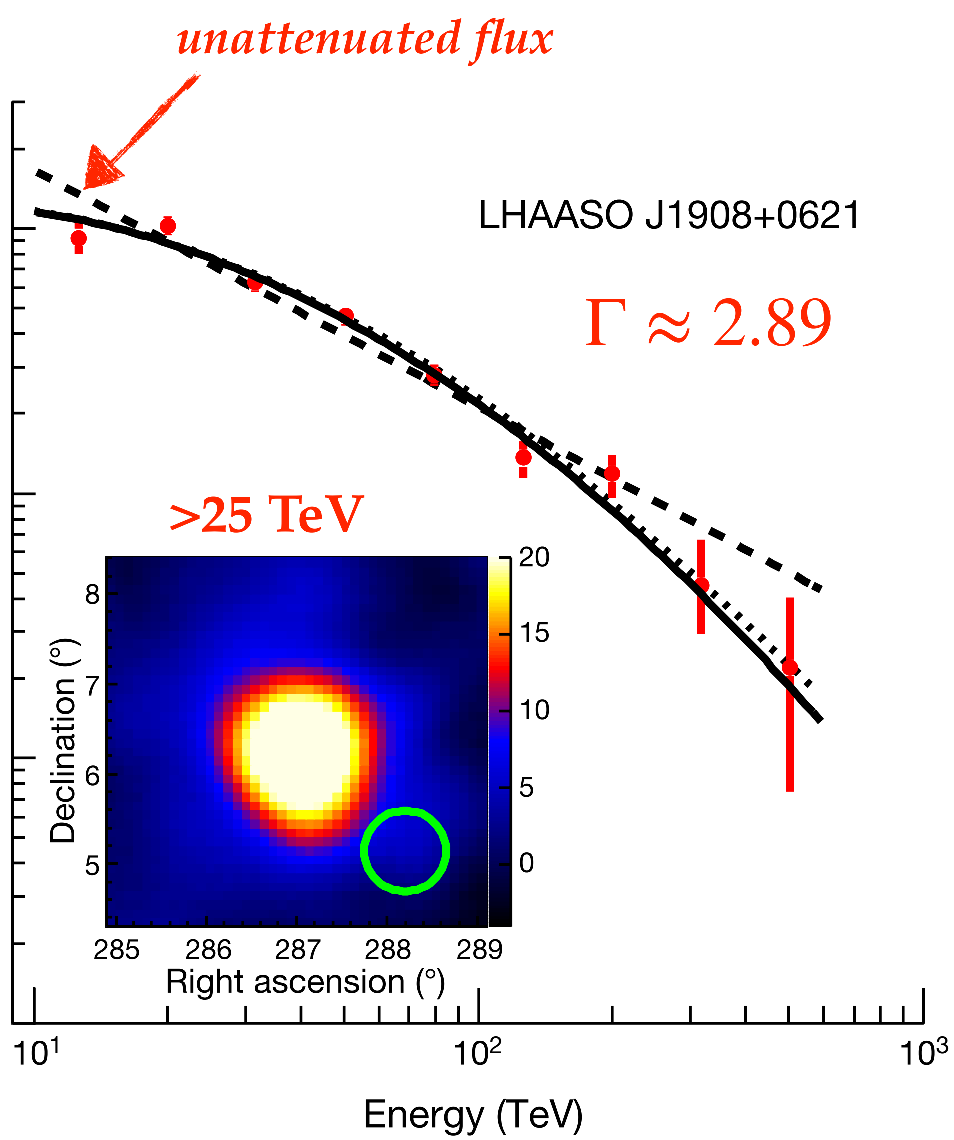

One of the most intriguing sources in the Galactic plane. MGRO J1908+06 spatially associates with an ***IceCube hotspot of neutrino emission***. Although the hotspot is not significant yet, this suggests a ***possible hadronic origin of the observed gamma-ray radiation.***

Highest energy photon 0.45 PeV => Ep > 2 PeV

confirmation of association with G40.5-0.5 would be ***the first evidence of a SNR operating as PeVatron***

soon LHAASO will announce detection of UHE γ-rays from W51 and γCygni
=> new developments are anticipated with exciting implications

Potential TeV counterparts

LHAASO Source	Possible Origin	Type	Distance (kpc)	Age (kyr)[a]	L_s (erg/s)[b]	Potential TeV Counterpart[c]
LHAASO J0534+2202	PSR J0534+2200	PSR	2.0	1.26	4.5×10^{38}	Crab, Crab Nebula
LHAASO J1825-1326	PSR J1826-1334	PSR	3.1 ± 0.2^d	21.4	2.8×10^{36}	HESS J1825-137, HESS J1826-130,
	PSR J1826-1256	PSR	1.6	14.4	3.6×10^{36}	2HWC J1825-134
LHAASO J1839-0545	PSR J1837-0604	PSR	4.8	33.8	2.0×10^{36}	2HWC J1837-065, HESS J1837-069,
	PSR J1838-0537	PSR	1.3^e	4.9	6.0×10^{36}	HESS J1841-055
LHAASO J1843-0338	SNR G28.6-0.1	SNR	9.6 ± 0.3^f	$< 2^f$	—	HESS J1843-033, HESS J1844-030,
						2HWC J1844-032
LHAASO J1849-0003	PSR J1849-0001	PSR	7^g	43.1	9.8×10^{36}	HESS J1849-000, 2HWC J1849+001
	W43	YMC	5.5^h	—	—	
LHAASO J1908+0621	SNR G40.5-0.5	SNR	3.4^i	$\sim 10 - 20^j$	—	MGRO J1908+06, HESS J1908+063,
	PSR 1907+0602	PSR	2.4	19.5	2.8×10^{36}	ARGO J1907+0627, VER J1907+062,
	PSR 1907+0631	PSR	3.4	11.3	5.3×10^{35}	2HWC 1908+063
LHAASO J1929+1745	PSR J1928+1746	PSR	4.6	82.6	1.6×10^{36}	2HWC J1928+177, 2HWC J1930+188,
	PSR J1930+1852	PSR	6.2	2.9	1.2×10^{37}	HESS J1930+188, VER J1930+188
	SNR G54.1+0.3	SNR	$6.3^{+0.8\ d}_{-0.7}$	$1.8 - 3.3^k$	—	
LHAASO J1956+2845	PSR J1958+2846	PSR	2.0	21.7	3.4×10^{35}	2HWC J1955+285
	SNR G66.0-0.0	SNR	2.3 ± 0.2^d	—	—	
LHAASO J2018+3651	PSR J2021+3651	PSR	$1.8^{+1.7\ l}_{-1.4}$	17.2	3.4×10^{36}	MGRO J2019+37, VER J2019+368,
	Sh 2-104	H II/YMC	$3.3 \pm 0.3^m/4.0 \pm 0.5^n$	—	—	VER J2016+371
LHAASO J2032+4102	Cygnus OB2	YMC	1.40 ± 0.08^o	—	—	TeV J2032+4130, ARGO J2031+4157,
	PSR 2032+4127	PSR	1.40 ± 0.08^o	201	1.5×10^{35}	MGRO J2031+41, 2HWC J2031+415,
	SNR G79.8+1.2	SNR candidate	—	—	—	VER J2032+414
LHAASO J2108+5157	—	—	—	—	—	—
LHAASO J2226+6057	SNR G106.3+2.7	SNR	0.8^p	$\sim 10^p$	—	VER J2227+608, Boomerang Nebula
	PSR J2229+6114	PSR	0.8^p	$\sim 10^p$	2.2×10^{37}	

The only firmly identified source is the Crab Nebula

LHAASO and ASTRI/CTA

The LHAASO angular resolution at PeV is about 0.2 deg

Crab apart, the majority of remaining sources represent ***diffuse γ-ray structures with angular extensions up to 1º***, and all of them are located along the Galactic plane

LHAASO has not observed PeVatrons but 'regions' emitting PeV gamma rays!

We need to ***improve the angular resolution*** to identify the emission zones.

Strong ***complementarity*** with Cherenkov Telescopes to improve the source identification

In addition, the effective area must increase of a factor of 10
because ***Super-PeVatrons*** emitting photons up to the ***10 PeV*** range
are expected, in particular in the South!

Homework for SWGO!

ASTRI is arriving!

Observations of ASTRI&CTA and eROSITA could be very helpful in localisation of PeVatrons inside the LHAASO UHE gamma-ray sources with high precision

ASTRI combined with LHAASO would be the most powerful tool for UHE gamma-ray astronomy in the coming years!

ASTRI very important for ***precise identification*** of PeV sources and information about their ***morphology***

→ Talk by Giuliani

PRELIMINARY	ASTRI Mini-Array	MAGIC	VERITAS	H.E.S.S.	HAWC	LHAASO	Tibet ASγ
Altitude [m]	2,390	2,200	1,268	1,800	4,100	4,410	4,300
FoV	$\sim 10°$	$\sim 3.5°$	$\sim 3.5°$	$\sim 5°$	2 sr	2 sr	2 sr
Angular Res.	0.05° (30 TeV)	0.07° (1 TeV)	0.07° (1 TeV)	0.06° (1 TeV)	0.15° (10 TeV)	(0.24–0.32)° (100 TeV)	$\sim$ 0.2° (100 TeV)
Energy Res.	12% (10 TeV)	16% (1 TeV)	17% (1 TeV)	15% (1 TeV)	30% (10 TeV)	(13–36)% (100 TeV)	20% (100 TeV)
Energy Range	(0.3-200) TeV	(0.05-20) TeV	(0.08-30) TeV	(0.02-30) TeV	(0.1-200) TeV	(0.1-1,000) TeV	(0.1-1,000) TeV

S. Vercellone 2022

The max photon energy event

Nature 594: 33-36 (2021)

- 1.42±0.13 PeV from the Cygnus region
- Chance probability due to cosmic ray background 0.028%

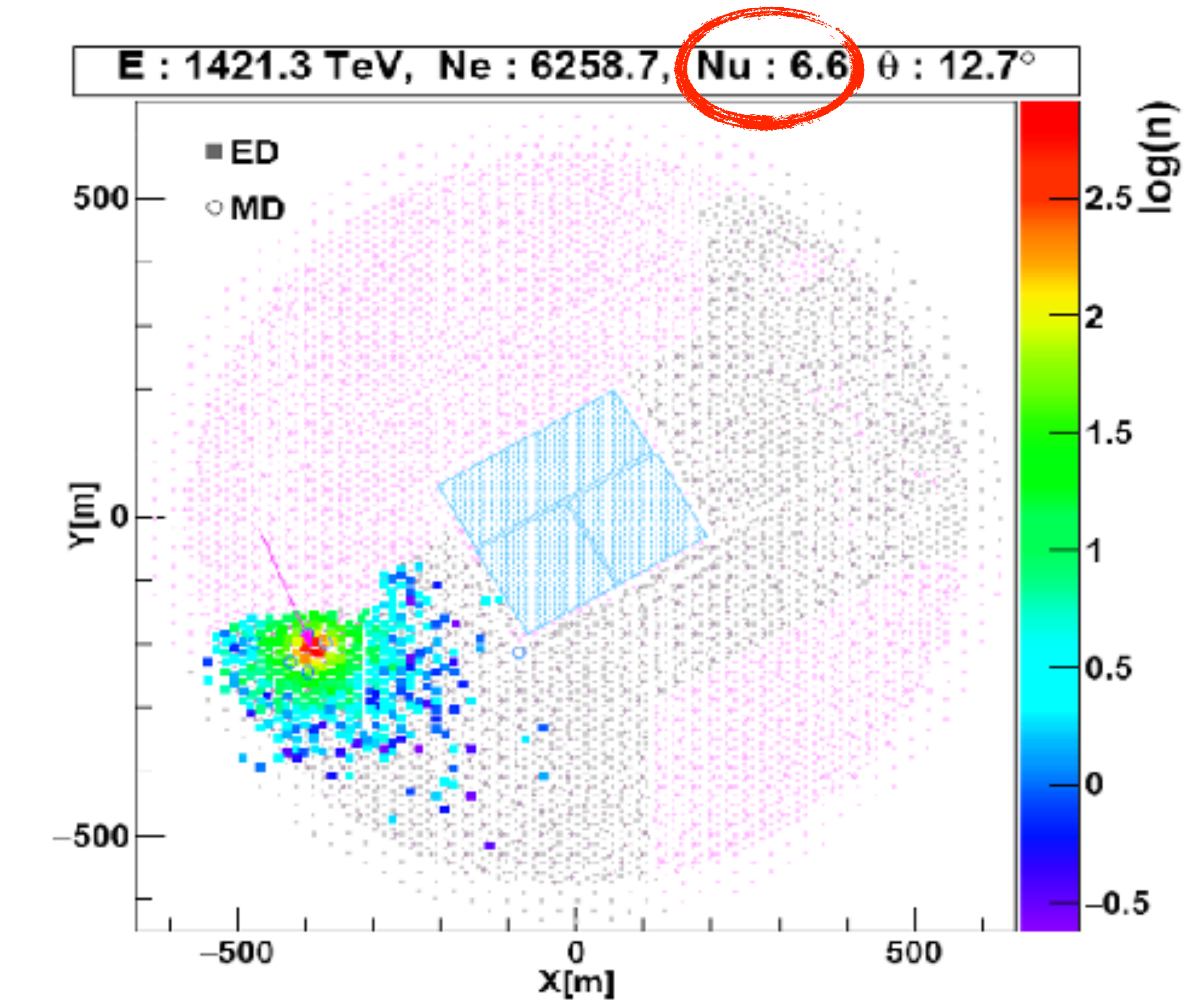

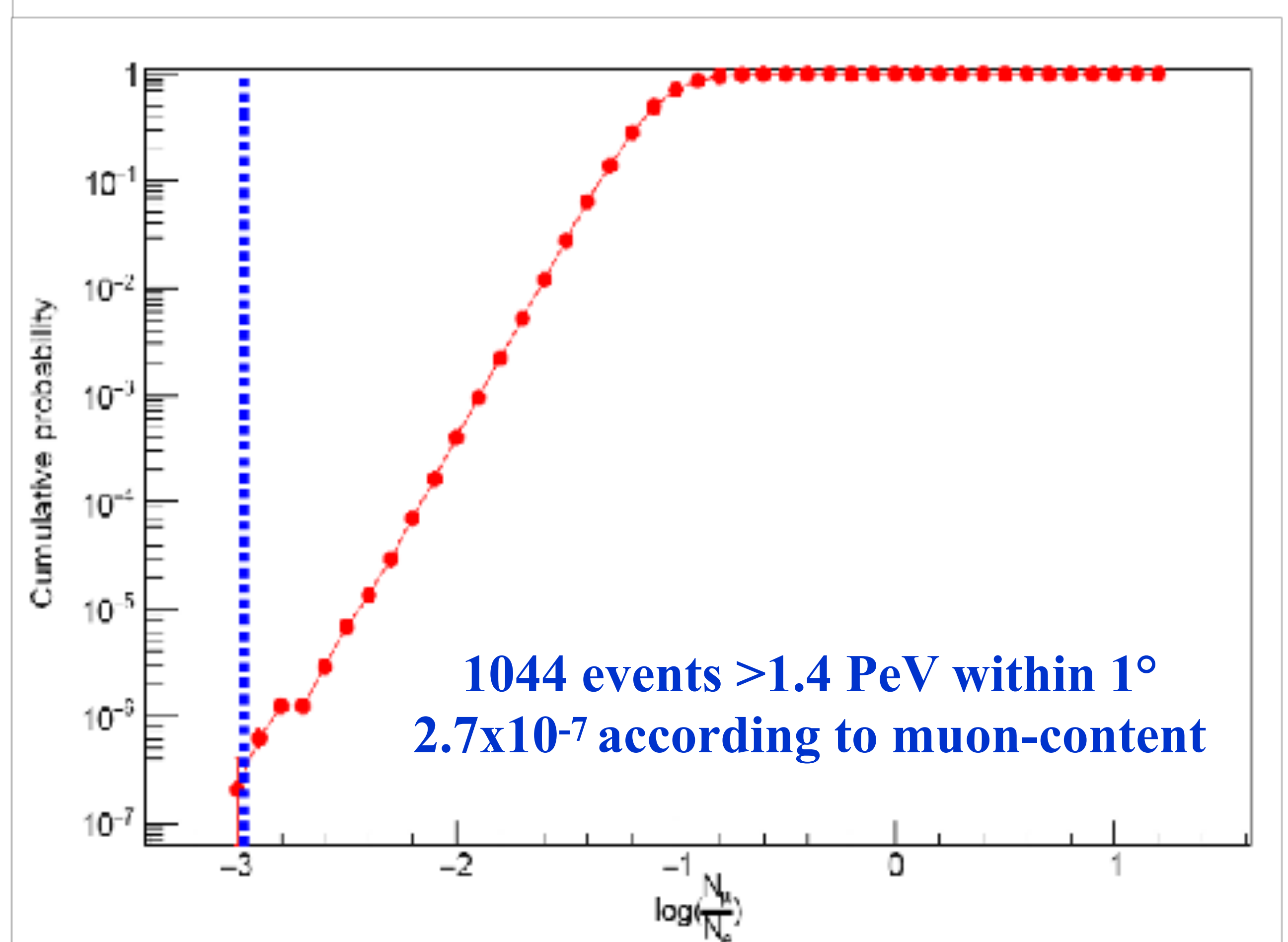

The Cygnus Cocoon by ARGO

The ***Cygnus Cocoon*** is a superbubble surrounding a region of OB2 massive star formation

The Cocoon, which seems to be related to the combination of many powerful SNR and stellar-wind shocks, ***has been detected at TeV energies by ARGO-YBJ for the first time.***

The Fermi/LAT view in the 10-100 GeV band

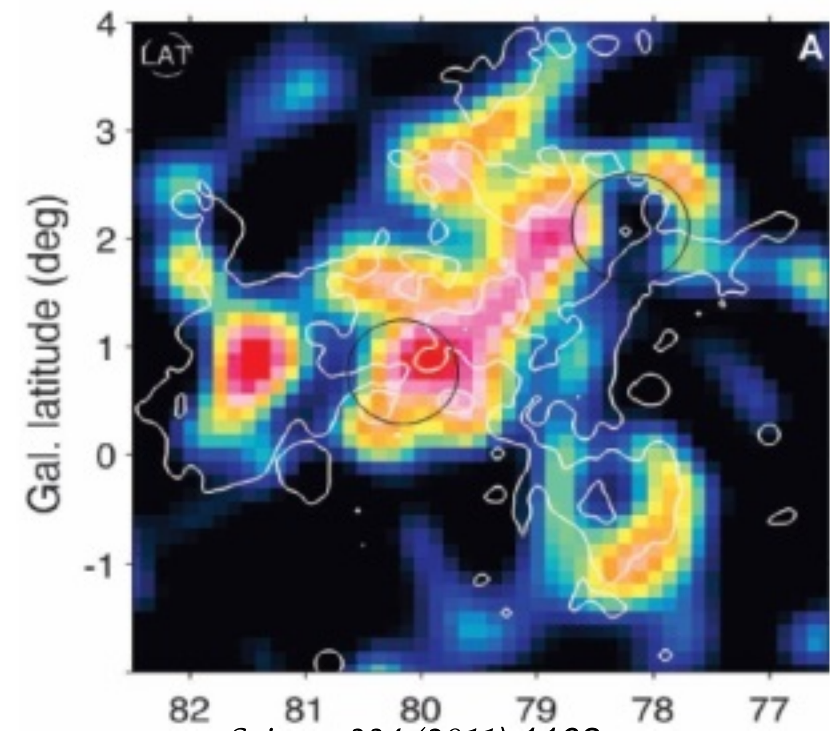

Science 334 (2011) 1103

This observation confirms a long-standing hypothesis that massive-star forming regions can accelerate particles to relativistic energies.

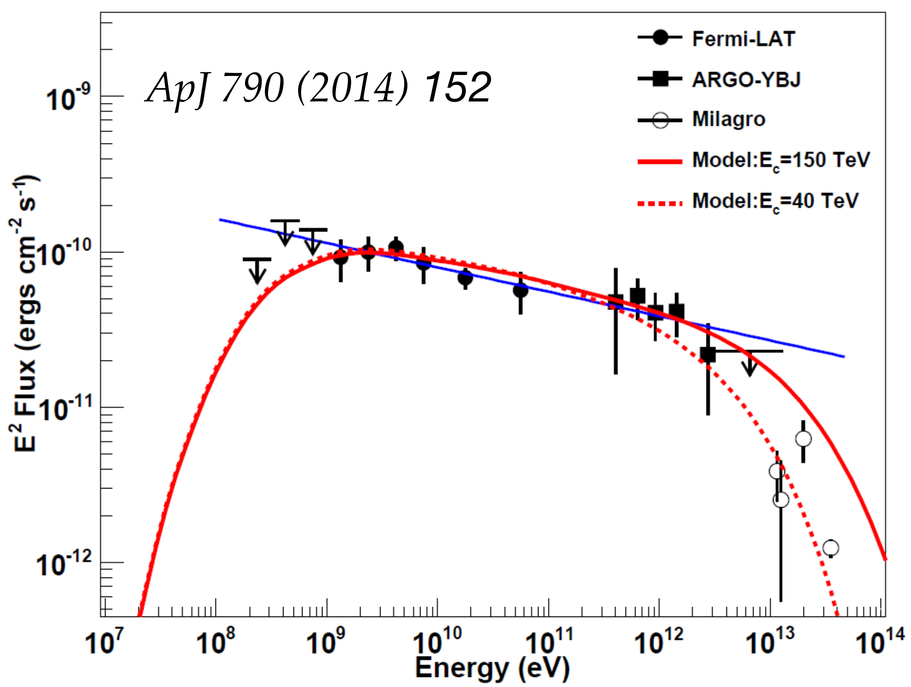

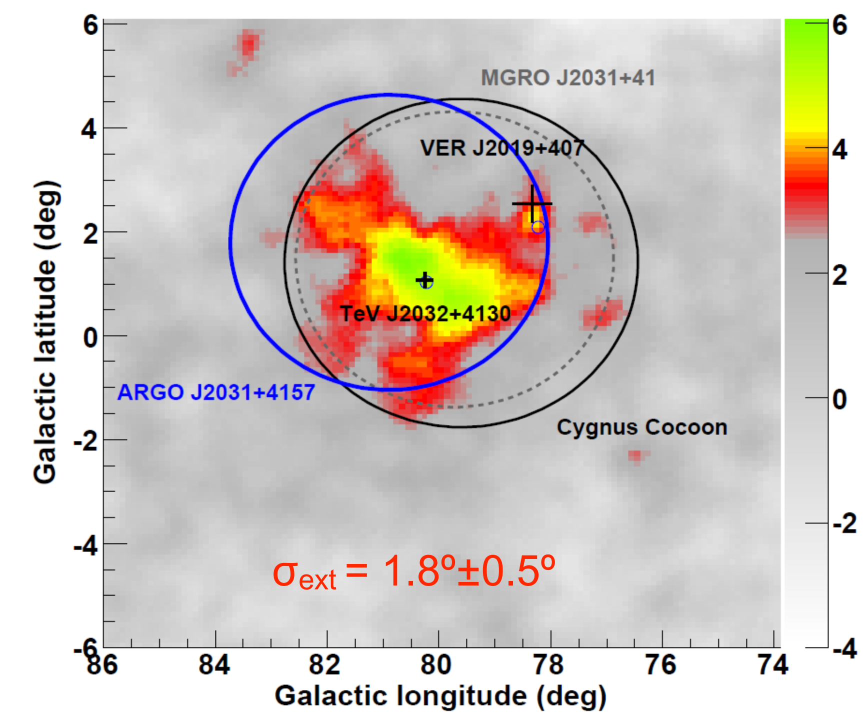

Spectrum of ARGO J2031+4157: $\frac{dN}{dE} \propto E^{-2.62\pm0.27}$

Combined Fermi-LAT&ARGO spectrum: $\frac{dN}{dE} \propto E^{-2.16\pm0.04}$

The Cygnus Cocoon by HAWC up to 200 TeV

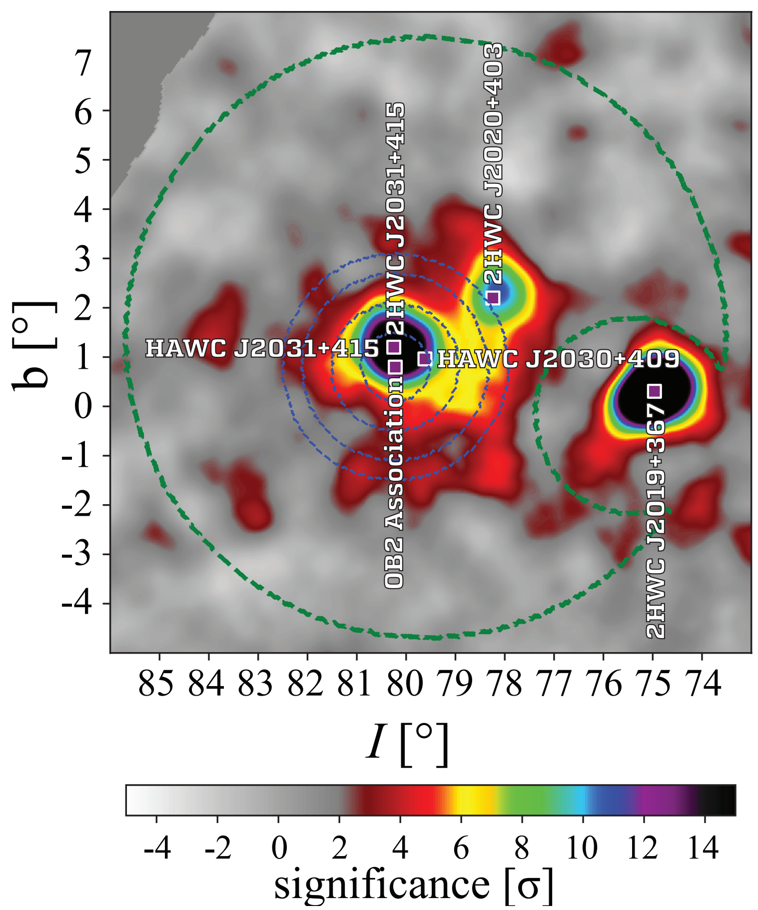

1343 days of measurements

Extension: 2.13° ± 0.15°(stat.) ± 0.06°(syst.)

The TeV measurements provide direct evidence that the Cygnus Cocoon accelerates CR protons above 100 TeV.

The ***leptonic origin*** of the γ-ray radiation is ***disfavored***, as uniquely responsible for the GeV and TeV flux observed.

The measured flux is likely originated by hadronic interactions.

Power law spectrum

$$dN/dE = N_0\,(E/E_0)^{\Gamma}$$

$$\Gamma = -2.64^{+0.05}_{-0.05}(\mathrm{stat.})^{+0.09}_{-0.03}(\mathrm{syst.})$$

HAWC Coll., Nature (2021)

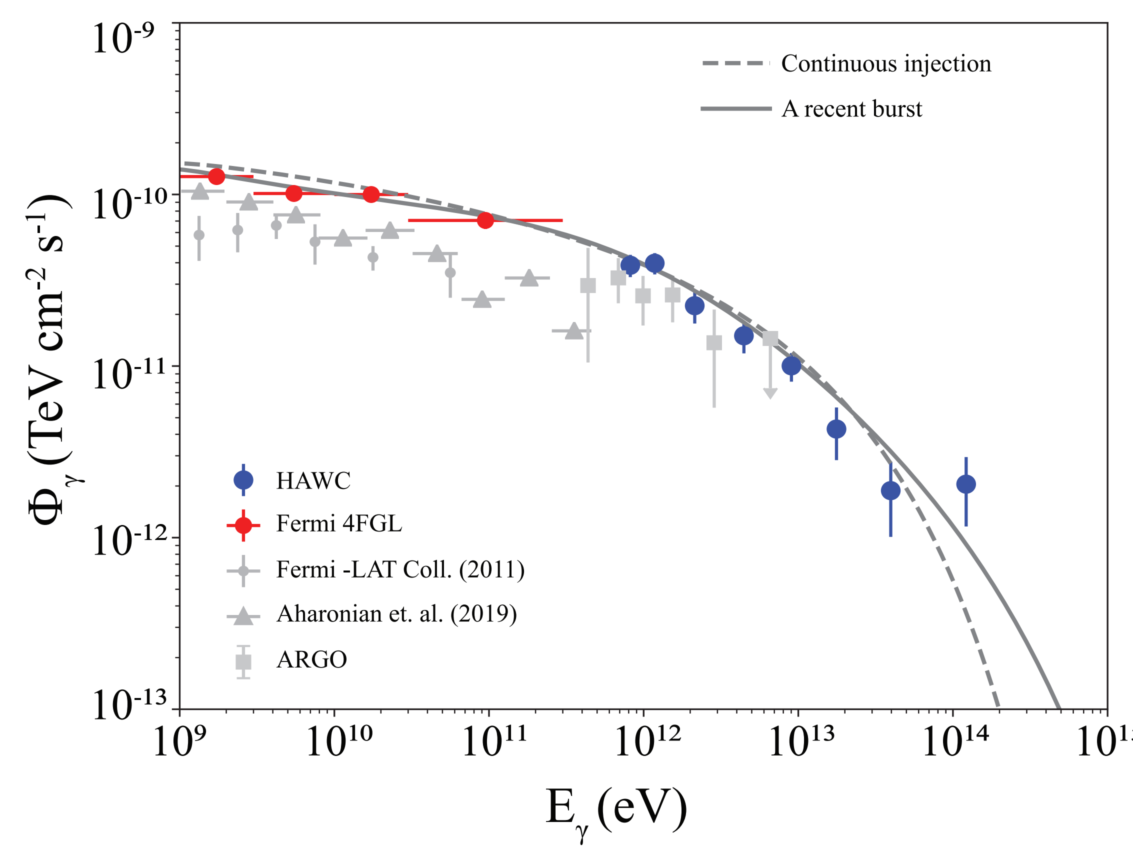

Radial distribution of CR density

in extended regions around ***Cygnus Cocoon***, Westerlund 1 Cocoon and in the CMZ of the Galactic Center

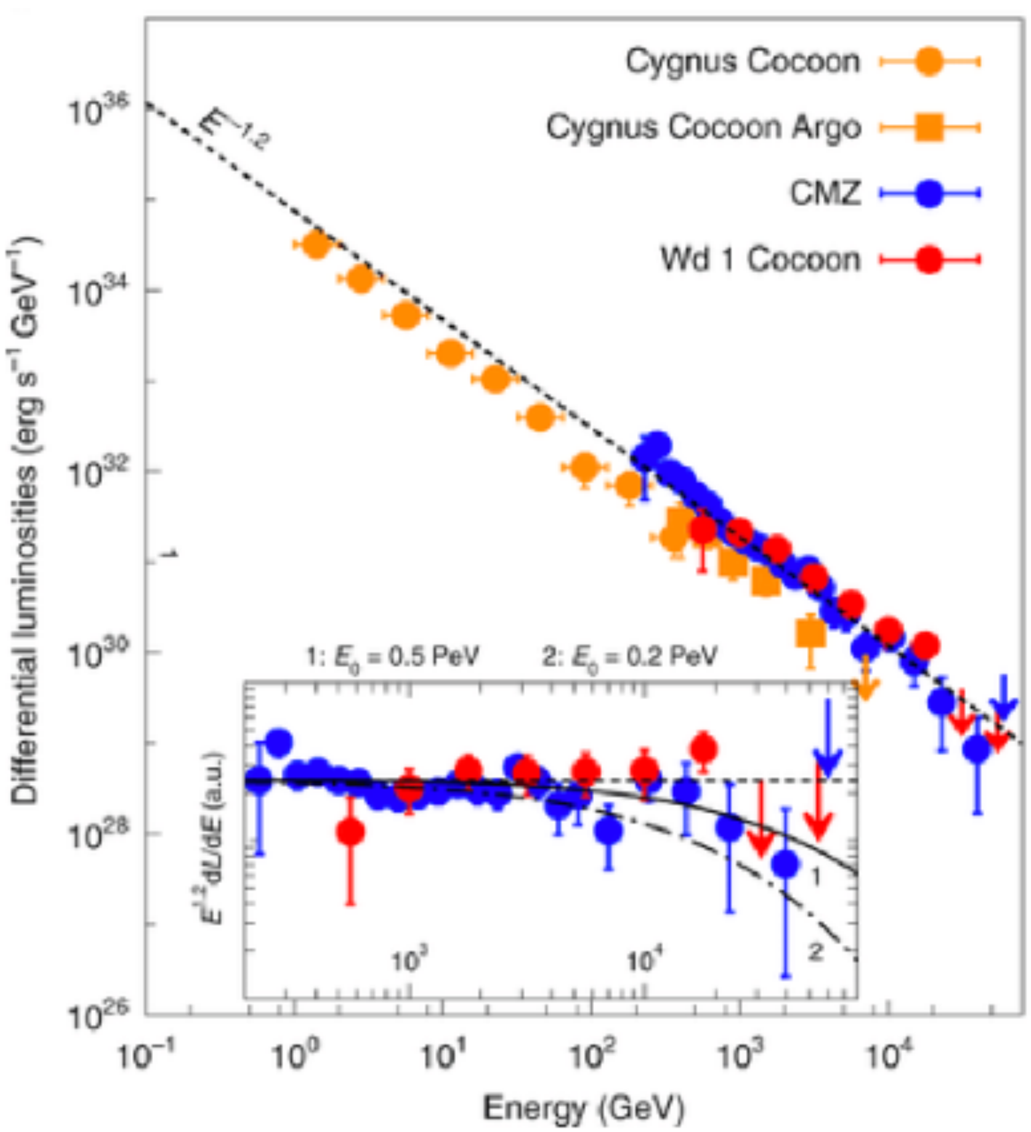

γ-ray luminosities of CR protons

F. Aharonian et al., Nature 2018

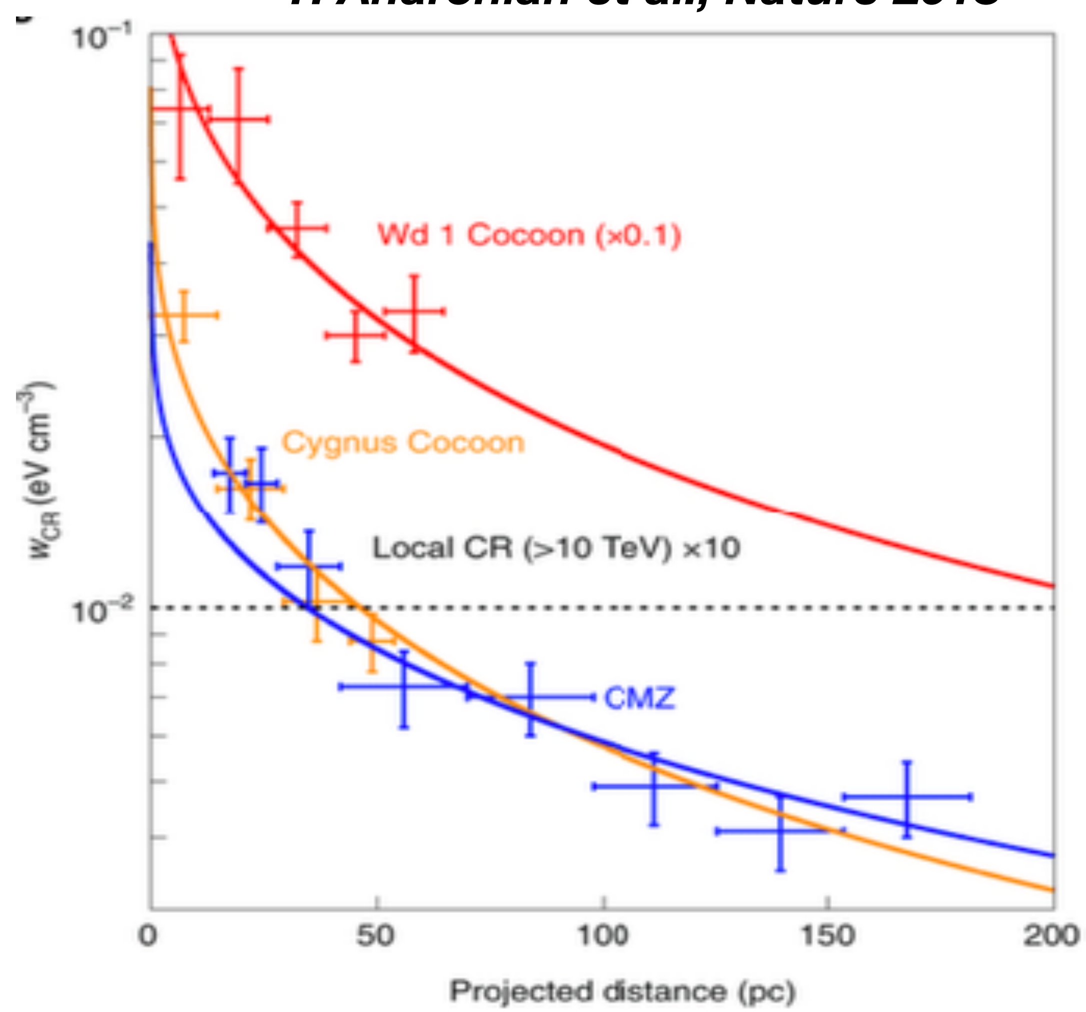

Radial distribution of CR protons

The density of CR protons responsible for γ-rays, ***declines as 1/r*** up to ≈50 pc from the stellar clusters Cyg OB2 and Westerlund 1.

1/r → continuous accelerator!

Massive Stars as PeVatrons

What do we expect ?

1/r ➔ continuous source

1/r² ➔ wind or ballistic motion

constant ➔ burst like source

The ***1/r decrement of the CR density*** with the distance from the star cluster is a distinct signature of ***continuous injection of CRs*** and their diffusion through ISM.

The analysis of γ-ray data show that ***the hard energy spectra of parent protons continue up to ~1 PeV***, and the efficiency of conversion of kinetic energy of powerful stellar winds can be as high as 10%.

This implies that ***the population of young massive stars can provide production of CRs at a rate of up to 10^{41} erg/s,*** which is sufficient to support the flux of Galactic CRs ***without invoking other source populations.***

What's next?

After the observation of more than 15 γ-sources above 100 TeV in the Northern hemisphere, an all-sky detector in the Southern hemisphere should be a high priority!

We expect Super-PeVatrons well beyond the PeV in the Inner Galaxy!

→ *we need a detector able to measure energy spectra up to 10 PeV*

2 different approaches:

SWGO: HAWC-based layout with only water Cherenkov detectors

Size & Fill factor

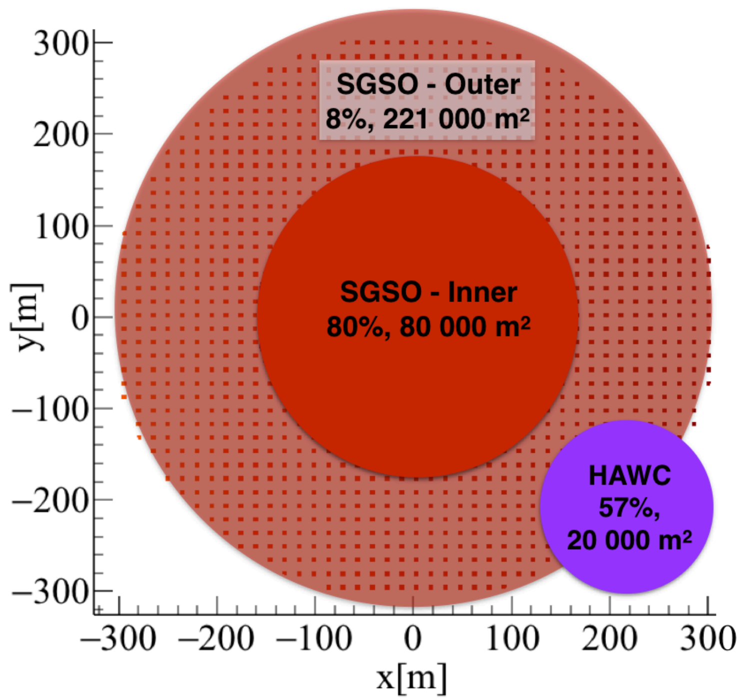

STACEX: RPC carpet above a water Cherenkov pond for muon detection + scintillator array to have statistics at PeV

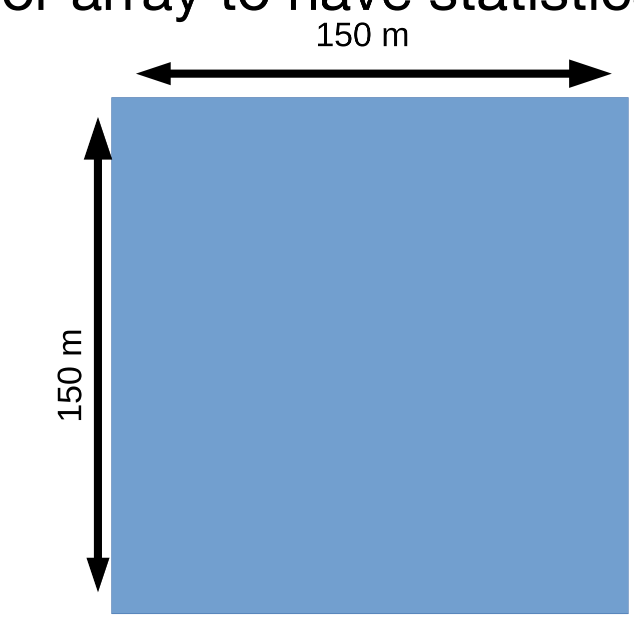

Much smaller full coverage core detector

SWGO: a water Cherenkov based array

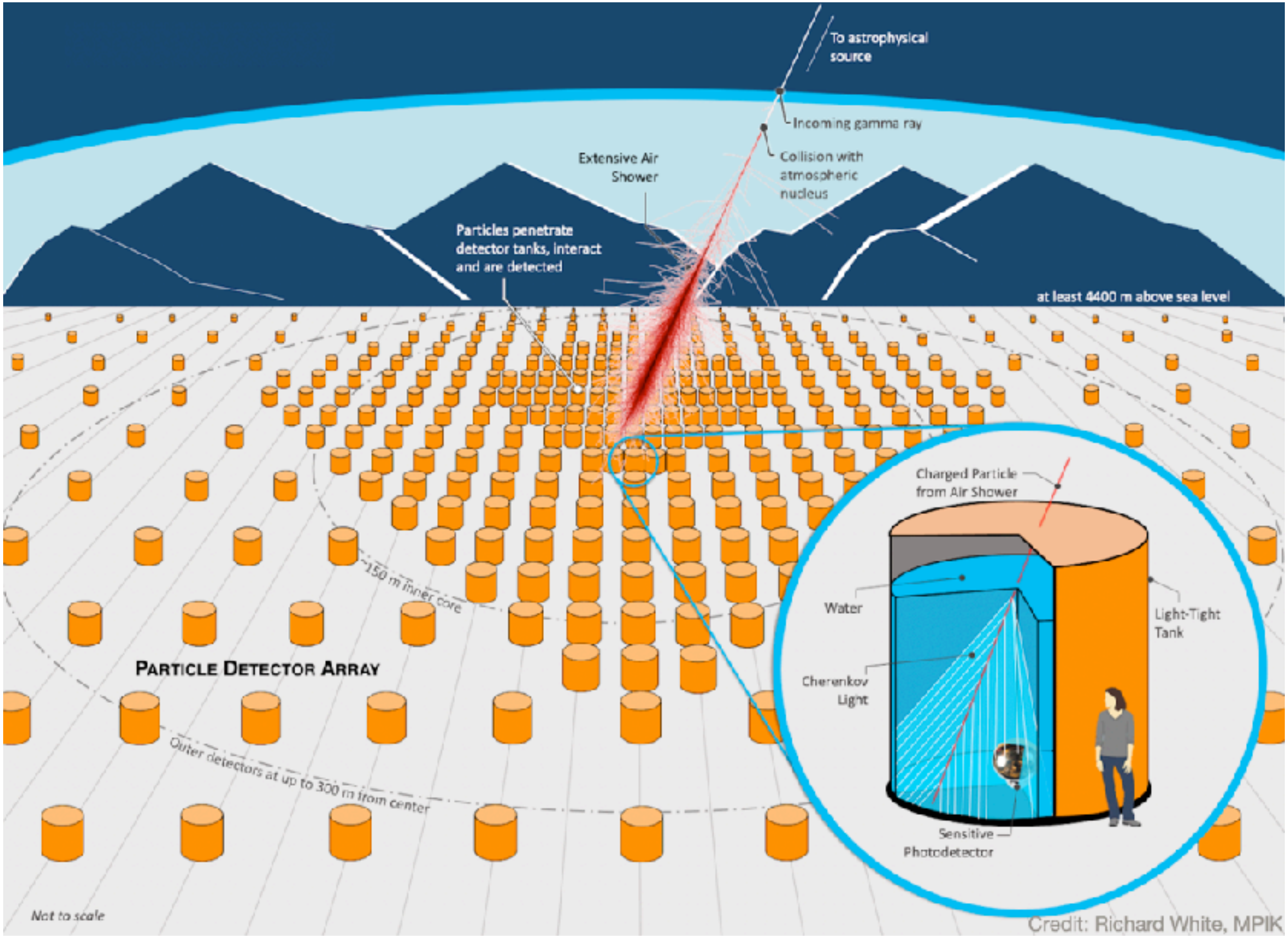

STACEX

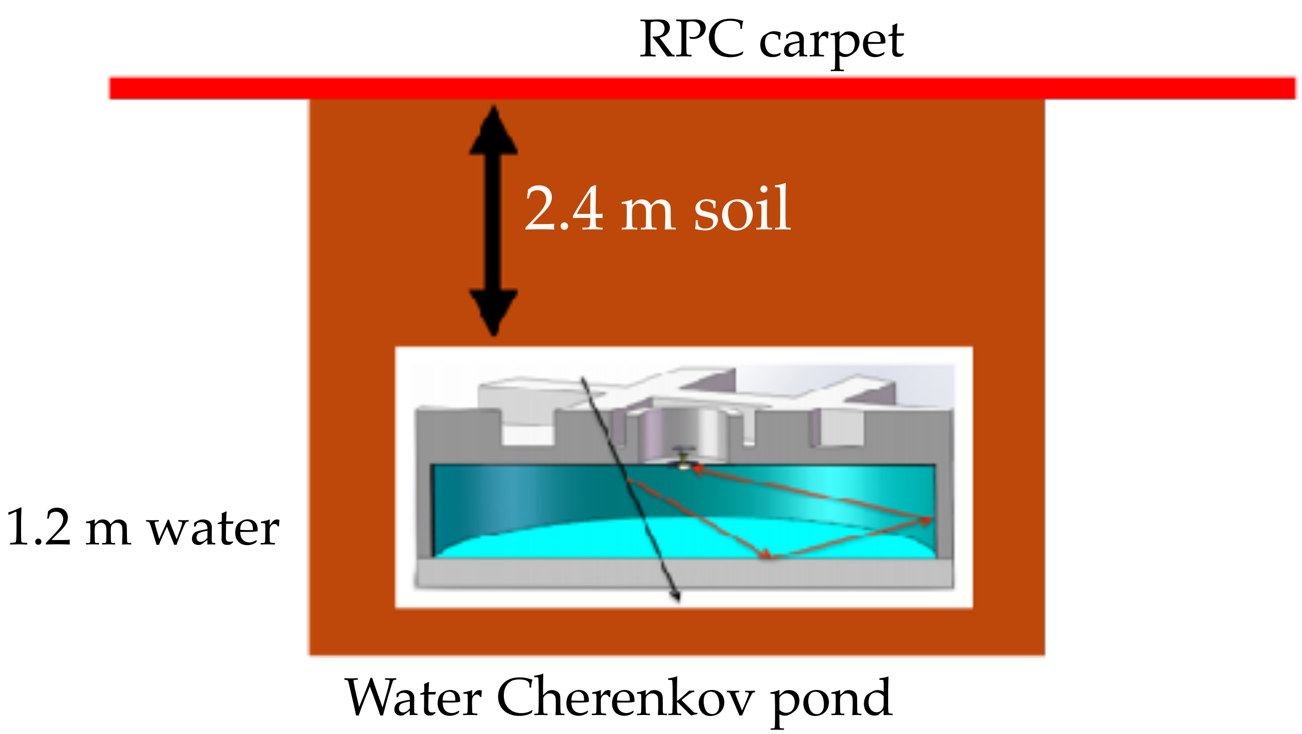

PROCEEDINGS OF SCIENCE

STACEX: RPC-based detector for a multi-messenger observatory in the Southern Hemisphere

Fernandez Gonzalo Rodriguez,[a,*] Bigongiari Ciro,[b] Bulgarelli Andrea,[c] Camarri Paolo,[d,e] Cardillo Martina,[a] Di Sciascio Giuseppe,[e] Fioretti Valentina,[c] Piano Giovanni,[a] Santonico Rinaldo[d,e] and Tavani Marco[a]

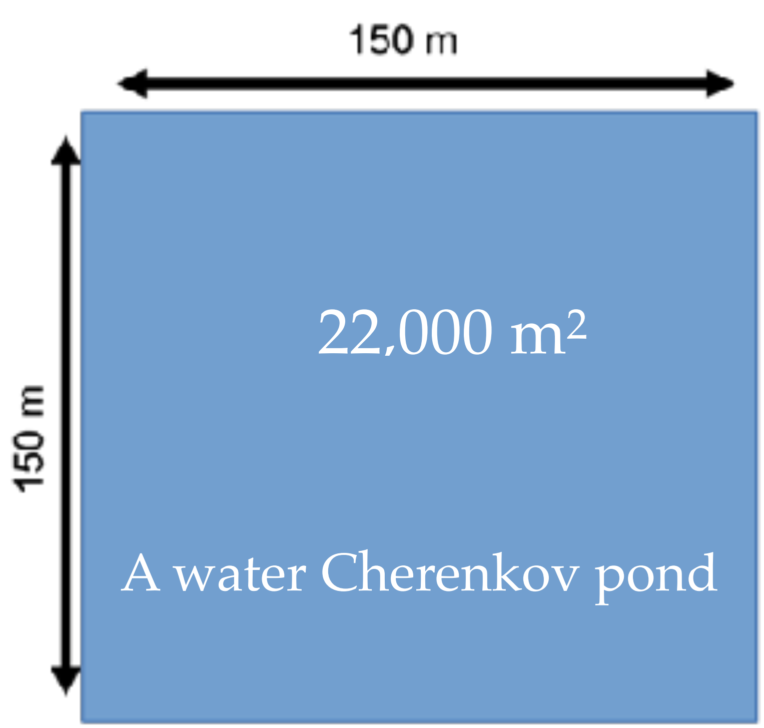

Few muons at low energy → full coverage pond to increase the bkg rejection capability at lower energies.

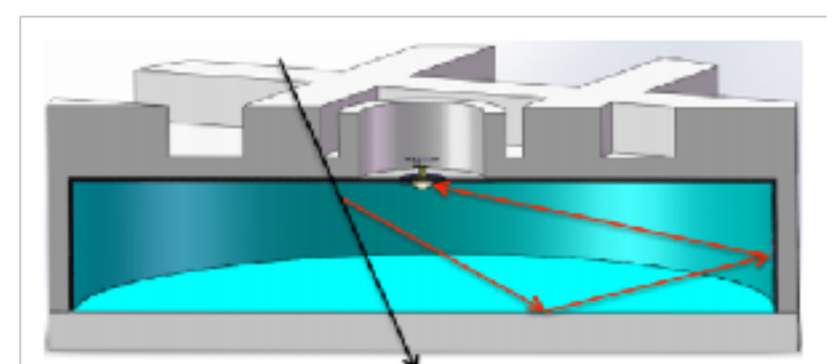

water Cherenkov detector LHAASO-like
1.2 m of water + 8″ PMT downward

Sensitivity of the "core" detector

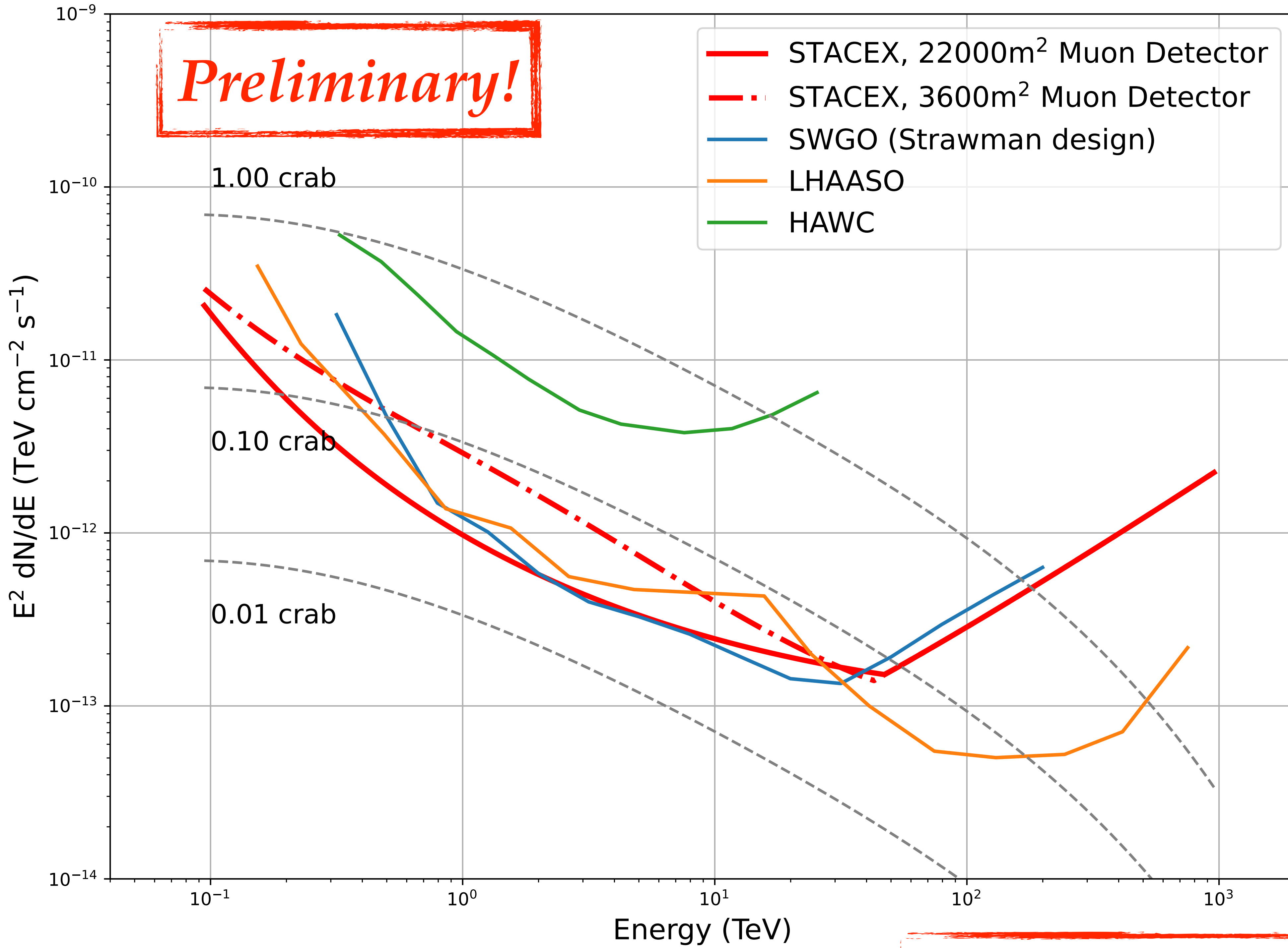

Bkg-free regime starts at ≈50 TeV

Conclusions

LHAASO is the most ambitious experiment to study Galactic Cosmic Rays being able to deal with all the main open problems of Cosmic Ray physics at the same time.

First year operation with half array ***opened the PeV gamma-sky to observations*** for the first time!

The recent detections by LHAASO

directly demonstrate the presence of electron and proton PeVatrons in the Milky Way

The Galaxy is full of PeVatrons!

Are the galactic proton PeVatrons linked to SNRs or YMCs or Sgr A* or all of of them?

- observations with LHAASO, eRosita, CTA/ASTRI and SWGO will tell us

CTA-South and ***SWGO*** in the Southern Hemisphere will explore the Inner Galaxy looking for Super-PeVatrons up to 10 PeV

The next challenge is to search for Super-PeVatrons in the Inner Galaxy!

LHAASO vs other EAS arrays

Experiment	g/cm^2	Detector	ΔE (eV)	e.m. Sensitive Area (m^2)	Instrumented Area (m^2)	Coverage
ARGO-YBJ	606	RPC/hybrid	$3 \cdot 10^{11} - 10^{16}$	6700	11,000	0.93 (central carpet)
BASJE-MAS	550	scint./muon	$6 \cdot 10^{12} - 3.5 \cdot 10^{16}$		10^4	
TIBET ASγ	606	scint./burst det.	$5 \cdot 10^{13} - 10^{17}$	380	3.7×10^4	10^{-2}
CASA-MIA	860	scint./muon	$10^{14} - 3.5 \cdot 10^{16}$	1.6×10^3	2.3×10^5	7×10^{-3}
KASCADE	1020	scint./mu/had	$2 - 90 \cdot 10^{15}$	5×10^2	4×10^4	1.2×10^{-2}
KASCADE-Grande	1020	scint./mu/had	$10^{16} - 10^{18}$	370	5×10^5	7×10^{-4}
Tunka	900	open Cher. det.	$3 \cdot 10^{15} - 3 \cdot 10^{18}$	-	10^6	-
IceTop	680	ice Cher. det.	$10^{16} - 10^{18}$	4.2×10^2	10^6	4×10^{-4}
LHAASO	600	Water C scintill/muon/hadron Wide FoV Cher. Tel.	$10^{12} - 10^{17}$	5.2×10^3	1.3×10^6	4×10^{-3} (KM2A)

		μ Sensitive Area (m^2)	Instrumented Area (m^2)	Coverage
LHAASO	4410	4.2×10^4	10^6	4.4×10^{-2}
TIBET ASγ	4300	4.5×10^3	3.7×10^4	1.2×10^{-1}
KASCADE	110	6×10^2	4×10^4	1.5×10^{-2}
CASA-MIA	1450	2.5×10^3	2.3×10^5	1.1×10^{-2}

✦ LHAASO Muon detector area: 4.2×10^4 m^2 + 8×10^4 m^2 (WCDA) ≈ *10^5 m^2* !!!

Water Cherenkov Detector Array

3 Arrays

1: 22,500 m^2 8”PMTs

2: 22,500 m^2 20”PMTs

3: 33,000 m^2 20”PMTs

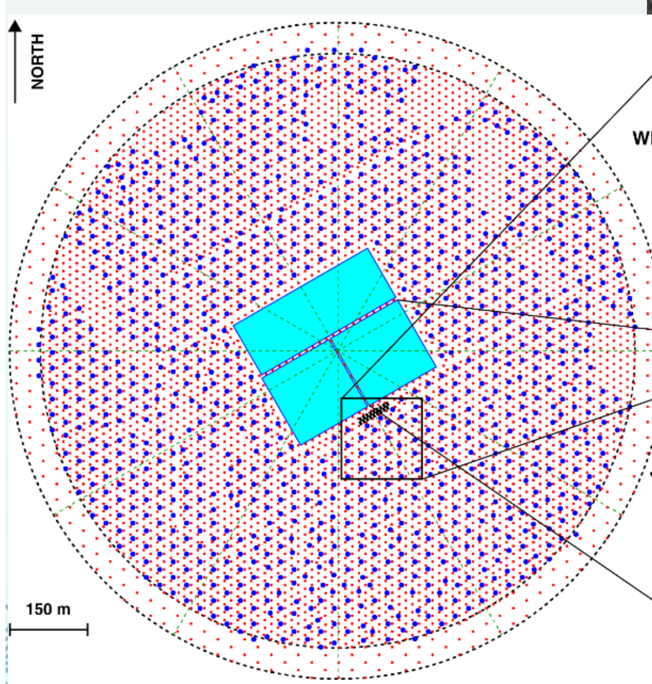

Water Cherenkov Detector Array

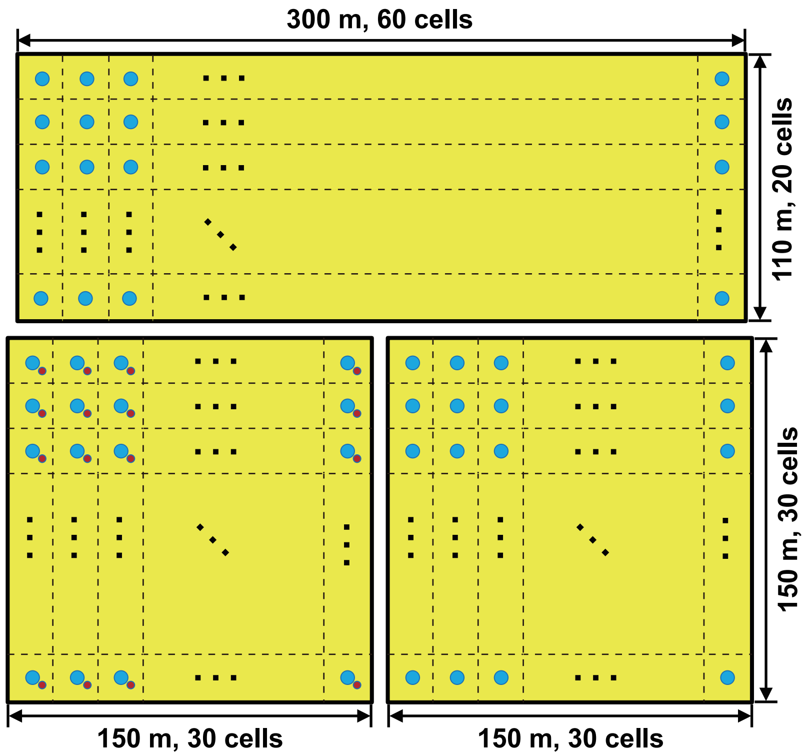

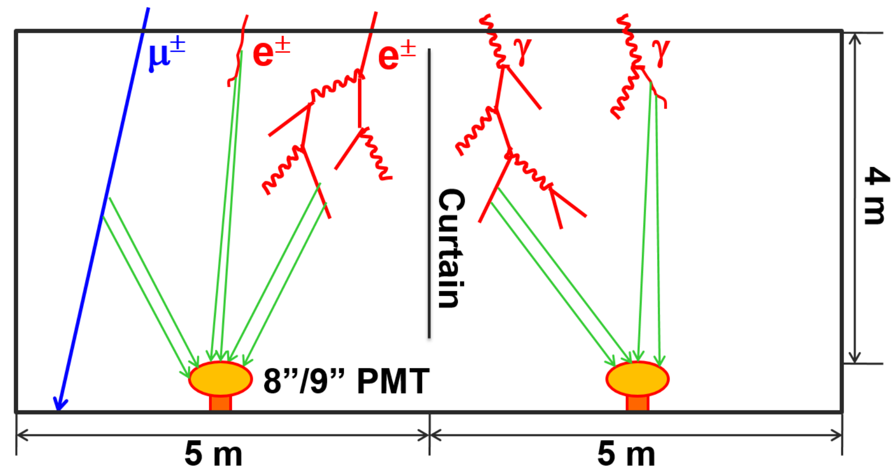

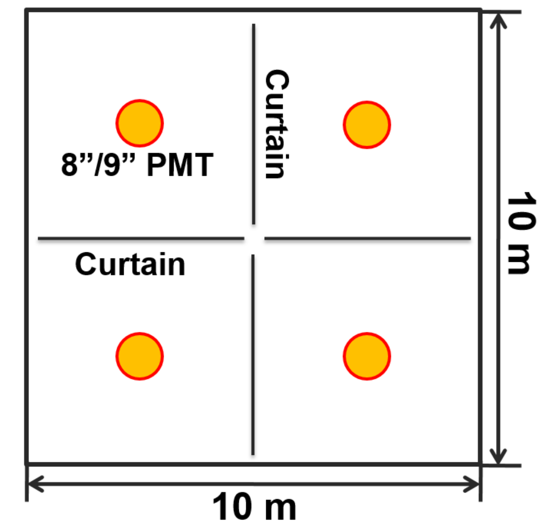

<table>
<tr><td>No.1 Pond</td><td rowspan="2">150m*150m, 900 cells</td><td>8-in PMT+ 1.5-in PMT</td></tr>
<tr><td>No.2 Pond</td><td rowspan="2">20-in PMT+ 3-in PMT</td></tr>
<tr><td>No.3 Pond</td><td>300m*110m, 1,320 cells</td></tr>
</table>

Item	Value
Cell area	25 m^2
Effective water depth	4 m
Water transparency	> 15 m (400 nm)
Precision of time measurement	0.5 ns
Dynamic range	1-4000 PEs
Time resolution	<2 ns
Charge resolution	40% @ 1 PE 5% @ 4000 PEs
Accuracy of charge calibration	<2%
Accuracy of time calibration	<0.2 ns
Total area	90,000 m^2
Total cells	3600

To enlarge the dynamic range, a *1.5-inch PMT* is placed aside each large PMT *in one of the two smaller ponds.*

To extend the dynamic range, a dynode of the PMT is also used for signal output together with the anode.

The *anode signal* is split into two parts for *time* and *charge* measurements, respectively, while the *dynode* signal is used only for *charge measurement of large signals*.

LHAASO: KM2A array

Electromagnetic particle detectors

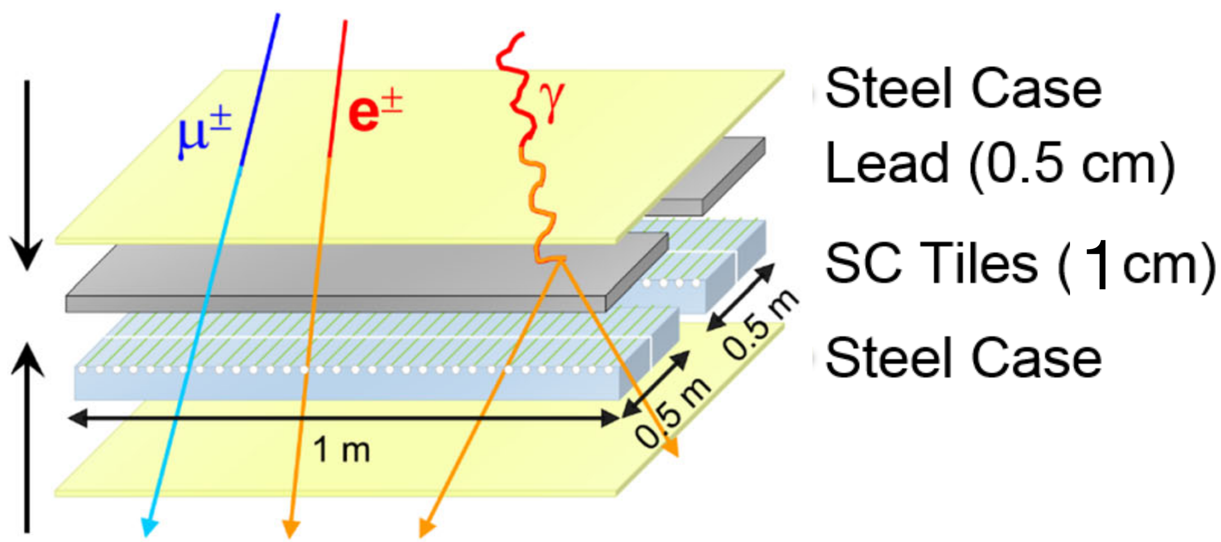

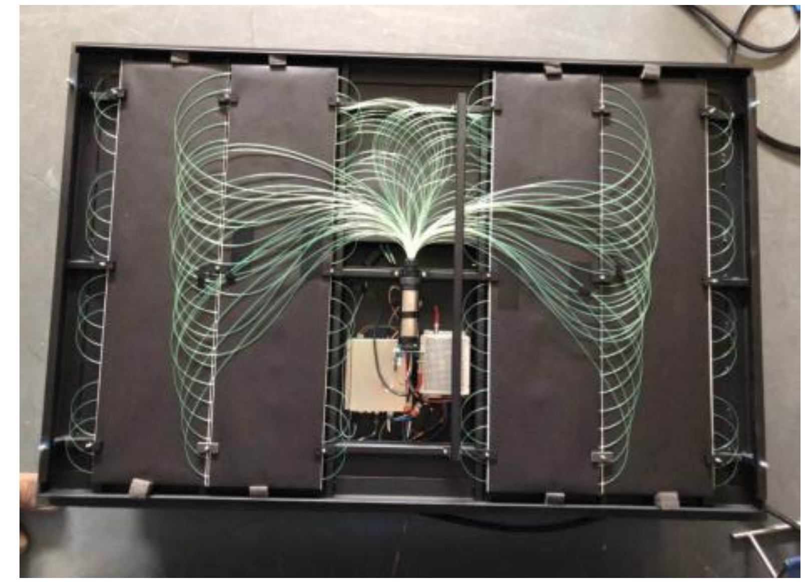

16 wavelength-shifting fibers (2.7 m in length and 1.5 mm in diameter) are embedded in 32 grooves (each 1.8 mm in depth and 1.6 mm in width) of each tile to collect scintillation light generated by charged particles and guide the scintillation light to a 1.5-inch PMT.

4 scintillation tiles
100 cm × 25 cm × 1 cm each

Effective Area: ***1 m²***

Detection Efficiency (>5 MeV): >95%

Dynamic Range: 1 - 10^4 particles

Time Resolution: < 2 ns

Particle counting resolution: 25% at 1 particle, 5% at 10^4 particles

PMT: 1.5 inch

The average *single rate* of an ED is *≈1.7 kHz* with a threshold of 1/3 particle

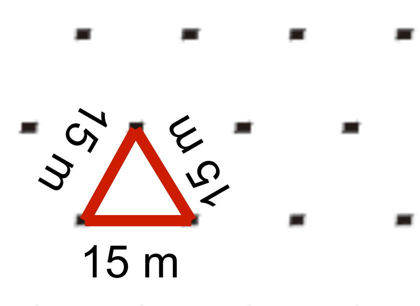

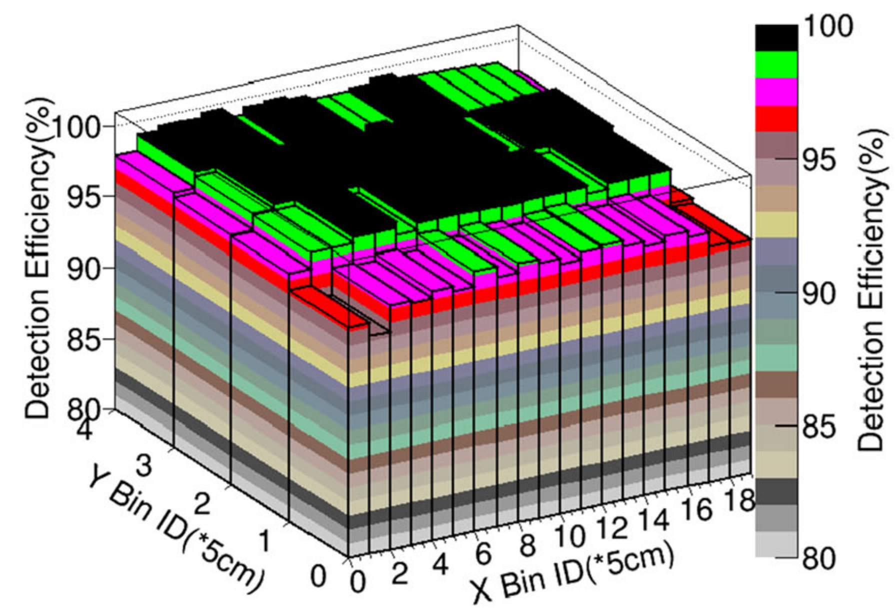

Detection efficiency for each 5 cm × 5 cm pixel

Water Cherenkov Muon Detector

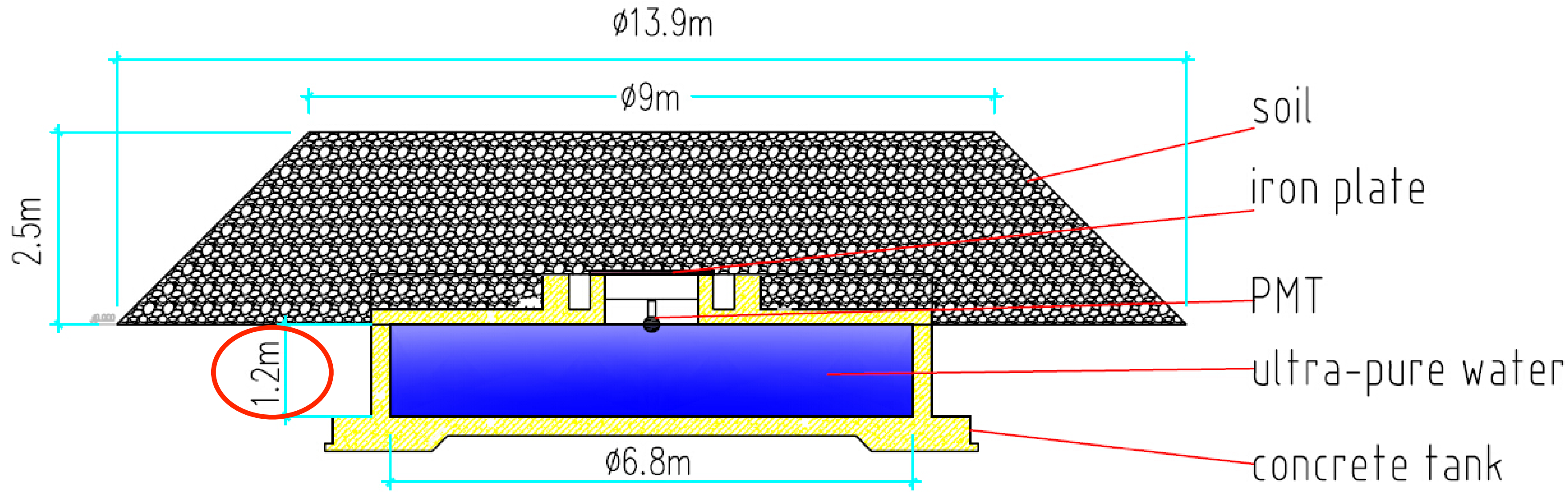

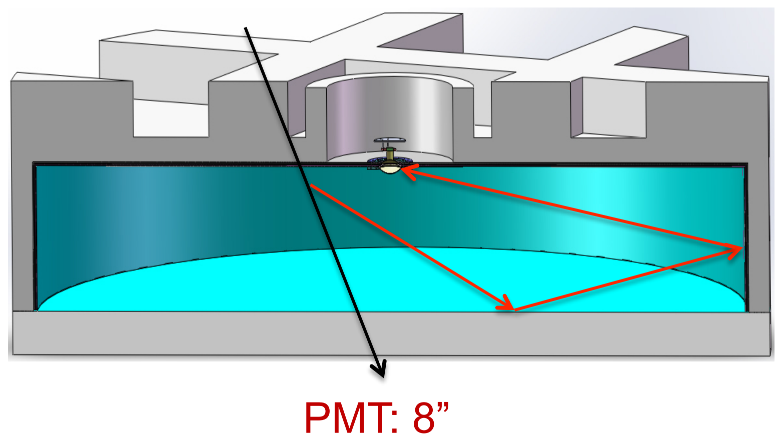

Item	Value
Area	36 m^2
Detection efficiency	>95%
Purity of N_μ	>95%
Time resolution	<10 ns
Dynamic range	1-10,000 particles
Particle counting resolution	25% @ 1 particle 5% @ 10,000 particles
Aging (<20%)	>10 years
Spacing	30 m
Total number of detectors	1221

The average *single rate* of an MD is *≈8 kHz* with a threshold of 0.4 particles

Wide FoV Cherenkov Telescope Array

Parameter	Requirement
Mirror area	>5 m^2
Number of pixels	1024 pixels
Pixel size	~0.5° /pixel
Field of view	16°×16°
Dynamic range	10 pe - 32000 pe
Resolution	<5%@1000 pe
Elevation angle adjustment range	0° - 90°, adjustment precision: <0.1°

Energy range: 30 TeV - 200 PeV

16 telescopes by the end of 2021

SiPM size: 15 mm×15 mm

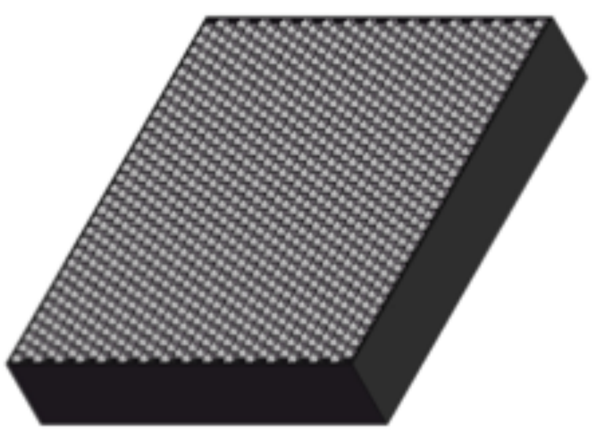

SiPM camera：32 × 32 SiPM pixels

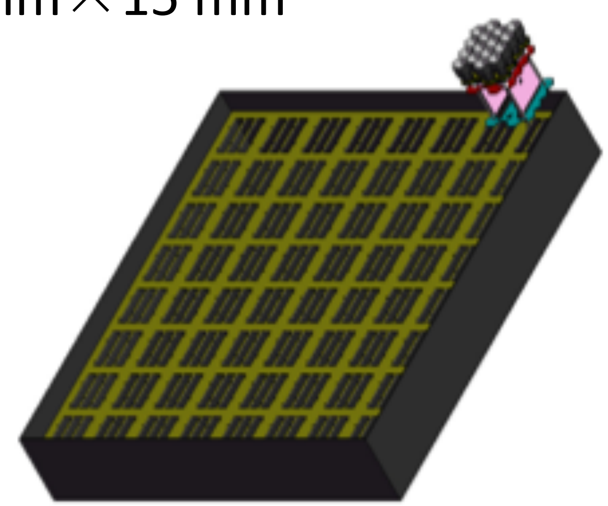

8 x 8 module camera box

64 × modules

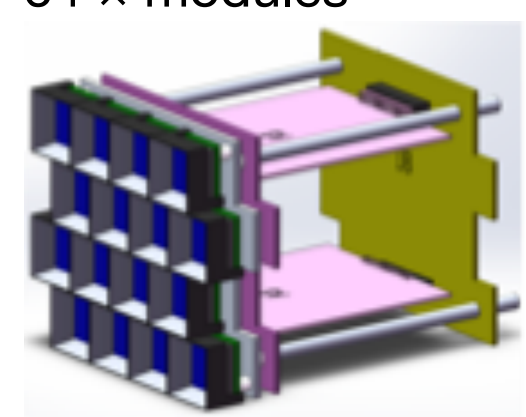

A module has 4×4 pixels